

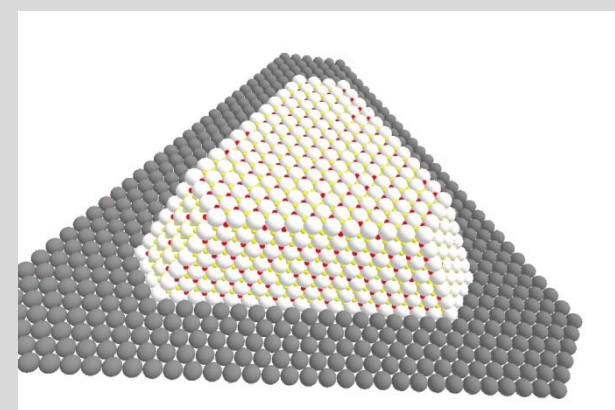
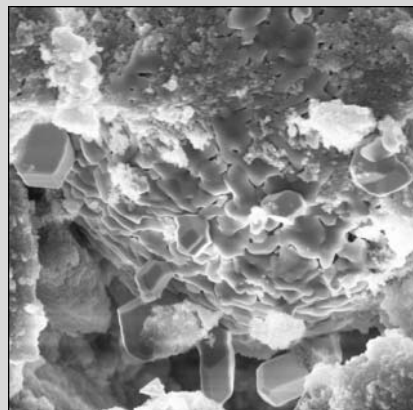
Kinetics – Interaction between Reaction, Mass and Heat Transfer

Lecture Series “Modern Methods in Heterogeneous Catalysis Research”, FHI, Berlin, 31.10.2014

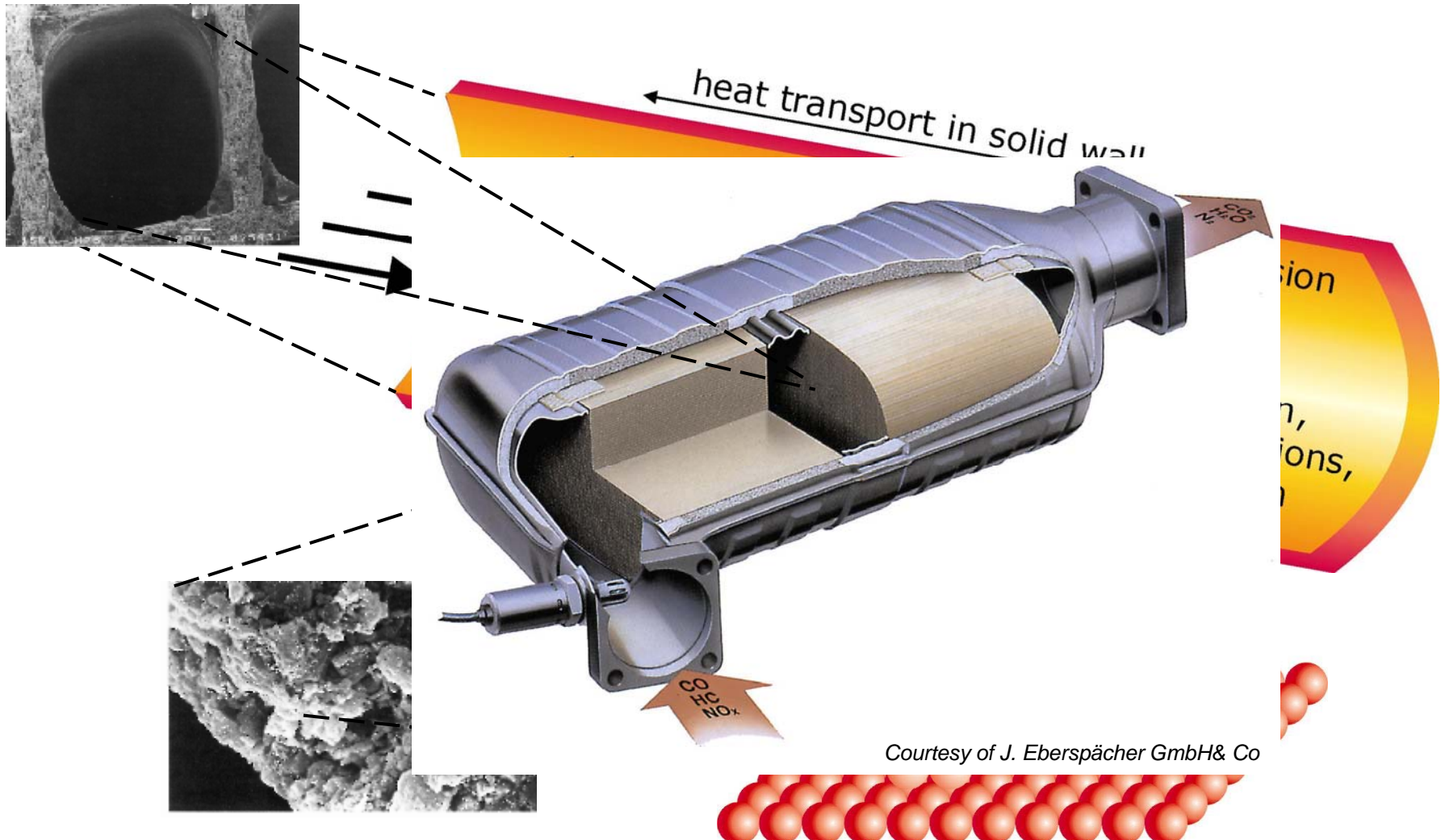
Olaf Deutschmann, Karlsruhe Institute of Technology (KIT)

Institute for Chemical Technology and Polymer Chemistry (ITCP)

Institute for Catalysis Research and Technology (IKFT)

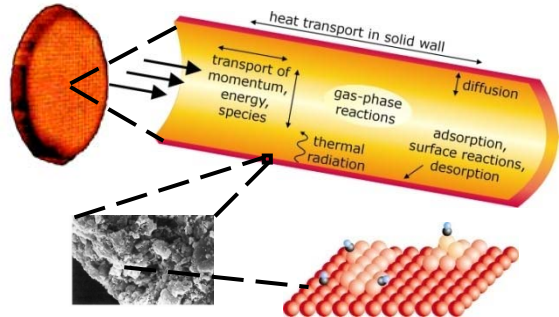


Complex interaction of physics and chemistry: Multi-scale modeling



Courtesy of J. Eberspächer GmbH& Co

Objective of this lecture: Introduction into the impact of mass and heat transfer on chemical kinetics



Physical-chemical processes occurring in catalytic reactors

- Surface micro kinetics
- Internal and external diffusion
- Flow field
- Heat transport
- Gas-phase micro kinetics
- Transient processes, Initial and boundary conditions
- Experimental methods, Modeling, Numerical Simulation

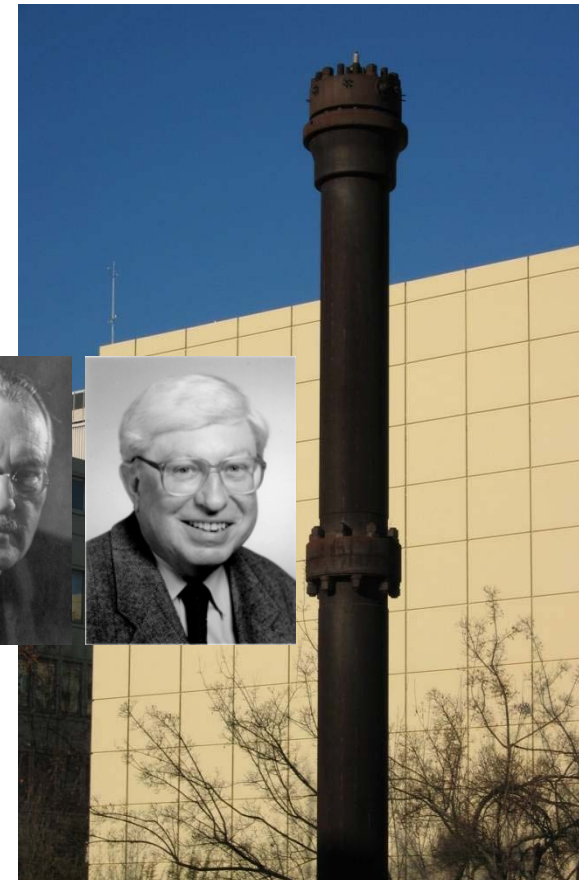
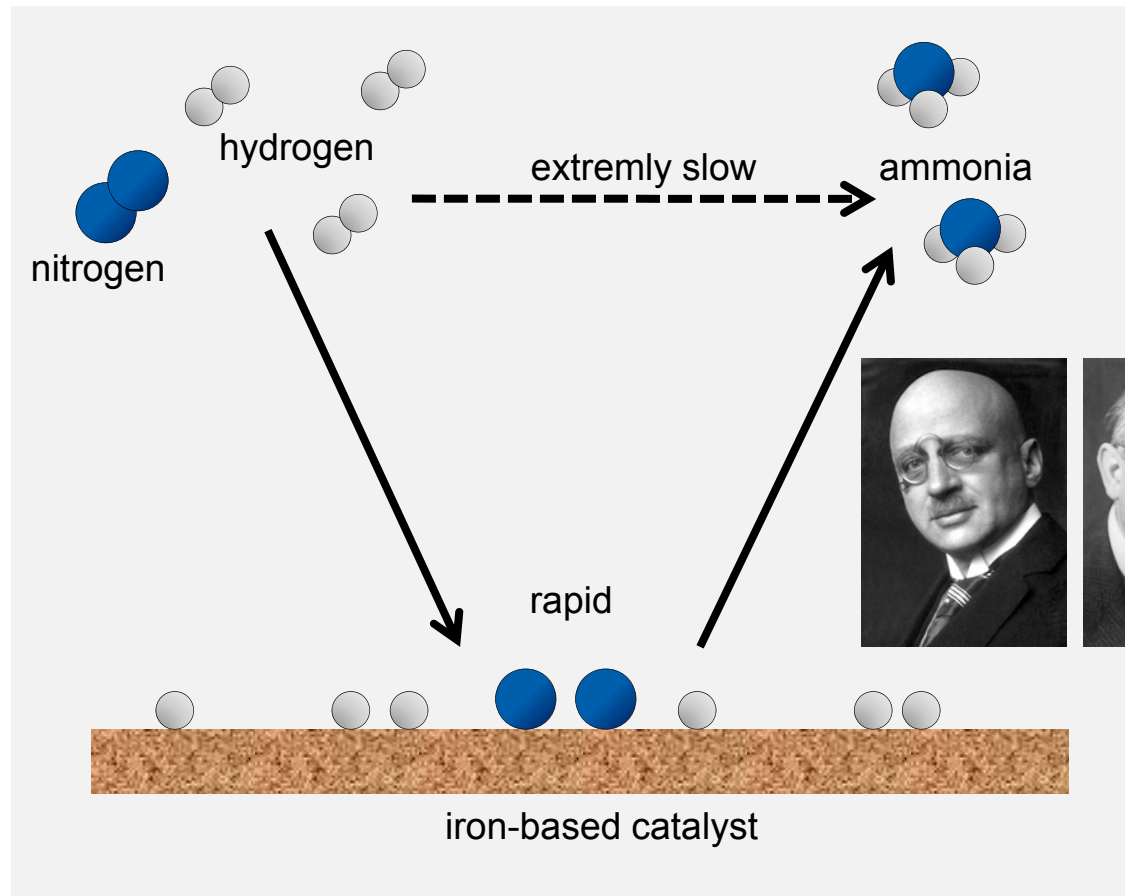
Kinetics – Interaction between Reaction, Mass and Heat Transfer: Outline



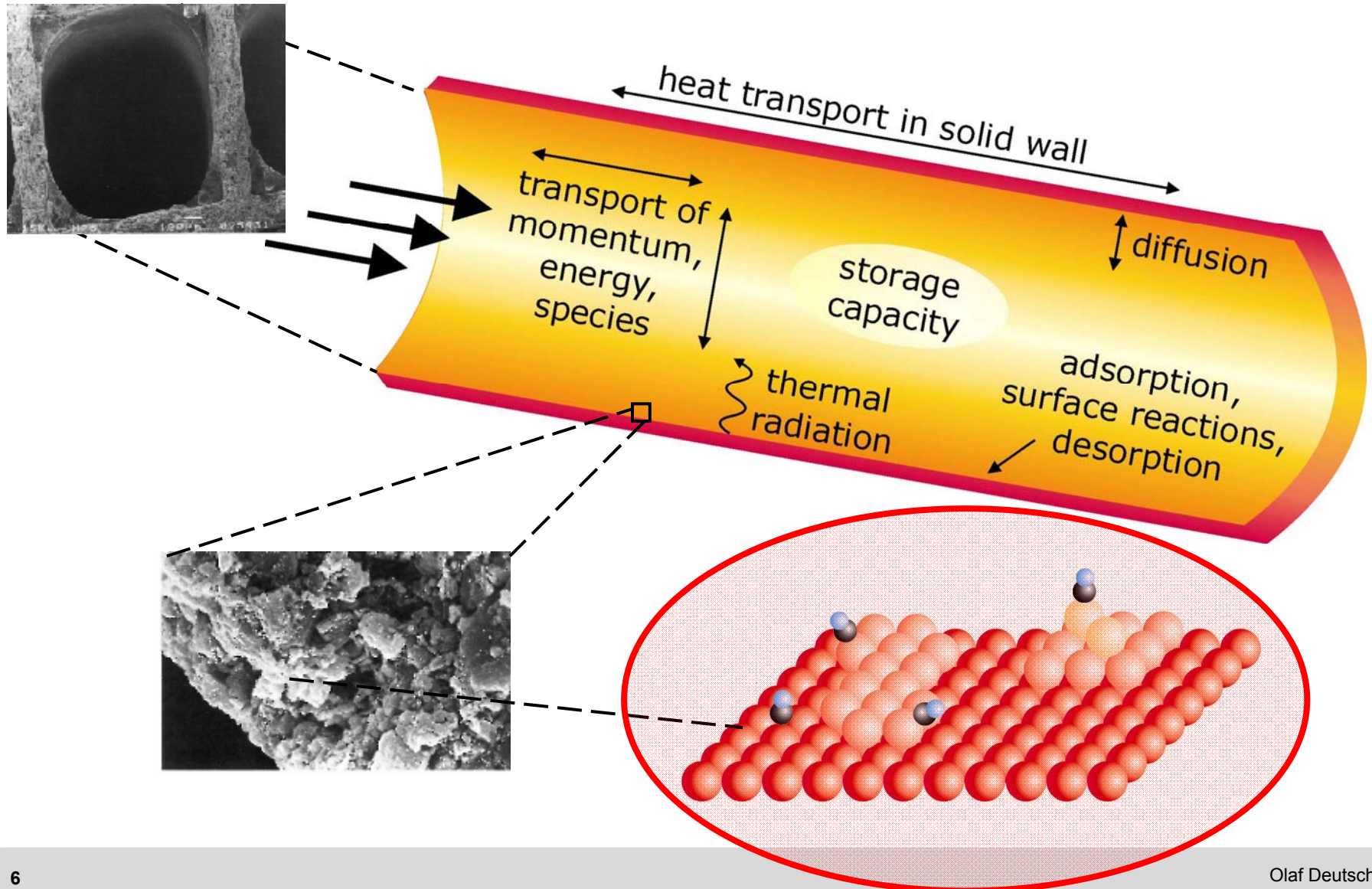
1. **Microkinetics of reactions on the catalytic surface**
2. Transport and reactions in porous media (internal diffusion)
3. Reactive flow and external diffusion
4. Gas-phase chemistry
5. Transient processes and heat transport

Micro kinetics of heterogeneous catalysis: ammonia synthesis studied since 1905

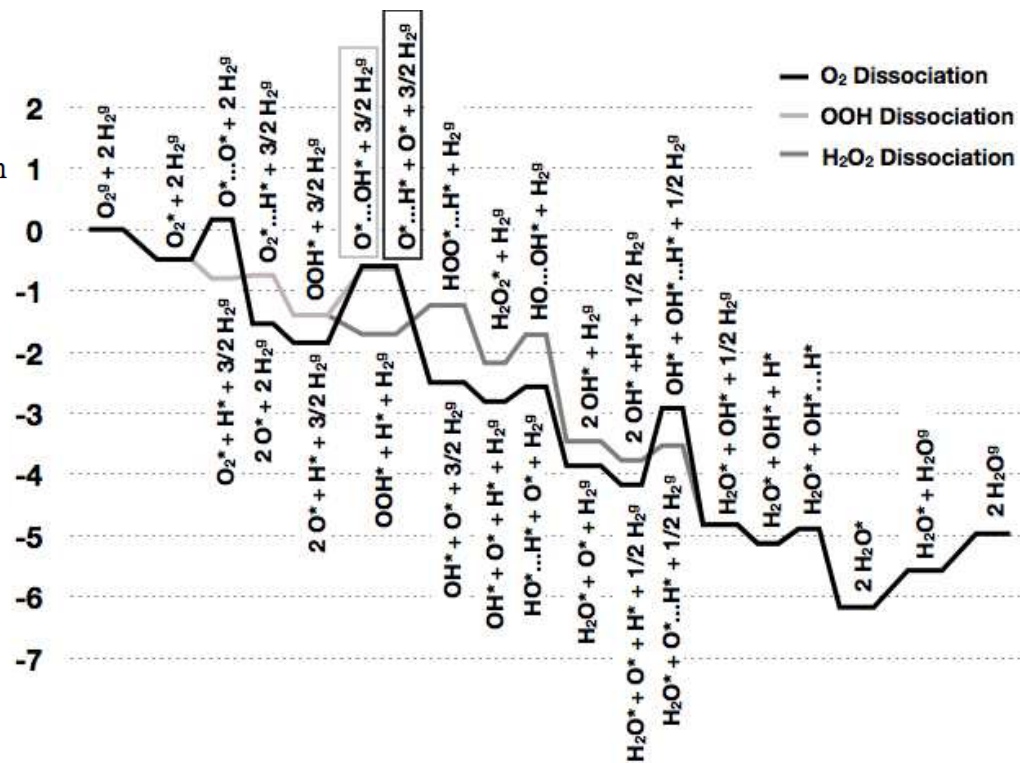
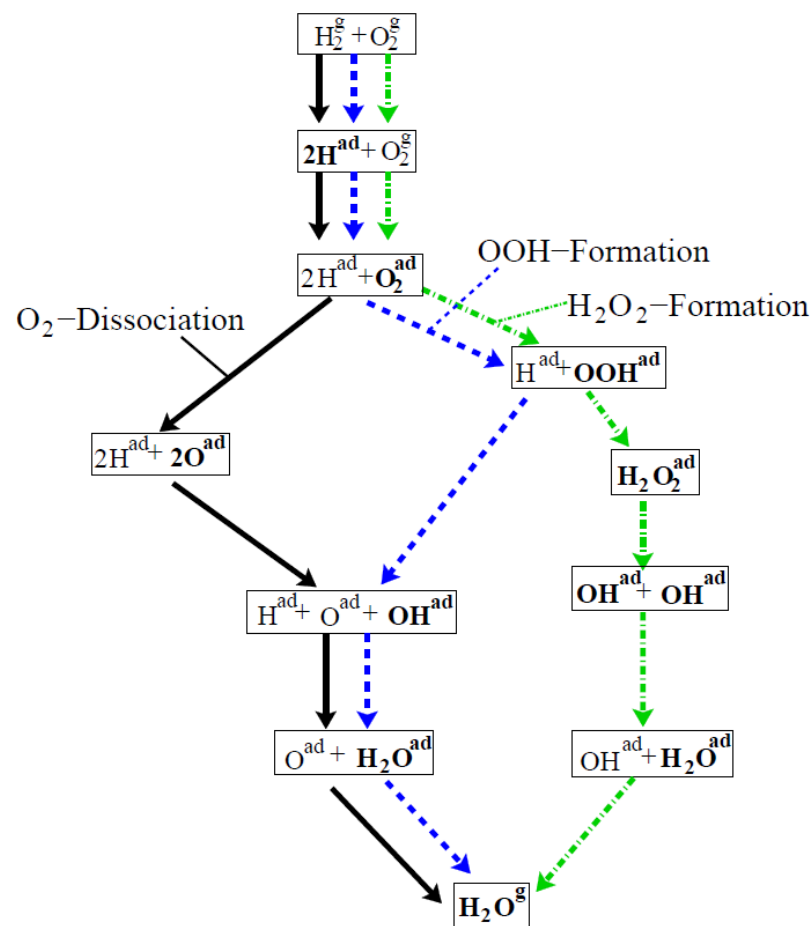
Haber/Karlsruhe, Bosch/BASF, Ertl/Berlin



Heterogeneous catalytic reactions

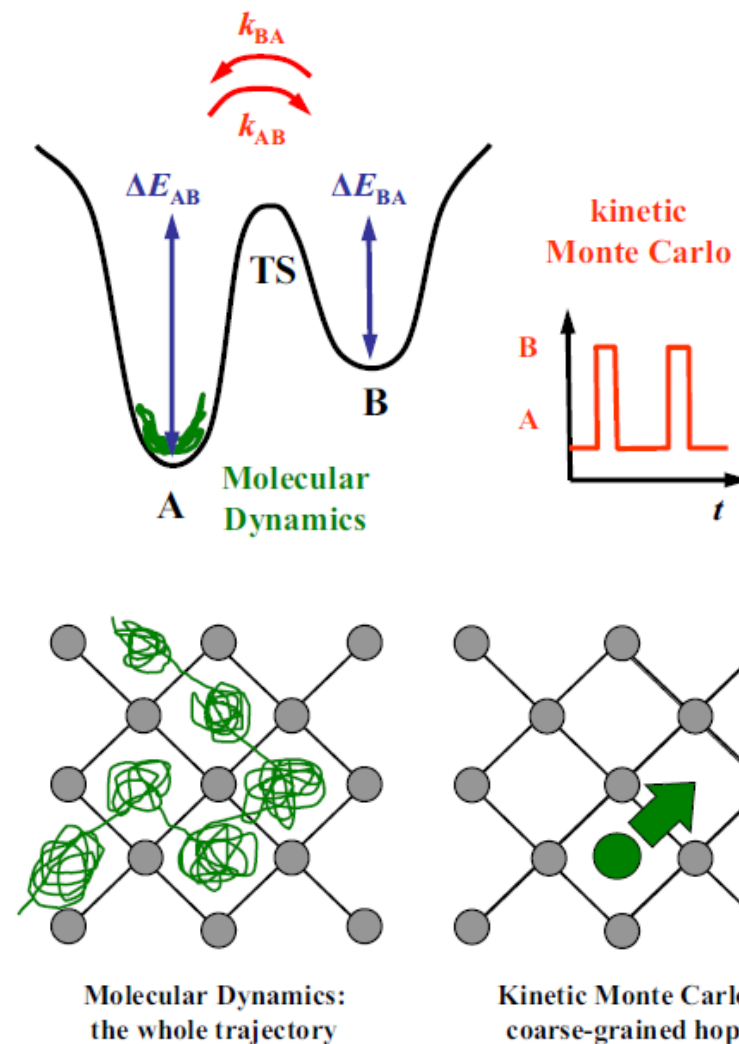


DFT - Simulation: Periodic boundary approach: H₂ oxidation over Pt(111)

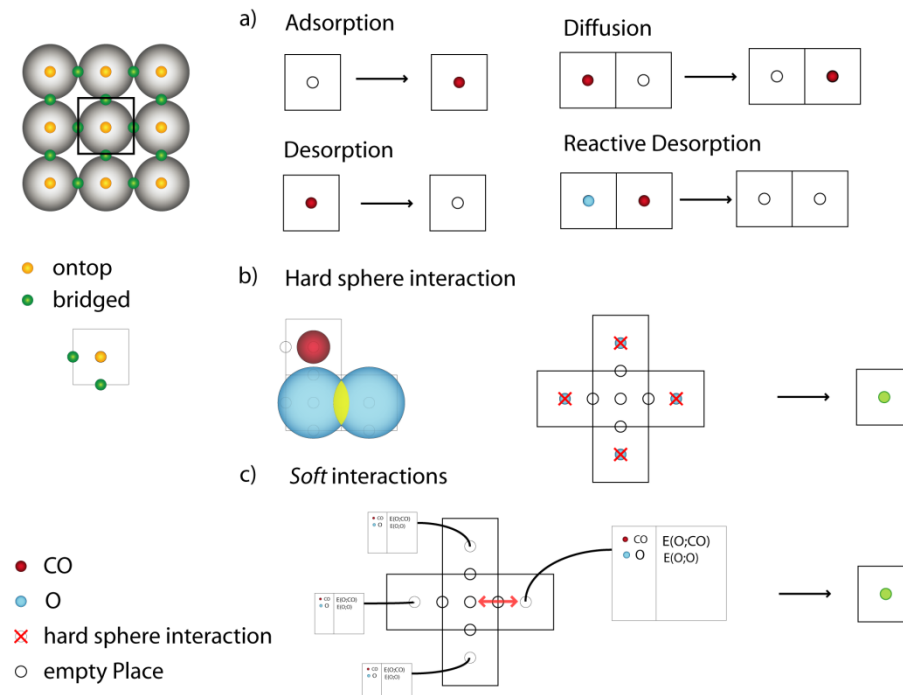


J.A. Keith, J. Anton, T.Jacob. Chapter 1 in Modeling Heterogeneous Catalytic Reactions. O. Deutschmann (Ed.), 2011

Molecular Dynamics vs. Monte Carlo Simulations

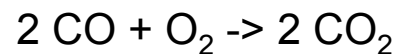
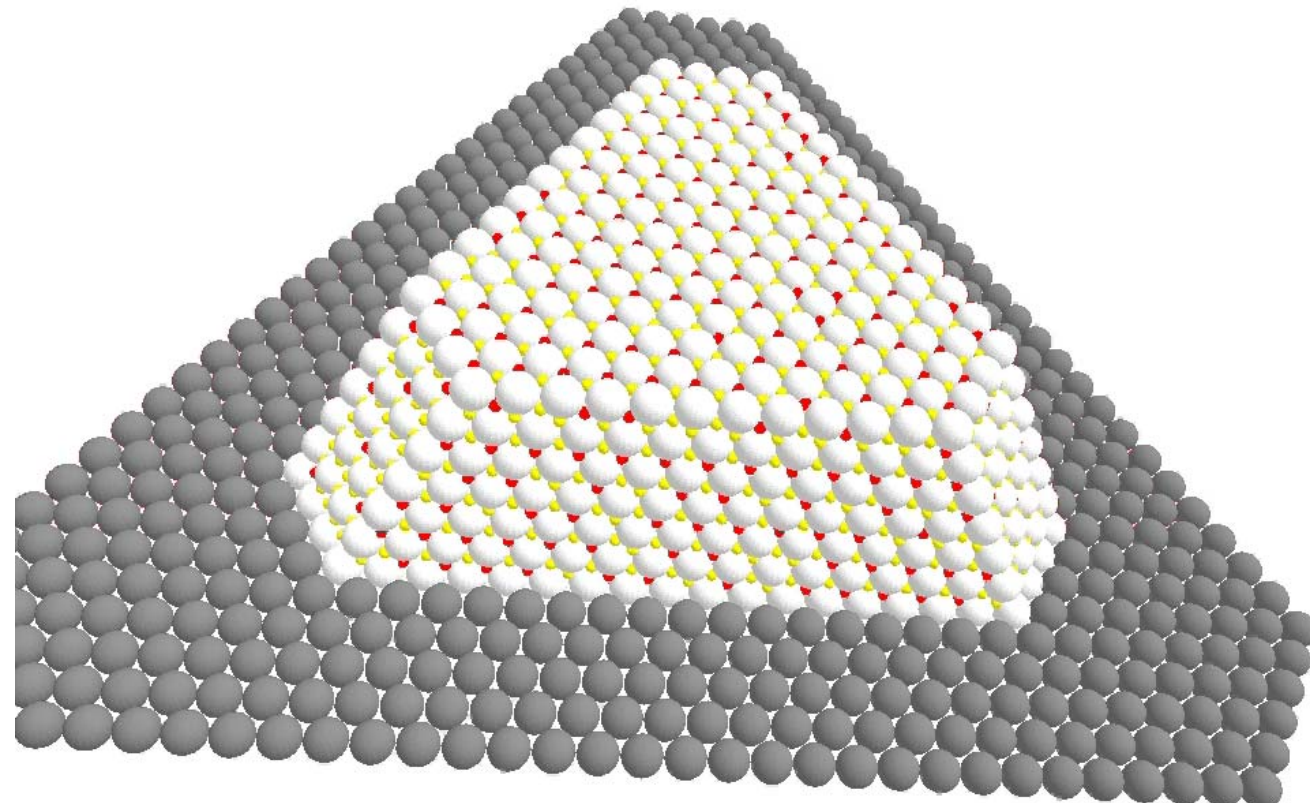


Formulation of reaction scheme



K. Reuter, Chapter 2 (left) and L. Kunz et al., Chapter 4 (right) in Modeling Heterogeneous Catalytic Reactions. O. Deutschmann (Ed.), 2011

Kinetic Monte Carlo Simulation of surface reactions and diffusion: CO oxidation on Pt nanoparticle



CO: blue O: red

Catalyst atom (Pt): white

Washcoat molecule (Al_2O_3): grey

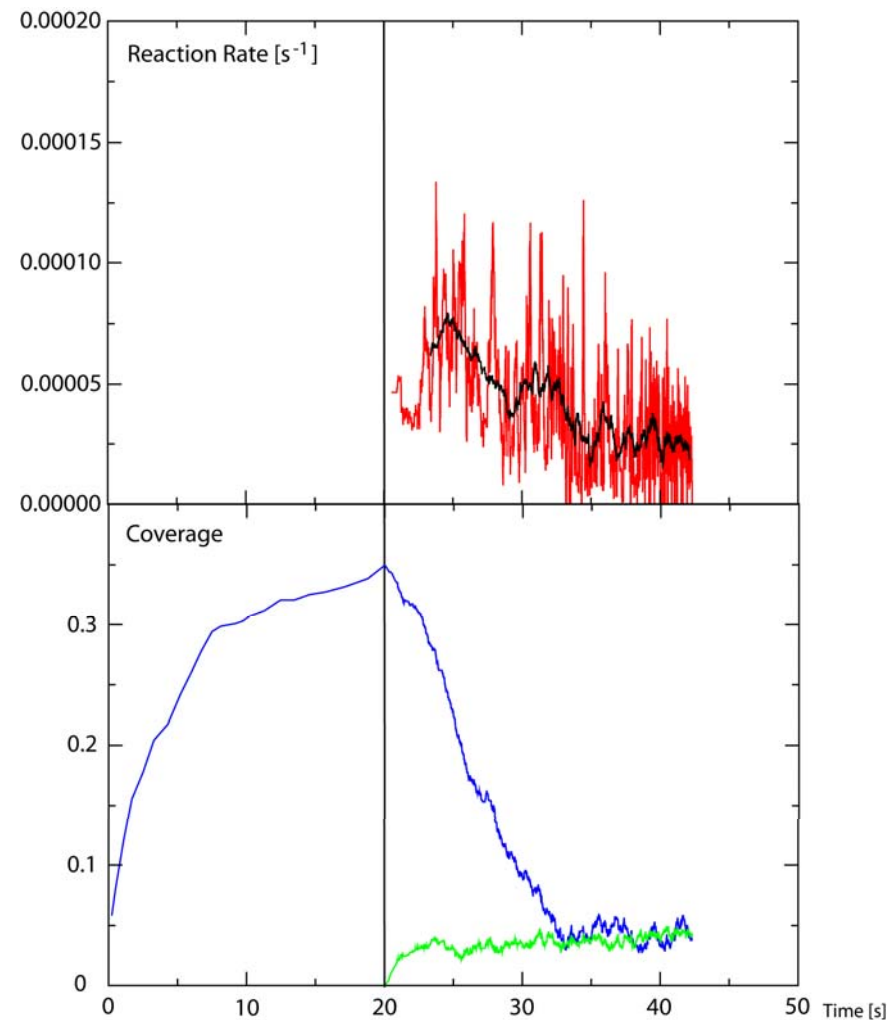
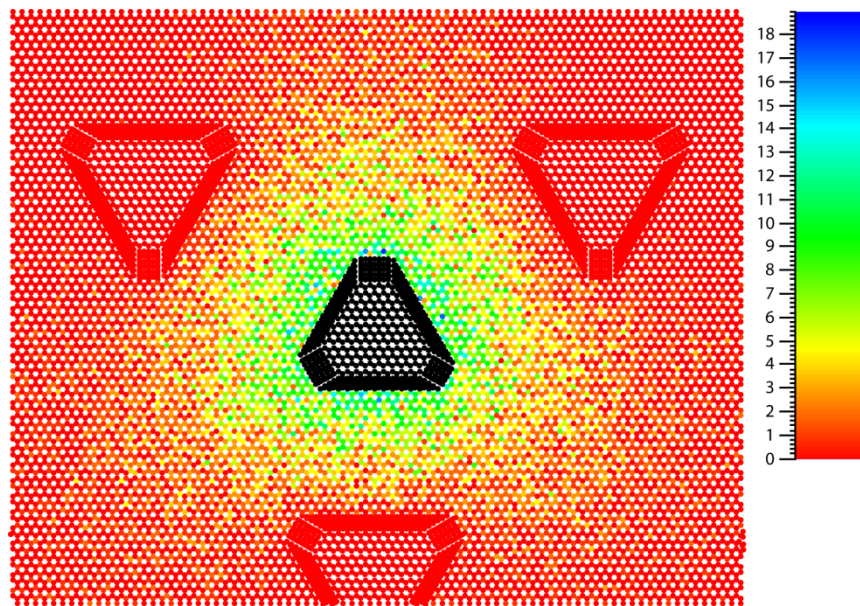
Adsorption sites: yellow

L. Kunz et al., Chapter 4 in *Modeling Heterogeneous Catalytic Reactions*. O. Deutschmann (Ed.), 2011

Kinetic Monte Carlo Simulation of surface reactions and diffusion: CO oxidation on Pt nanoparticle

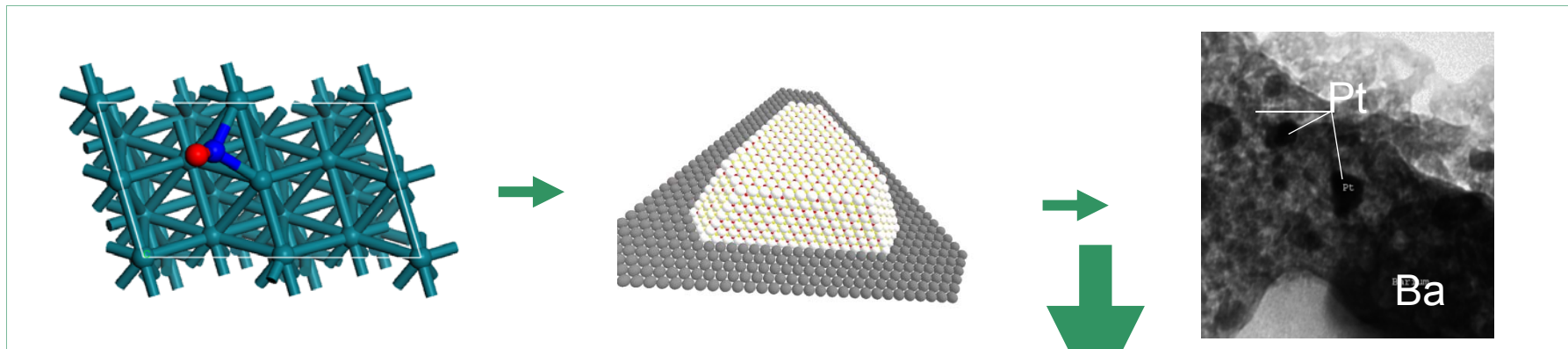
Results of simulations:

- coverages over time on each facet
- reaction rates of each process
- number of times each process was used



L. Kunz et al., Chapter 4 in Modeling Heterogeneous Catalytic Reactions. O. Deutschmann (Ed.), 2011

Modeling heterogeneous reactions: Molecular picture leads to mechanistic model



Surface coverage

$$\Theta_i = \frac{c_i \sigma_i}{\Gamma} \quad \frac{\partial \Theta_i}{\partial t} = \frac{\dot{s}_i M_i}{\Gamma}$$

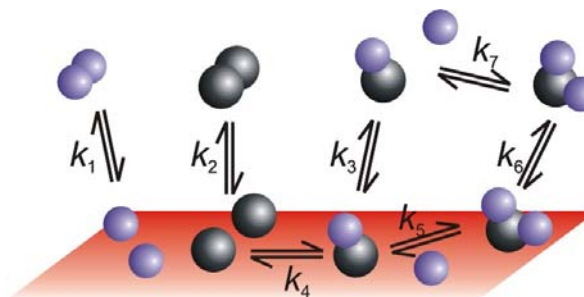
Surface reaction rate

$$\dot{s}_i = \sum_{k \in R} \nu_{ik} k_{f_k} \prod_{j \in S} c_j^{\nu'_{jk}}$$

Rate expression

$$k_{f_k} = A_k T^{\beta_k} \exp\left[\frac{-E_{a_k}}{RT}\right] \prod_{i=1}^{N_s} \Theta_i^{\mu_{i_k}} \exp\left[\frac{\varepsilon_{i_k} \Theta_i}{RT}\right]$$

Locally resolved reaction rates depending on gas-phase concentration and surface coverages



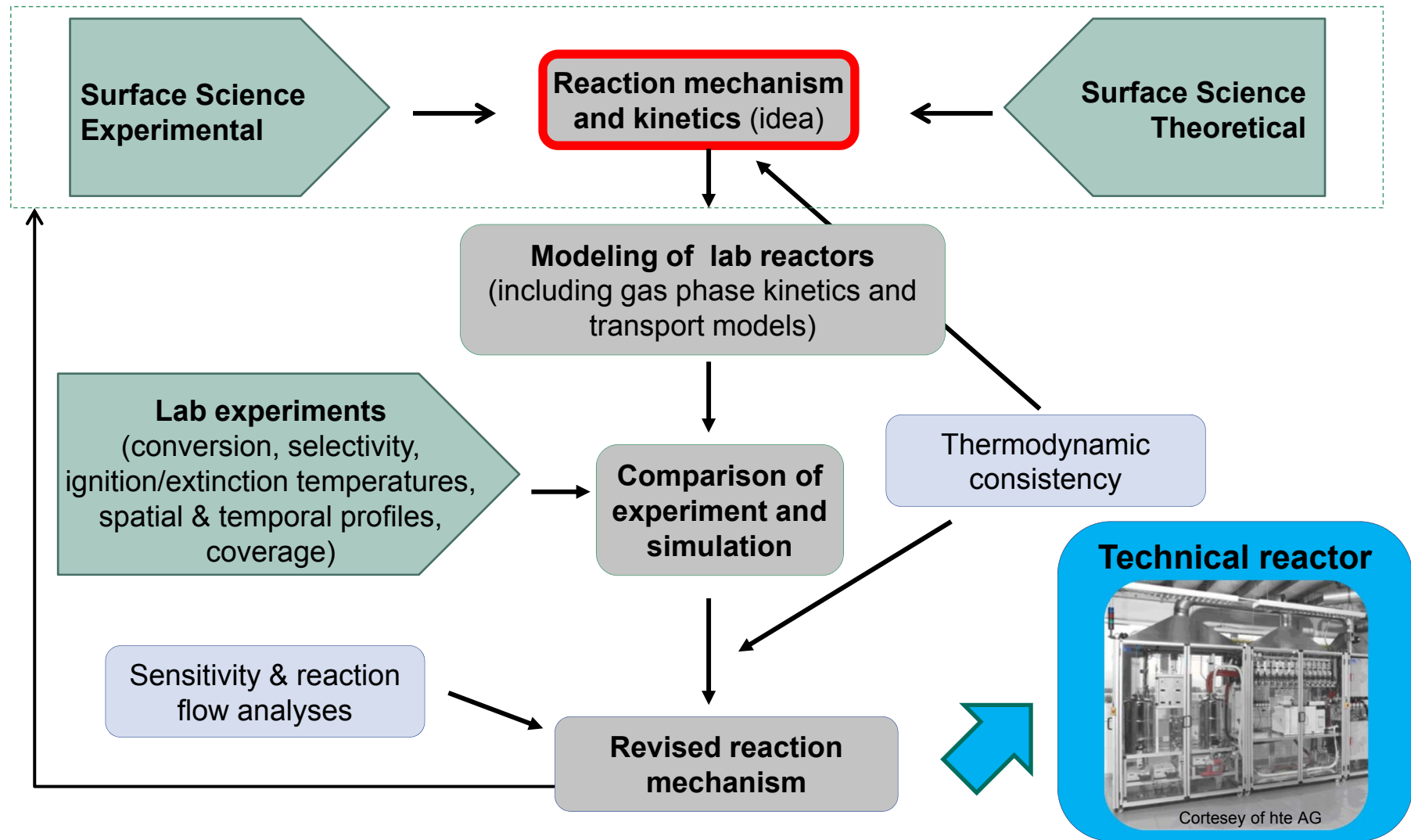
O. Deutschmann. Chapter 6.6 in
Handbook of Heterogeneous Catalysis, 2007

Proposed surface reaction mechanism for three-way catalyst: Mean field approximation

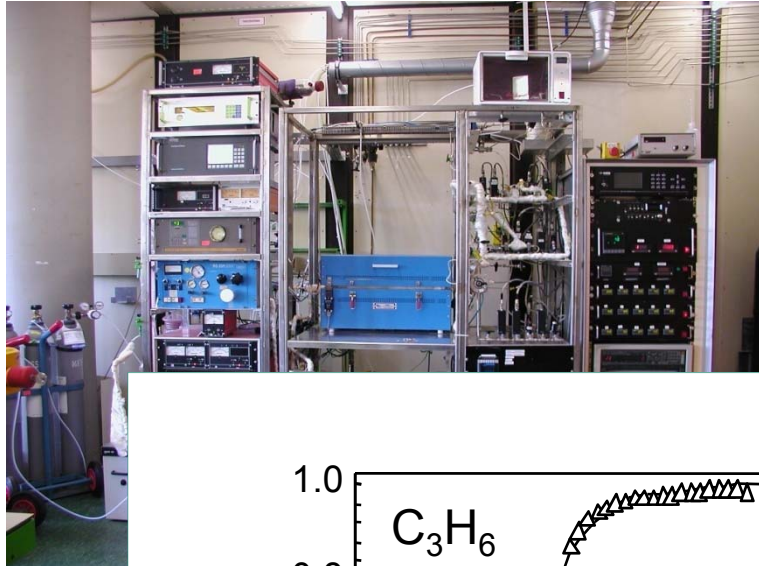
	A (mole, cm, s)	E_a (kJ/mol)				
Adsorption/desorption reactions						
$C_3H_6 + Pt(s) + Pt(s) \rightarrow C_3H_6(s)$	$S^0 = 0.98$		$C_2H_3(s) + O(s) \rightarrow CH_3CO(s) + Pt(s)$	3.7×10^{19}	62.3	
$C_3H_6(s) \rightarrow Pt(s) + Pt(s) + C_3H_6$	3.7×10^{12}	74.4	$CH_3CO(s) + Pt(s) \rightarrow C_2H_3(s) + O(s)$	7.9×10^{20}	191.4	$+60\Theta_{O(s)}$
$C_3H_6 + Pt(s) + O(s) \rightarrow C_3H_5(s) + OH(s)$	$S^0 = 0.05$		$CH_3(s) + CO(s) \rightarrow CH_3CO(s) + Pt(s)$	3.7×10^{21}	82.9	
$\mu(\Theta_{Pt(s)}) = -0.9$			$CH_3CO(s) + Pt(s) \rightarrow CH_3(s) + CO(s)$	1.8×10^{23}	6.1	$+33\Theta_{CO(s)}$
$C_3H_5(s) + OH(s) \rightarrow O(s) + Pt(s) + C_3H_6$	3.7×10^{21}	31.0	$CH_3(s) + O(s) \rightarrow OH(s) + CH_2(s)$	3.7×10^{21}	36.6	
$CH_4 + Pt(s) + Pt(s) \rightarrow CH_3(s) + H(s)$	$S^0 = 0.01$		$OH(s) + CH_2(s) \rightarrow CH_3(s) + O(s)$	2.3×10^{22}	26.0	
$O_2 + Pt(s) + Pt(s) \rightarrow O(s) + O(s)$	$S^0 = 0.07$		$CH_2(s) + O(s) \rightarrow OH(s) + CH(s)$	3.7×10^{21}	25.1	
$O(s) + O(s) \rightarrow Pt(s) + Pt(s) + O_2$	3.2×10^{21}	224.7	$OH(s) + CH(s) \rightarrow CH_2(s) + O(s)$	1.2×10^{21}	26.8	
			$CH(s) + O(s) \rightarrow OH(s) + C(s)$	3.7×10^{21}	25.1	
			$OH(s) + C(s) \rightarrow CH(s) + O(s)$	1.9×10^{21}	214.2	
$H_2 + Pt(s) + Pt(s) \rightarrow H(s) + H(s)$	$S^0 = 0.046$		Carbon monoxide oxidation			
			$CO(s) + O(s) \rightarrow CO_2(s) + Pt(s)$	3.7×10^{21}	48.2	
$H(s) + H(s) \rightarrow Pt(s) + Pt(s) + H_2$	2.1×10^{21}	69.1	$CO_2(s) + O(s) \rightarrow OH(s) + OH(s)$	2.5×10^{20}	38.2	
			$CO(s) + OH(s) \rightarrow HCOO(s) + Pt(s)$	3.7×10^{21}	94.2	
$H_2O + Pt(s) \rightarrow H_2O(s)$	$S^0 = 0.75$		$HCOO(s) + Pt(s) \rightarrow CO(s) + OH(s)$	1.3×10^{21}	0.9	
$H_2O(s) \rightarrow Pt(s) + H_2O$	5.0×10^{13}	49.2	$HCOO(s) + O(s) \rightarrow OH(s) + CO_2(s)$	3.7×10^{21}	0.0	
$CO_2 + Pt(s) \rightarrow CO_2(s)$	$S^0 = 0.005$		$OH(s) + CO_2(s) \rightarrow HCOO(s) + O(s)$	2.8×10^{21}	151.1	
$CO_2(s) \rightarrow Pt(s) + CO_2$	3.6×10^{10}	23.7	$HCOO(s) + Pt(s) \rightarrow H(s) + CO_2(s)$	3.7×10^{21}	0.0	
$CO + Pt(s) \rightarrow CO(s)$	$S^0 = 0.84$		$H(s) + CO_2(s) \rightarrow HCOO(s) + Pt(s)$	2.8×10^{21}	90.1	
$CO(s) \rightarrow Pt(s) + CO$	2.1×10^{13}	136.2	Reactions of hydroxyl species			
			$CO(s) + Pt(s) \rightarrow C(s) + O(s)$			
$NO + Pt(s) \rightarrow NO(s)$	$S^0 = 0.85$		Reactions of NO and NO_2			
$NO(s) \rightarrow Pt(s) + NO$	2.1×10^{12}	80.7	$NO(s) + Pt(s) \rightarrow N(s) + O(s)$	5.0×10^{20}	107.8	
$NO_2 + Pt(s) \rightarrow NO_2(s)$	$S^0 = 0.9$		$N(s) + O(s) \rightarrow NO(s) + Pt(s)$	1.0×10^{21}	122.6	
$NO_2(s) \rightarrow Pt(s) + NO_2$	1.4×10^{13}	61.0	$O(s) + NO \rightarrow NO_2(s)$	2.0×10^{13}	111.3	
$N_2O + Pt(s) \rightarrow N_2O(s)$	$S^0 = 0.025$					
$N_2O(s) \rightarrow Pt(s) + N_2O$	1.2×10^{10}	0.7	$NO_2(s) \rightarrow O(s) + NO$	3.3×10^{14}	115.5	
$N(s) + N(s) \rightarrow Pt(s) + Pt(s) + N_2$	3.7×10^{21}	113.9	$N(s) + NO(s) \rightarrow N_2O(s) + Pt(s)$	1.0×10^{21}	90.9	
			$N_2O(s) + Pt(s) \rightarrow N(s) + NO(s)$	2.9×10^{24}	133.1	
			$O(s) + NO(s) \rightarrow NO_2(s) + Pt(s)$	1.3×10^{17}	133.0	$+75\Theta_{CO(s)}$
Surface reactions						
Propylene oxidation						
$C_3H_6(s) \rightarrow C_3H_5(s) + H(s)$	1.0×10^{13}	75.4	$NO_2(s) + Pt(s) \rightarrow O(s) + NO(s)$	8.1×10^{18}	58.0	
$C_3H_5(s) + H(s) \rightarrow C_3H_6(s)$	3.7×10^{21}	48.8	$H(s) + NO(s) \rightarrow OH(s) + N(s)$	1.2×10^{21}	25.0	
$C_3H_5(s) + Pt(s) \rightarrow C_2H_3(s) + CH_2(s)$	3.7×10^{21}	108.2				$+80\Theta_{CO(s)}$
$C_2H_3(s) + CH_2(s) \rightarrow C_3H_5(s) + Pt(s)$	3.7×10^{21}	3.3	$OH(s) + N(s) \rightarrow H(s) + NO(s)$	6.4×10^{21}	99.9	
$C_2H_3(s) + Pt(s) \rightarrow CH_3(s) + C(s)$	3.7×10^{21}	46.0	$NO_2(s) + H(s) \rightarrow OH(s) + NO(s)$	3.9×10^{21}	20.0	
$CH_3(s) + C(s) \rightarrow C_2H_3(s) + Pt(s)$	3.7×10^{21}	46.5	$OH(s) + NO(s) \rightarrow NO_2(s) + H(s)$	6.1×10^{22}	175.3	
$CH_3(s) + Pt(s) \rightarrow CH_2(s) + H(s)$	1.3×10^{22}	70.4				
$CH_2(s) + H(s) \rightarrow CH_3(s) + Pt(s)$	2.9×10^{22}	0.4				
$CH_2(s) + Pt(s) \rightarrow CH(s) + H(s)$	7.0×10^{22}	59.2				
$CH(s) + H(s) \rightarrow CH_2(s) + Pt(s)$	8.1×10^{21}	0.7				
$CH(s) + Pt(s) \rightarrow C(s) + H(s)$	3.1×10^{22}	0.0				
$C(s) + H(s) \rightarrow CH(s) + Pt(s)$	5.8×10^{21}	128.9				
$C_3H_5(s) + O(s) \rightarrow C_3H_4(s) + OH(s)$	5.0×10^{21}	70.0				
$C_3H_4(s) + 4O(s) + 2Pt(s) \rightarrow 3C(s) + 4OH(s)$	2.6×10^{64}	0.0 ^a				

D. Chatterjee, O. Deutschmann, J. Warnatz. Faraday Discuss. 119 (2001) 371
 J. Koop, O. Deutschmann. Appl. Catal. B: Env. 91 (2009) 47

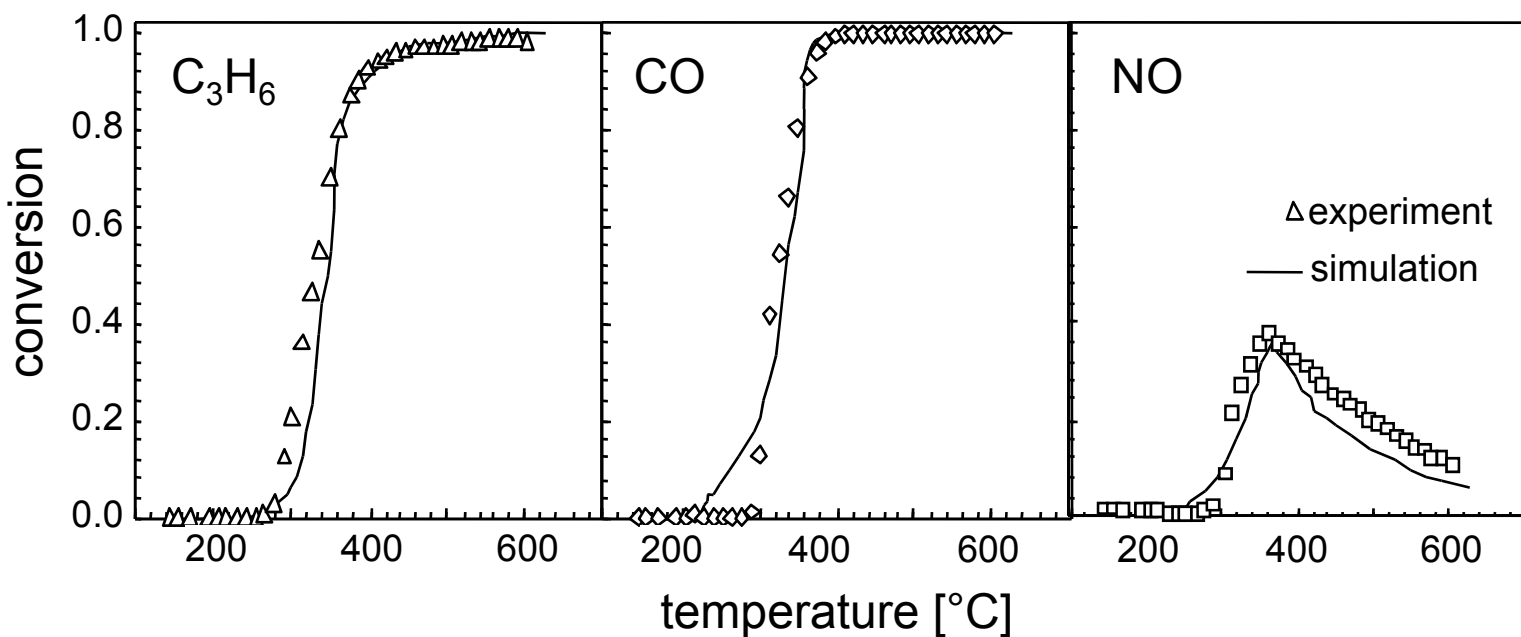
Development of micro kinetic models for simulations of catalytic reactors



Conversion of a synthetic exhaust in a real three way catalyst: Steady-state conditions



Laboratory experiments at well-defined conditions, e.g. differentially operated reactors (no gradients), are used for first model evaluation

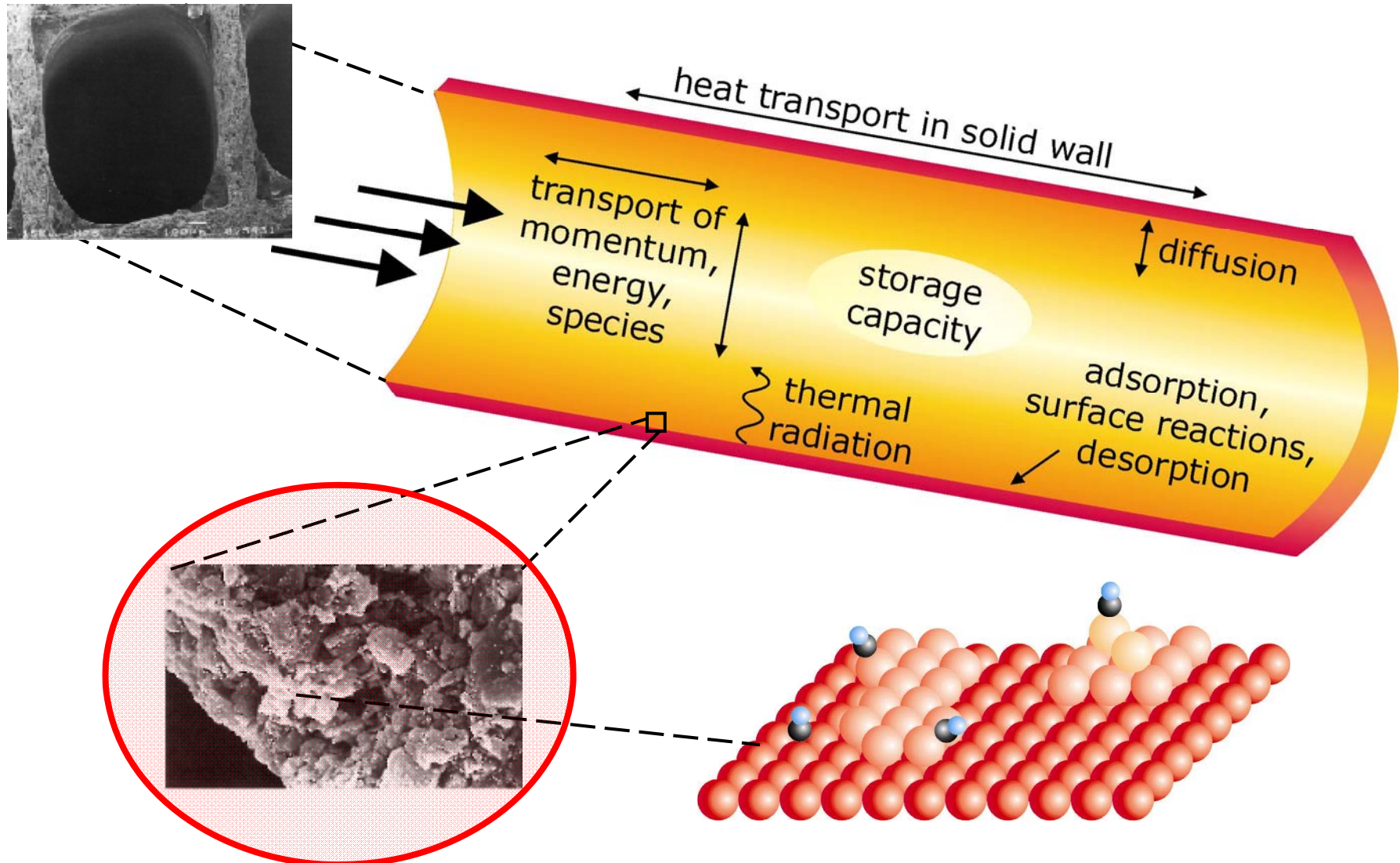


Kinetics – Interaction between Reaction, Mass and Heat Transfer: Outline

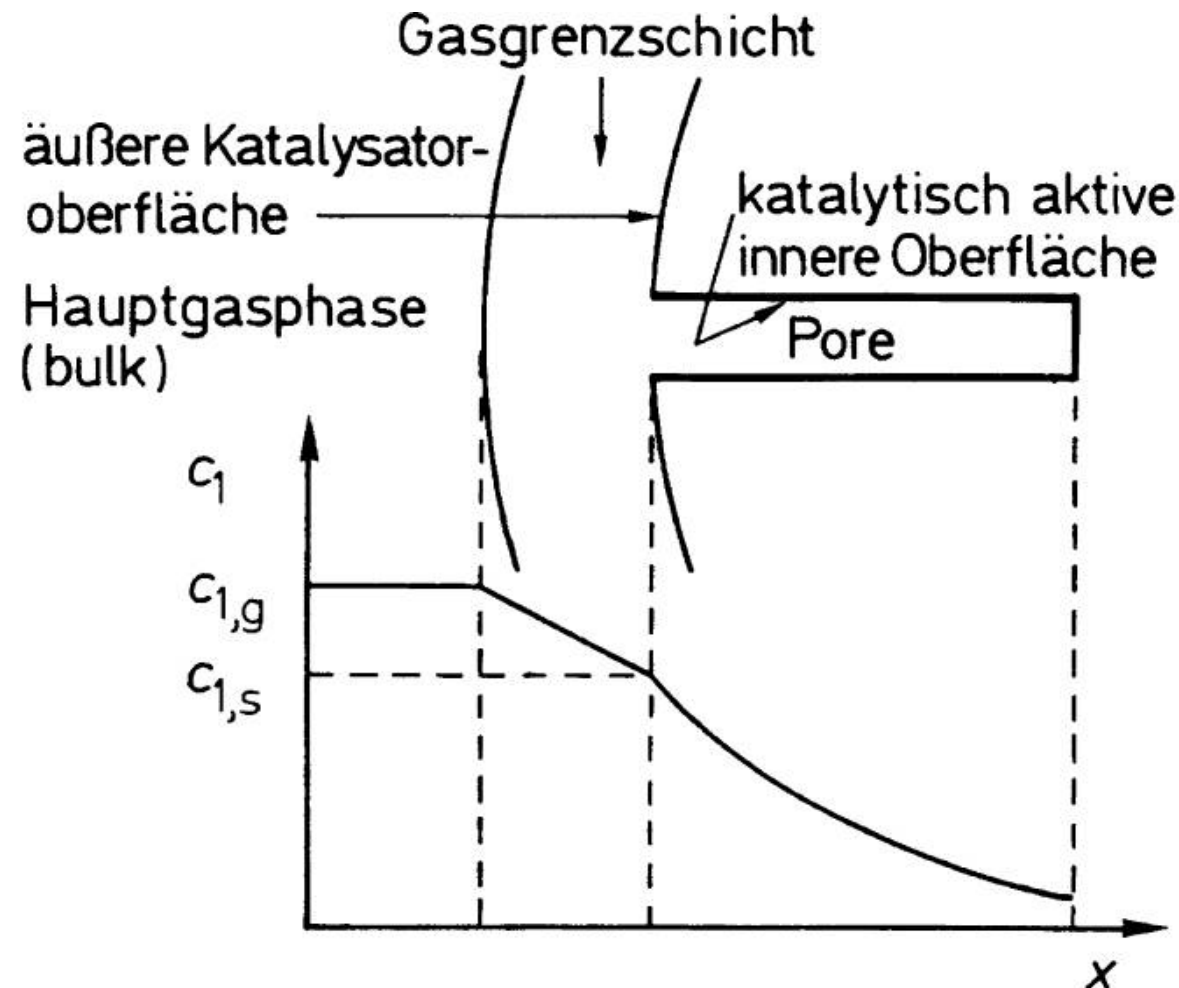


1. Microkinetics of reactions on the catalytic surface
2. **Transport and reactions in porous media (internal diffusion)**
3. Reactive flow and external diffusion
4. Gas-phase chemistry
5. Transient processes and heat transport

Coupling of internal diffusion and reaction

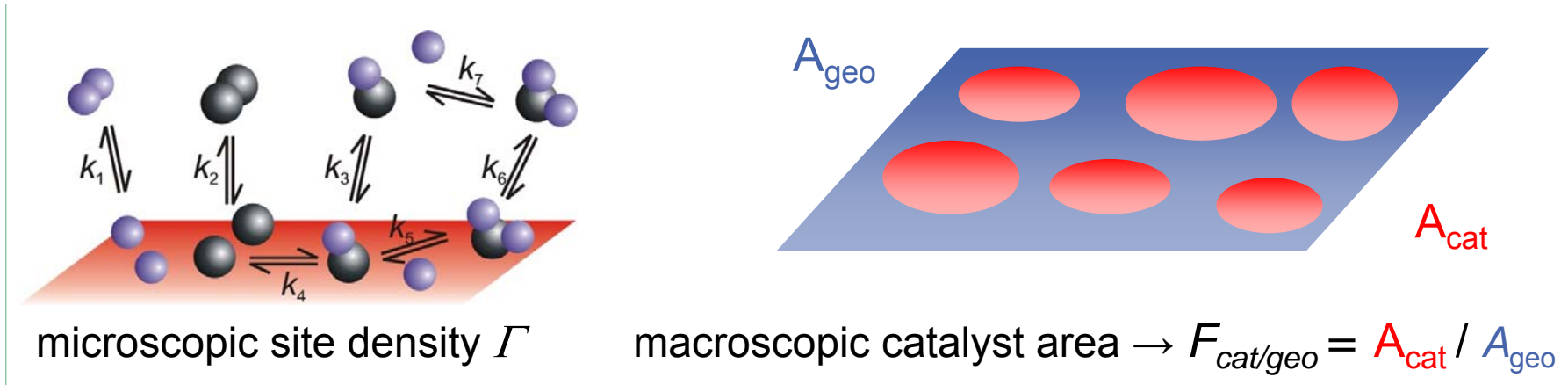


Stofftransporthemmung für einen porösen Katalysator

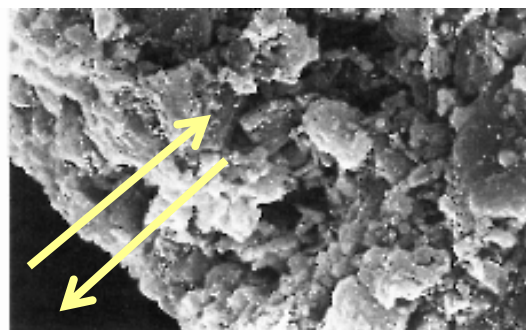


© 2006 Wiley-VCH, Weinheim
 Baerns / Technische Chemie
 ISBN: 3-527-31000-2 Abb-04-03-01

Coupling of surface reaction rate and flow field - Modeling transport limitation of reaction rate



$$j_{i,s} = F_{\text{cat/geo}} \eta_i M_i \dot{s}_i$$

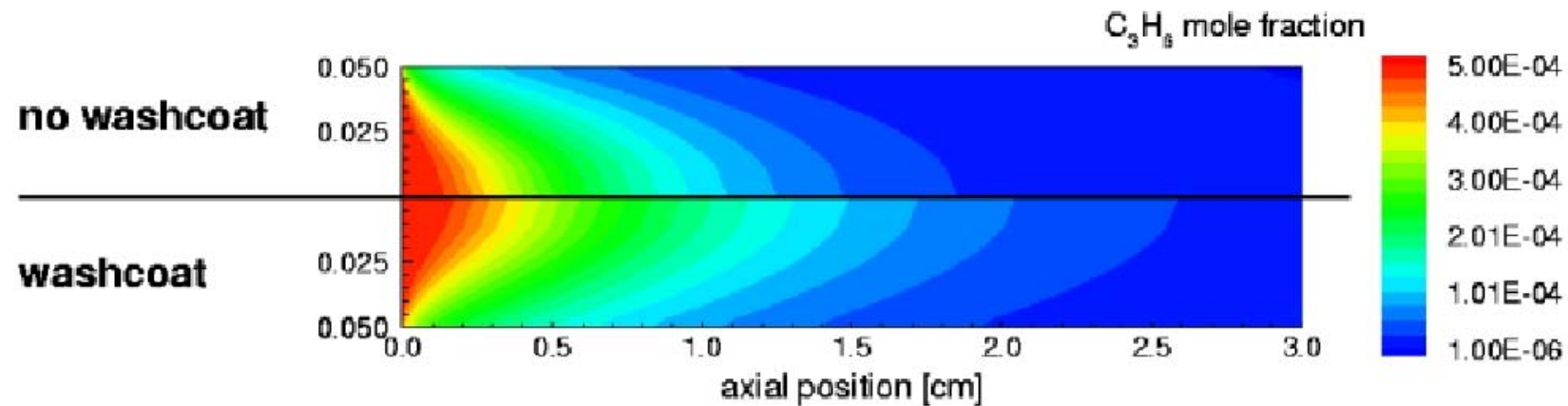


Effectiveness factor

$$\eta_i = \frac{\tanh(\Phi_i)}{\Phi_i}$$

$$\Phi_i = L \sqrt{\frac{\dot{s}_i \gamma}{D_{\text{eff},i} c_{i,0}}}$$

HC-SCR on Pt/Al₂O₃: Impact of washcoat transport limitation on conversion

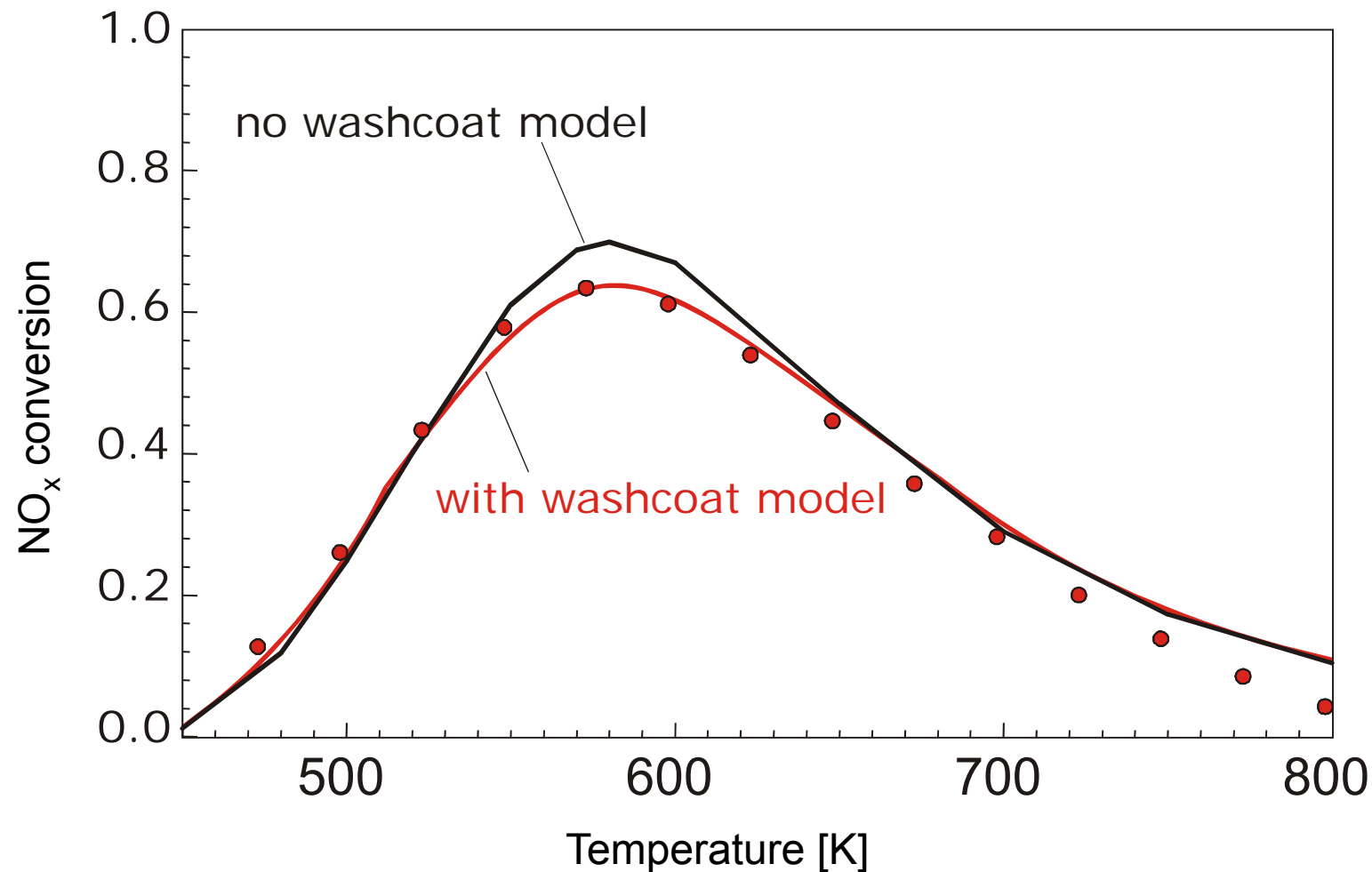


Conditions:

500 ppm C₃H₆, 500 ppm NO, 5 Vol.-% O₂, in N₂, 6 slpm, $u = 0.63$ m/s; $T = 570$ K

D. Chatterjee, O. Deutschmann, 2000

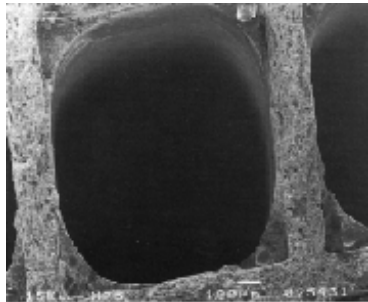
NO oxidation on Pt/Al₂O₃: Impact of washcoat transport limitation on conversion



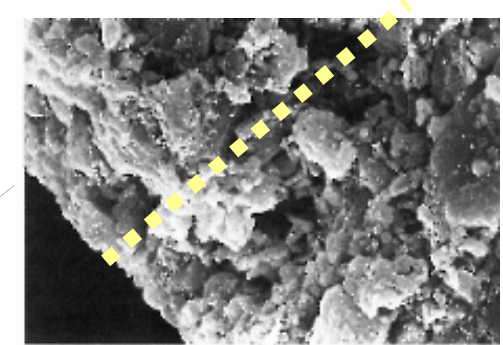
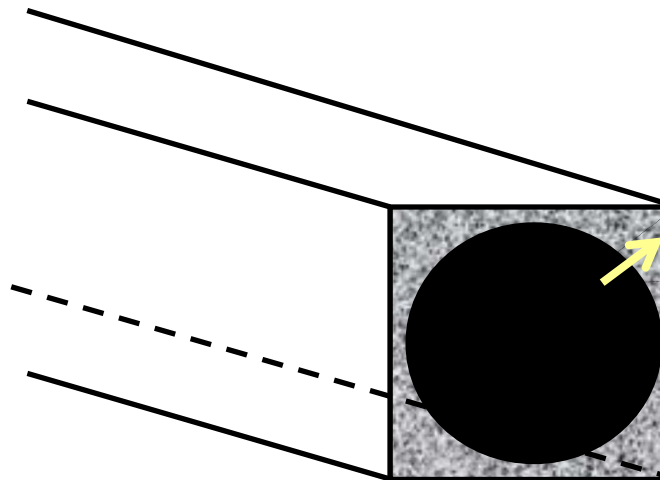
Conditions: 500 ppm NO, 1 Vol.-% O₂ in N₂

D. Chatterjee, O. Deutschmann, 2000

Modeling reaction and transport in porous media: 1d reaction-diffusion equations



Washcoat is treated as continuum



Discretization of the washcoat
normal to the gas-phase-
washcoat boundary at each
radial and axial position

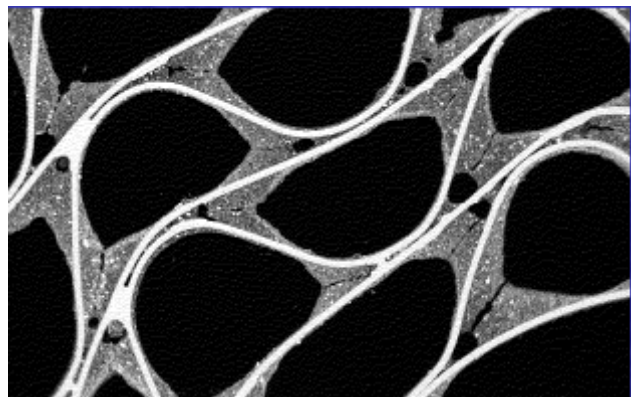
$$D_{\text{eff},i} \frac{\partial c_i^W}{\partial r} + \gamma M_i \dot{s}_i = 0 \quad (i = 1, \dots, N_g)$$

$$\dot{s}_i = \sum_{k=1}^{K_s} v_{ik} k_{f_k} \prod_{j=1}^{N_g + N_s} c_j^{v_{jk}}$$

$$\dot{s}_i = 0 \quad (i = N_g + 1, \dots, N_g + N_s)$$

$$j_i^{\text{surf}} = j_{r,i}^W(r=0) = -D_{\text{eff},i} \left. \frac{\partial c_i^W}{\partial r} \right|_{r=0}$$

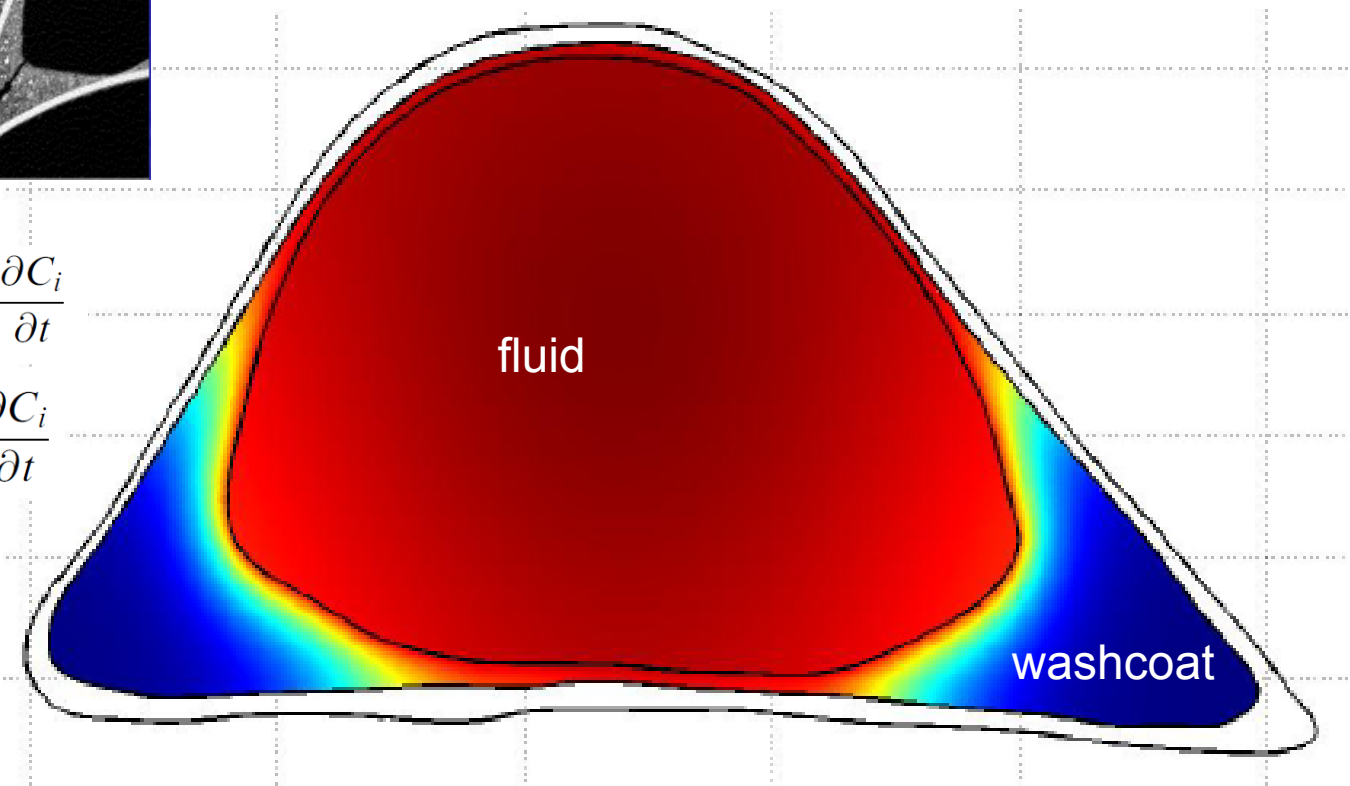
Understanding the interaction of diffusion and reaction: Potential for reduced catalyst costs by zone coating



Reactant concentration in a complex shaped channel

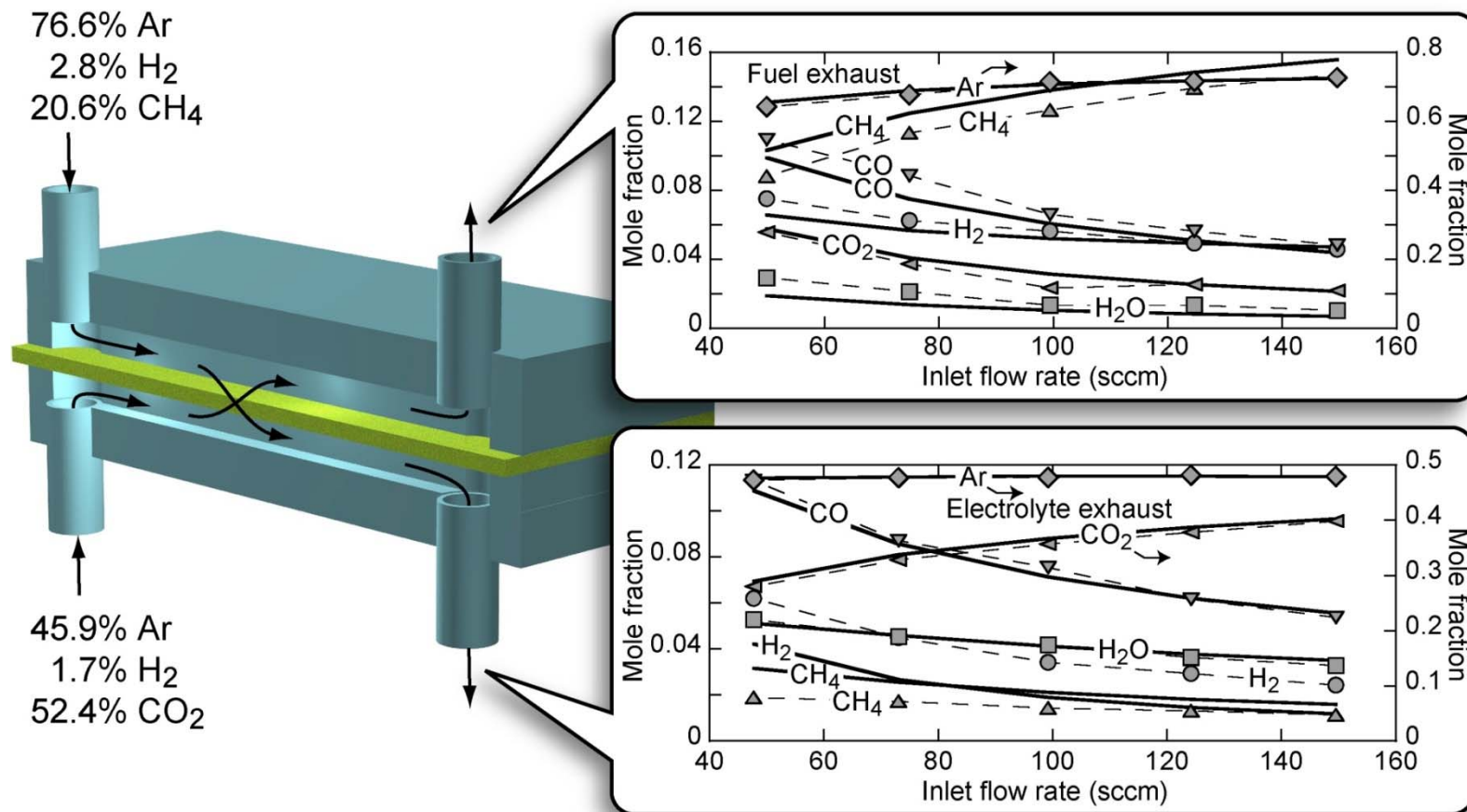
$$\nabla \cdot (D_i \nabla C_i) - \nabla \cdot (v C_i) = \frac{\partial C_i}{\partial t}$$

$$(D_{\text{eff}})_i \nabla^2 C_i - (-R_i) = \varepsilon \frac{\partial C_i}{\partial t}$$



R.E. Hayes, B. Liu, M. Votsmeier. Chem. Eng. Sci. 60 (2005) 2037.

Experimental set-up for the evaluation of transport and reaction kinetics in a Ni/YSZ membrane: CH₄ dry reforming

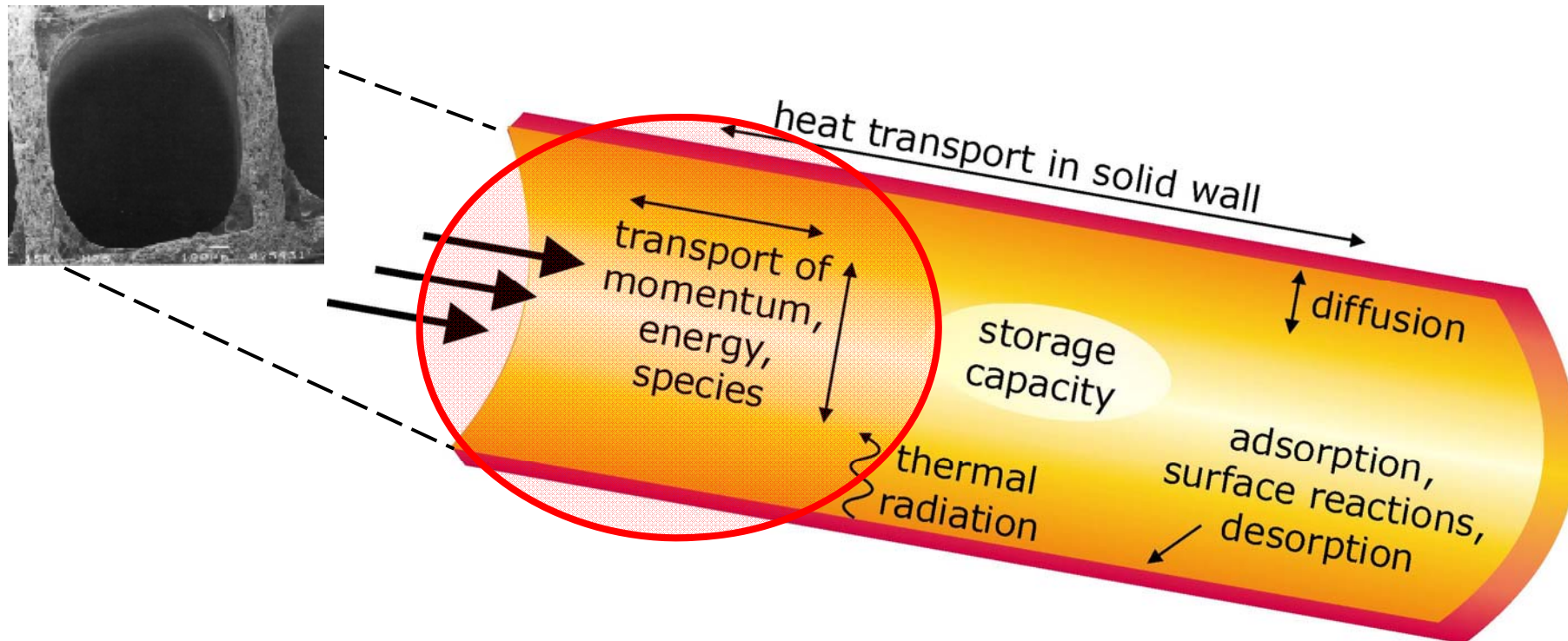


Kinetics – Interaction between Reaction, Mass and Heat Transfer: Outline



1. Microkinetics of reactions on the catalytic surface
2. Transport and reactions in porous media (internal diffusion)
3. **Reactive flow and external diffusion**
4. Gas-phase chemistry
5. Transient processes and heat transport

Modeling the flow in the channel



General:

Transient 3D Navier-Stokes equations + species mass balances + heat balances

Simplifying assumptions often made:

No direct transients, cylindrical channel, no axial (and radial) diffusion

Most general approach for modeling laminar flow fields: Transient 3D Navier-Stokes equations

Total mass

$$\frac{\partial \rho}{\partial t} + \frac{\partial(\rho v_i)}{\partial x_i} = S_m$$

Momentum

$$\frac{\partial(\rho v_i)}{\partial t} + \frac{\partial(\rho v_i v_j)}{\partial x_j} + \frac{\partial p}{\partial x_i} + \frac{\partial \tau_{ij}}{\partial x_j} = \rho g_i$$

$$\tau_{ij} = -\mu \left(\frac{\partial v_i}{\partial x_j} + \frac{\partial v_j}{\partial x_i} \right) + \left(\frac{2}{3} \mu - \kappa \right) \delta_{ij} \frac{\partial v_k}{\partial x_k}$$

Species' mass

$$\frac{\partial(\rho Y_i)}{\partial t} + \frac{\partial(\rho v_j Y_i)}{\partial x_j} + \frac{\partial(j_{i,j})}{\partial x_j} = R_i^{\text{hom}}$$

$$j_{i,j} = -\rho \frac{Y_i}{X_i} D_i^M \frac{\partial X_i}{\partial x_j} - \frac{D_i^T}{T} \frac{\partial T}{\partial x_j}$$

Heat transport

$$\frac{\partial(\rho h)}{\partial t} + \frac{\partial(\rho v_j h)}{\partial x_j} + \frac{\partial j_{q,j}}{\partial x_j} = \frac{\partial p}{\partial t} + v_j \frac{\partial p}{\partial x_j} - \tau_{jk} \frac{\partial v_j}{\partial x_k} + S_h$$

$$j_{q,j} = -\lambda \frac{\partial T}{\partial x_j} + \sum_{i=1}^{N_g} h_i j_{i,j}$$

solid phase

$$\frac{\partial(\rho h)}{\partial t} - \frac{\partial}{\partial x_j} \left(\lambda \frac{\partial T}{\partial x_j} \right) = S_h$$

$$S_{h,\text{ext rad}} = -\varepsilon \sigma (T_{\text{solid}}^4 - T_{\text{ref}}^4) A$$

temperature

$$h = \sum_{i=1}^{N_g} Y_i h_i(T)$$

Equation of state
(perfect gas)

$$p = \frac{\rho R T}{\sum_{i=1}^{N_g} X_i M_i}$$

$$X_i = \frac{1}{\sum_{j=1}^{N_g} Y_j / M_j} \frac{Y_i}{M_i}$$

Model simplification by assuming a cylindrical channel and neglecting axial diffusion: Boundary-layer equations

Total mass flux

$$\frac{\partial(\rho u)}{\partial z} = -\frac{1}{r} \frac{\partial(r\rho v)}{\partial r}$$

Axial momentum flux

$$\frac{\partial(\rho uu)}{\partial z} = -\frac{1}{r} \frac{\partial(r\rho vu)}{\partial r} - \frac{\partial p}{\partial z} + \frac{1}{r} \frac{\partial}{\partial r} \left(\eta r \frac{\partial u}{\partial r} \right) + \rho g_z$$

Enthalpy flux

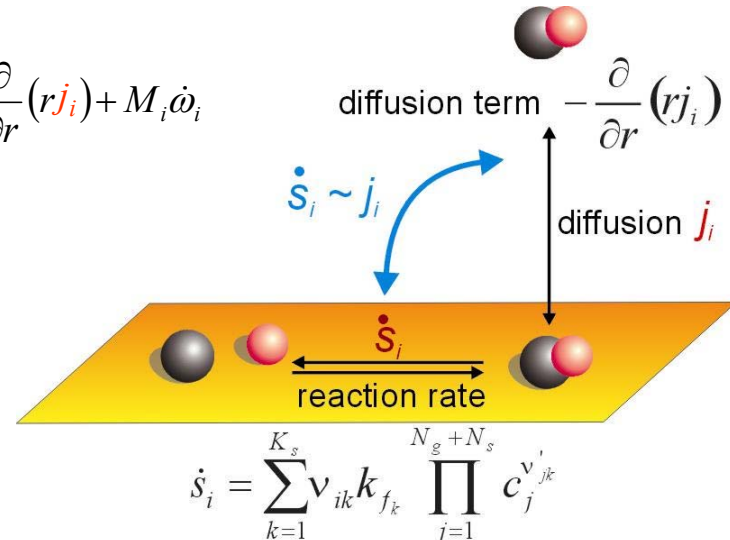
$$\frac{\partial(\rho uh)}{\partial z} = -\frac{1}{r} \frac{\partial(r\rho vh)}{\partial r} + u \frac{\partial p}{\partial z} - \frac{1}{r} \frac{\partial}{\partial r} (rq_r)$$

Species mass flux

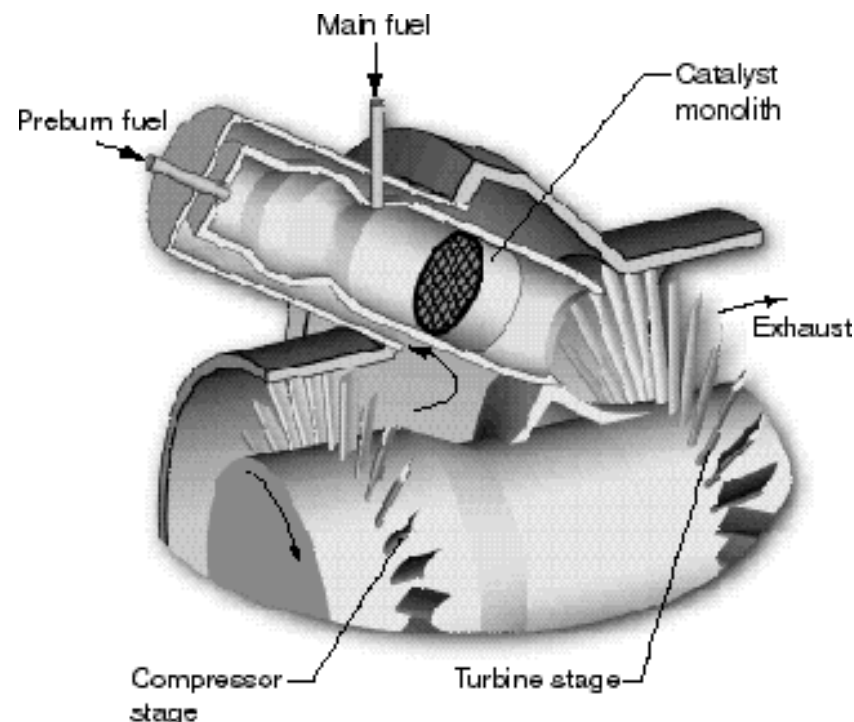
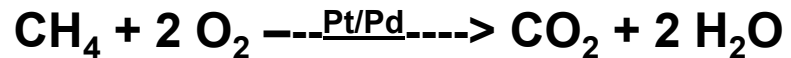
$$\frac{\partial(\rho u Y_i)}{\partial z} = -\frac{1}{r} \frac{\partial(r\rho v Y_i)}{\partial r} - \frac{1}{r} \frac{\partial}{\partial r} (rj_i) + M_i \dot{s}_i$$

Coupling between surface reactions and flow field:

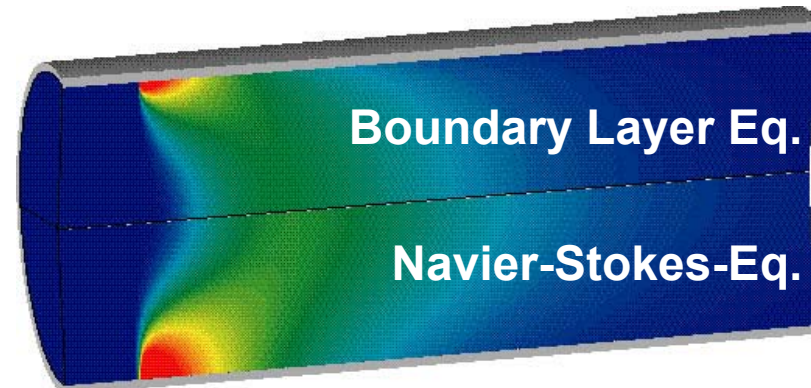
$$j_{i,wall} = F_{\text{cat/geo}} \eta_i M_i \dot{s}_i$$



Catalytic combustion of natural gas in catalytic channel: 2D Navier-Stokes and 2D Boundary layer approach



Picture: Courtesy of Robert J. Kee, Colorado School of Mines



L. L. Raja, R. J. Kee, O. Deutschmann, J. Warnatz, L. D. Schmidt. *Catalysis Today* 59 (2000) 47-60.

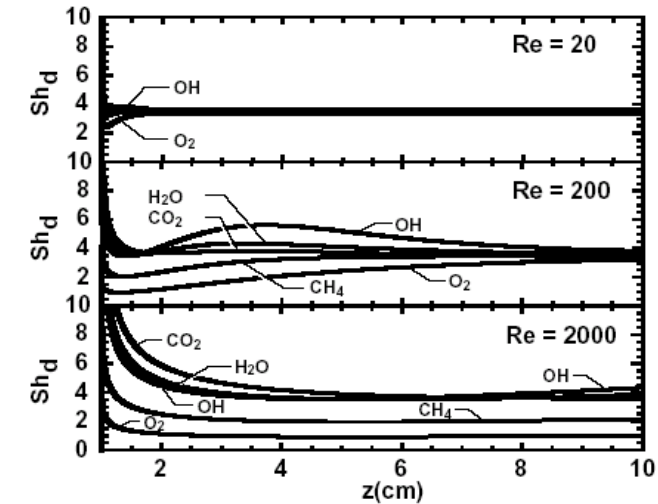
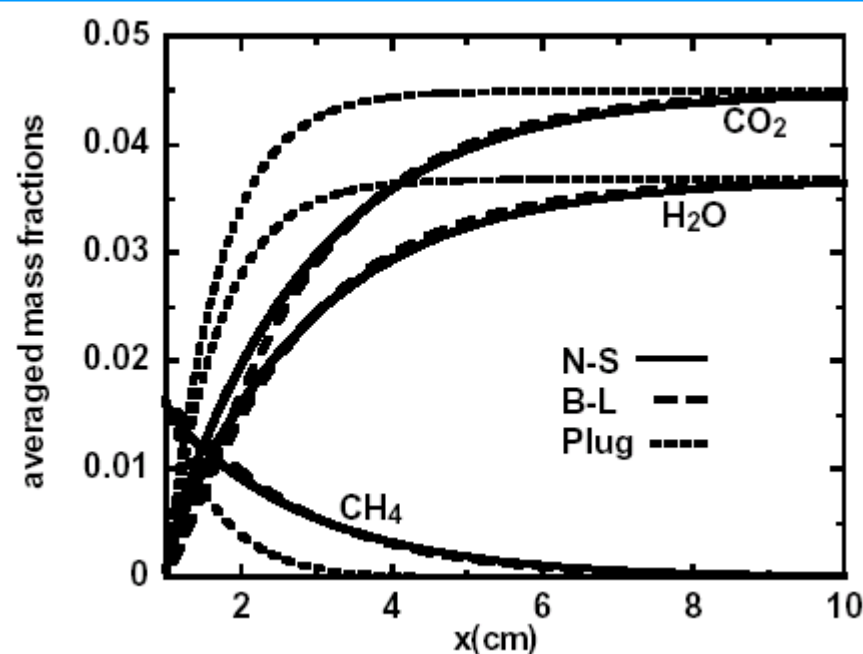
Computed CO concentrations in single monolith channel

⇒ No significant differences

⇒ Axial diffusion can be neglected

Catalytic combustion of natural gas in catalytic channel: 2D Navier-Stokes, 2D Boundary layer, and 1d Plug flow approach

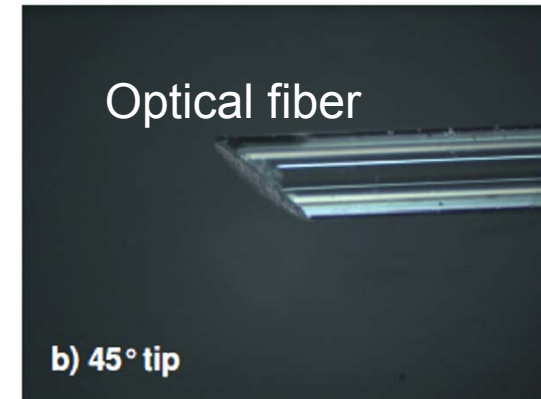
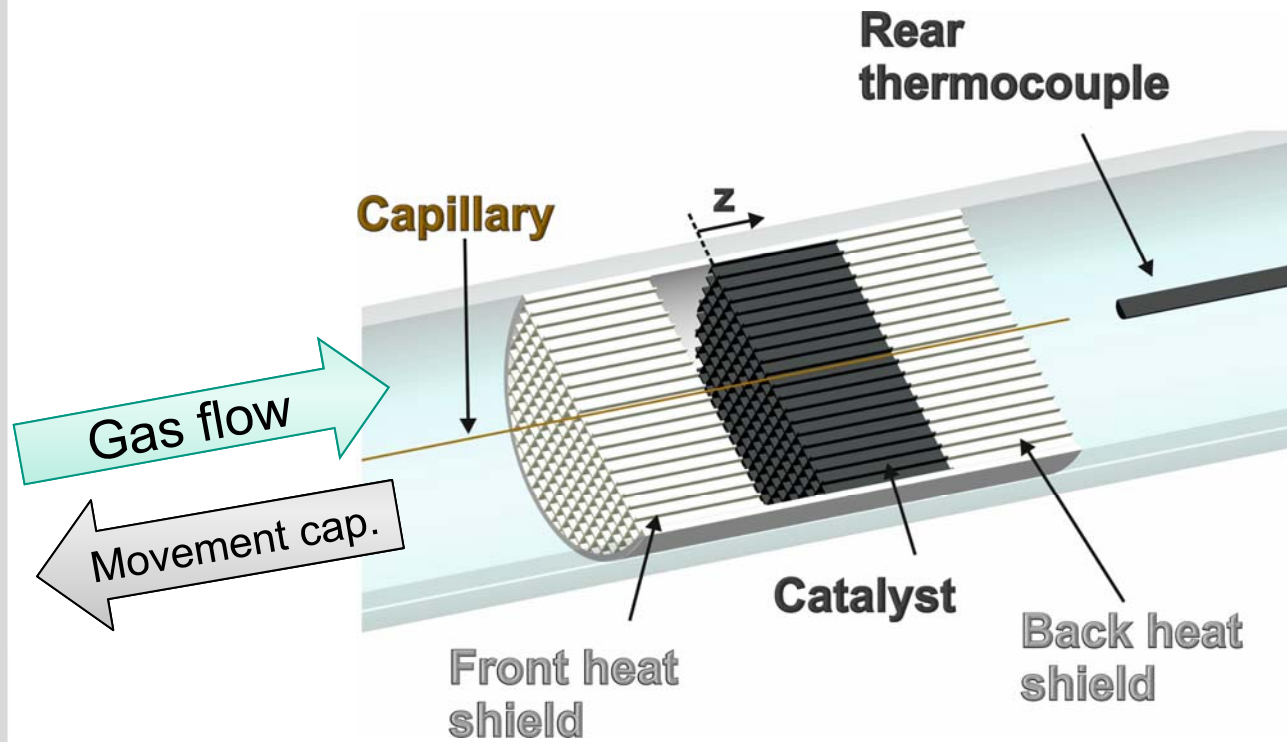
1D – Plug-Flow-Model over estimates conversion



Use of mass transfer coefficient is difficult due to large reaction rate causing strong variation of the Sherwood number

L. L. Raja, R. J. Kee, O. Deutschmann, J. Warnatz, L. D. Schmidt. *Catalysis Today* 59 (2000) 47-60.

In-Situ Sampling Technique



$\frac{A}{A + \text{channel}} = 2,96\%$
A. Donazzi, D. Livio, A. Beretta, G. Groppi, P. Forzatti, Applied Catalysis A: General, 402 (2011) 41.

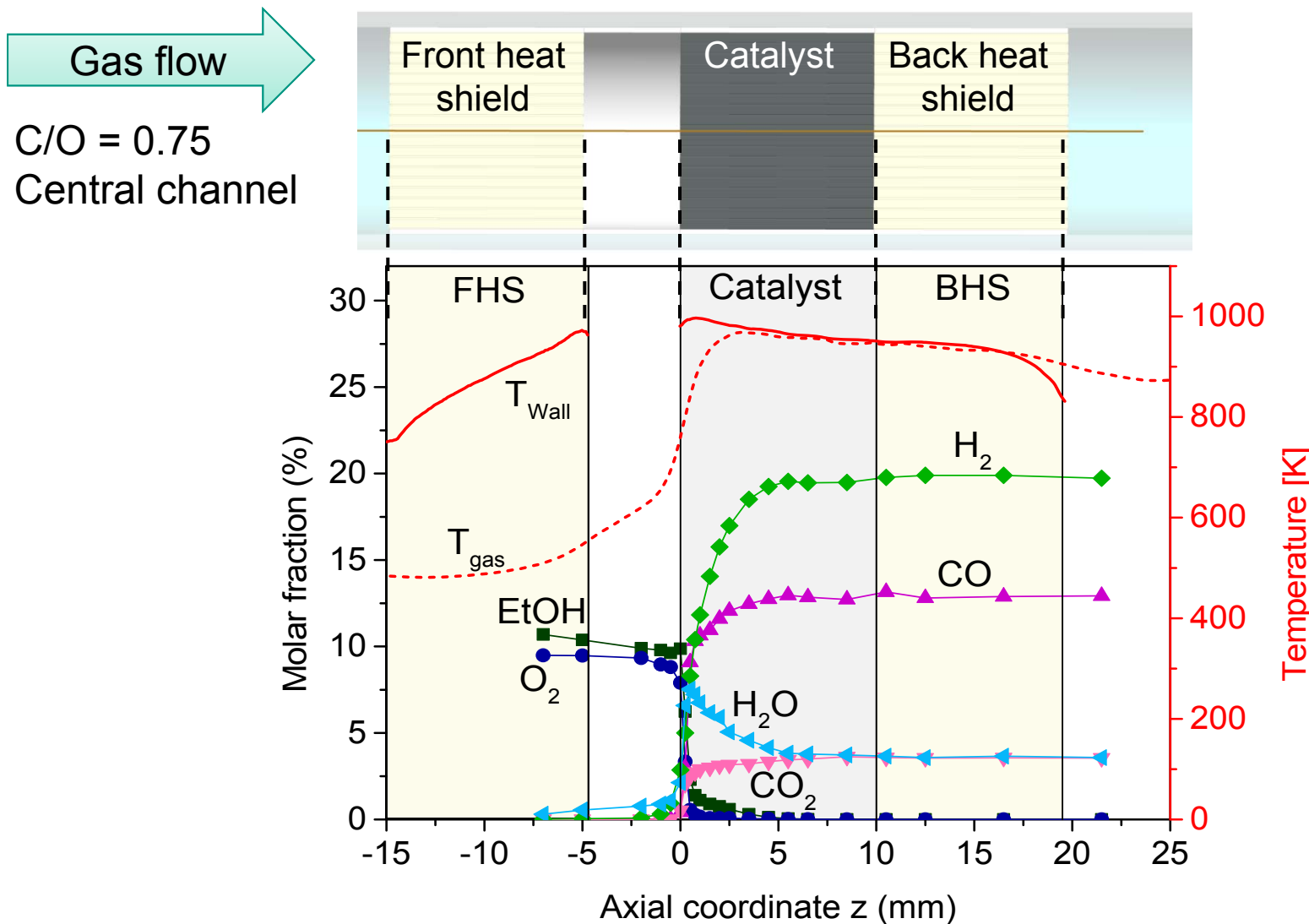
- Movement capillary: with motorized linear stage
 - Response time 0.25 ms due to fast tip (rotating linearly around the capillary)
 - Outer diameter = 170 µm Thermocouple
 - Analysis of gas samples: FT IR, MS

R. Horn, K.A. Williams, N.J. Degenstein, L.D. Schmidt, J. Catal., 242 (2006) 92.

D. Livio, C. Diehm, A. Donazzi, A. Beretta, G. Groppi, O. Deutschmann, Appl. Catal. A 467 (2013) 530.

Partial oxidation of ethanol over Rh/Al₂O₃

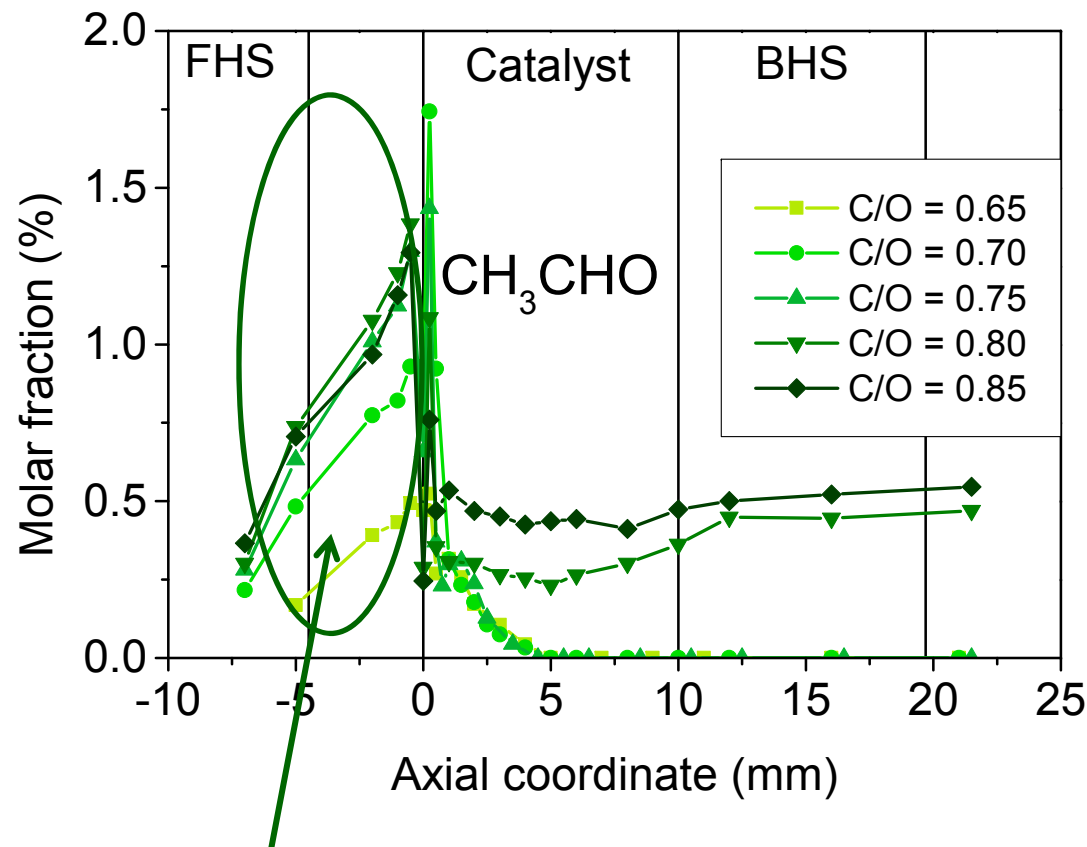
Concentration and temperature profiles in axial direction



D. Livio, C. Diehm, A. Donazzi, A. Beretta, G. Groppi, O. Deutschmann, Appl. Catal. A 467 (2013) 530

Partial oxidation of ethanol over Rh/Al₂O₃

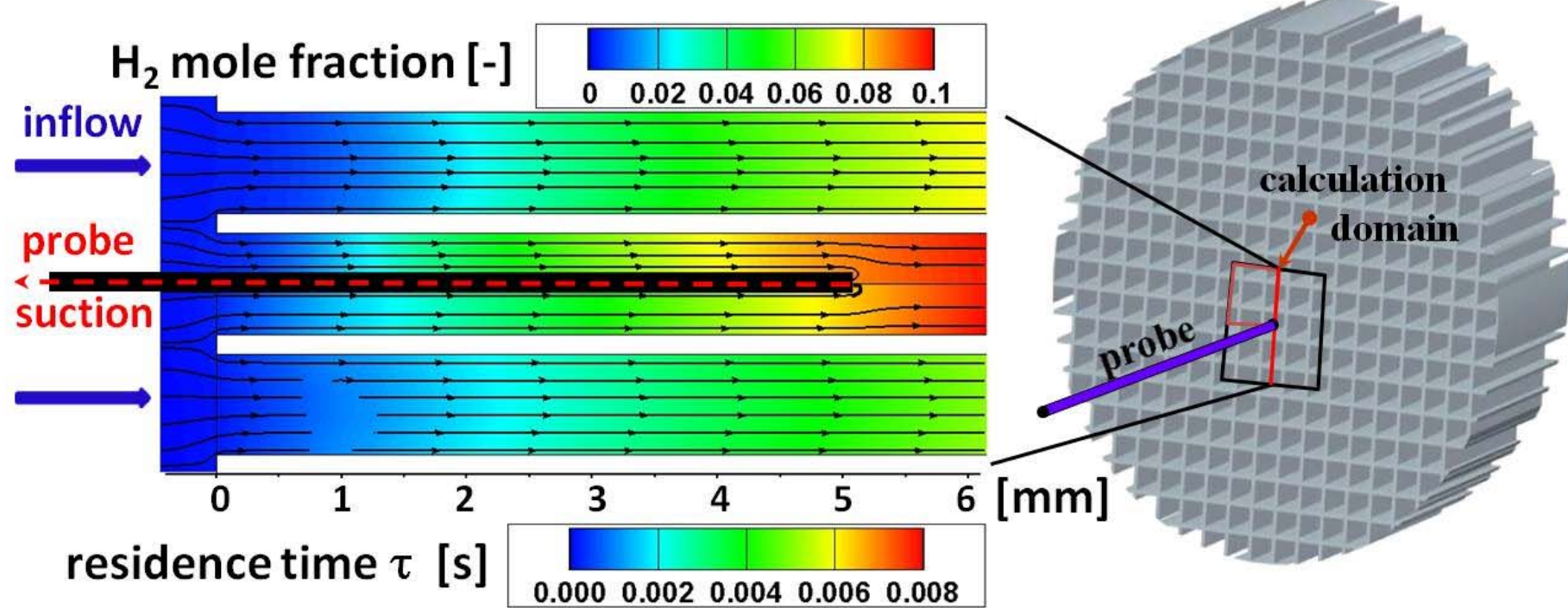
Formation of acetaldehyde in the gas phase



Increasing formation of acetaldehyde with rising ethanol concentration in feed

D. Livio, C. Diehm, A. Donazzi, A. Beretta, G. Groppi, O. Deutschmann, Appl. Catal. A 467 (2013) 530

CFD simulations of impact of capillary on profiles: Hydrogen profile and residence time

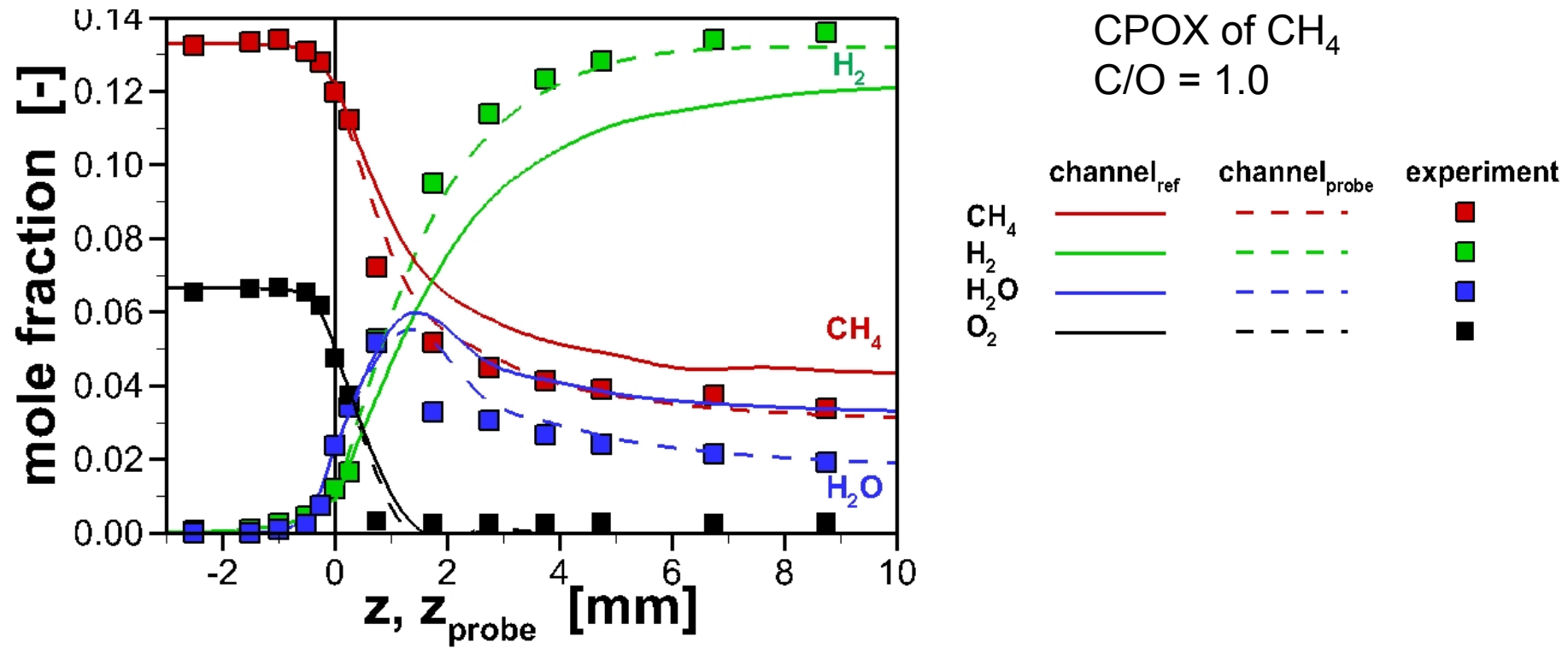


CPOX of CH_4 over Rh/Al_2O_3
 $C/O = 1$
Probe tip at $z = 5$ mm

M. Hettel, C. Diehm, B. Torkashvand, O. Deutschmann, Catalysis Today 216 (2013) 2.

Impact of capillary on spatial profiles

Comparison of measured and modeled data

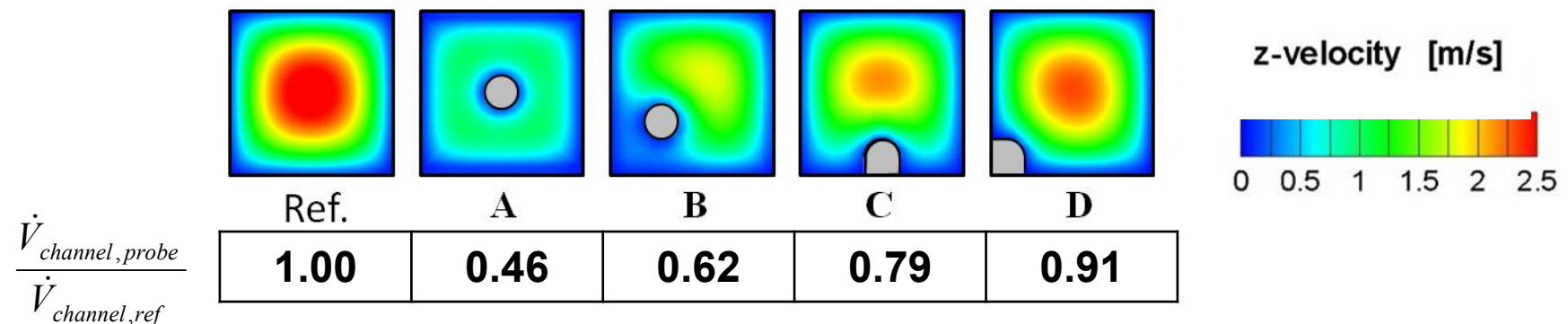


- Decrease of reactant concentrations upstream of catalyst both in simulation and experiment
→ Diffusion due to high temperature and high concentration gradients

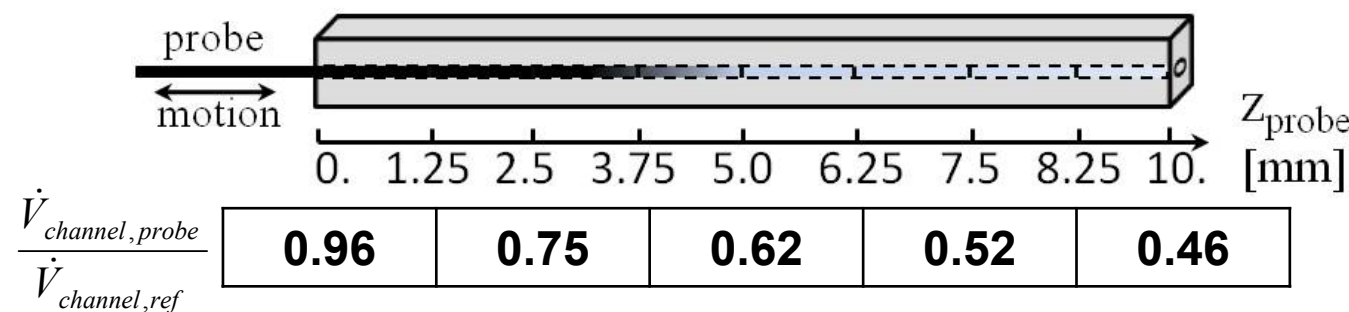
M. Hettel, C. Diehm, B. Torkashvand, O. Deutschmann, *Catalysis Today*, 2013

Impact of axial and radial position of capillary on volumetric flux though probe channel

Impact of radial position of capillary on axial velocity and volumetric flux

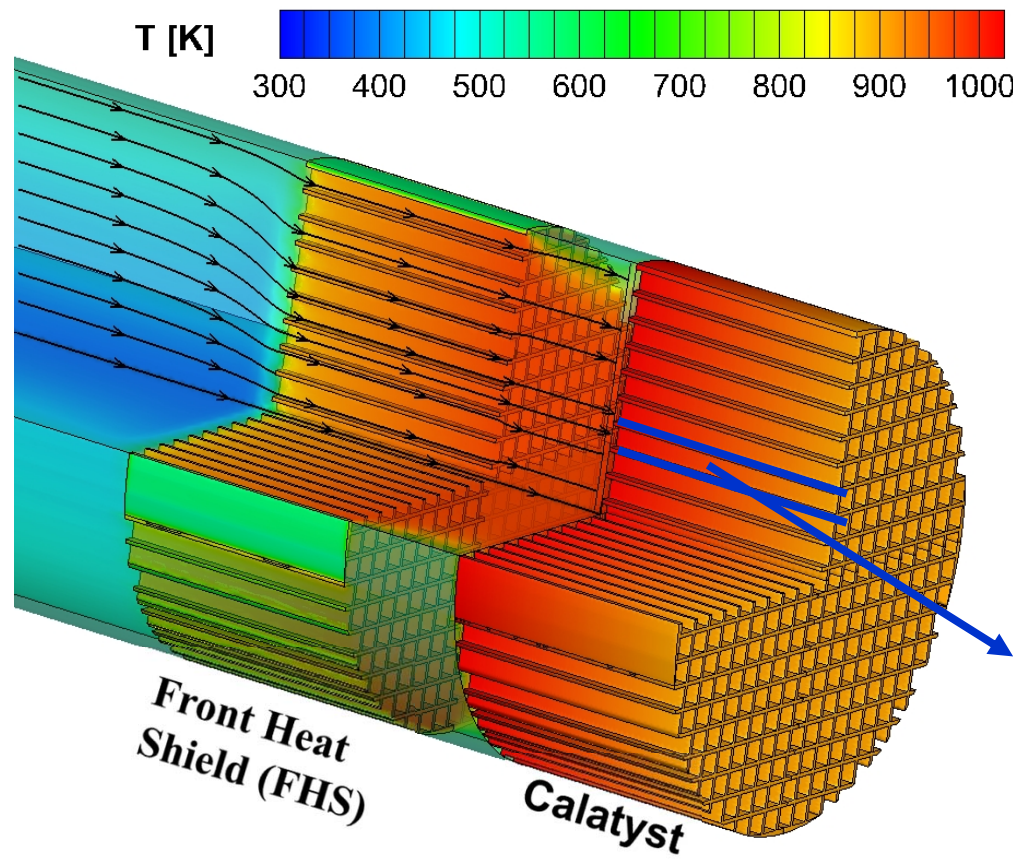


Impact of axial position of the tip for central location on volumetric flux



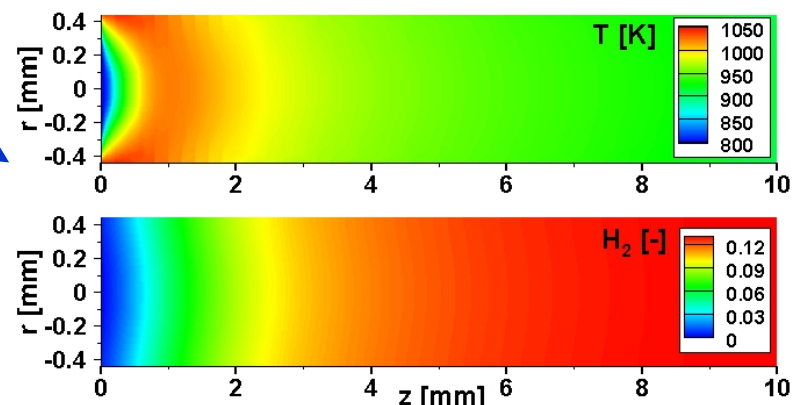
M. Hettel, C. Diehm, B. Torkashvand, O. Deutschmann, Catalysis Today 216 (2013) 2.

Syngas Formation in CPOX of CH₄ on Rh: CFD simulation using OpenFoam and DETCHEM



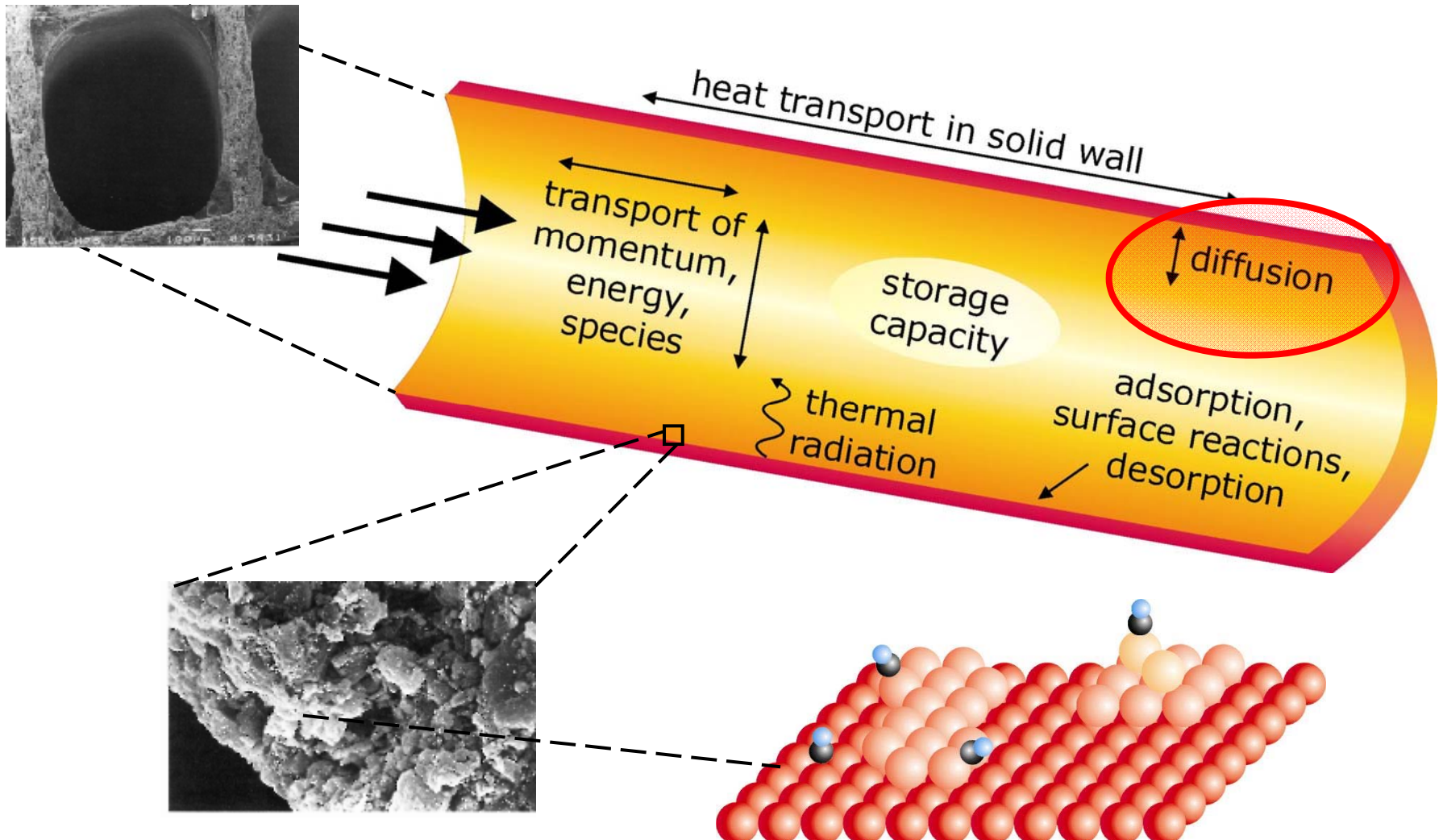
CH₄+O₂ in N₂
C/O = 1.0
Rh (10 mm)

Surface mechanism for
CPOX of CH₄ on Rh
(38 reactions, 6 gas-phase species,
11 adsorbed species)



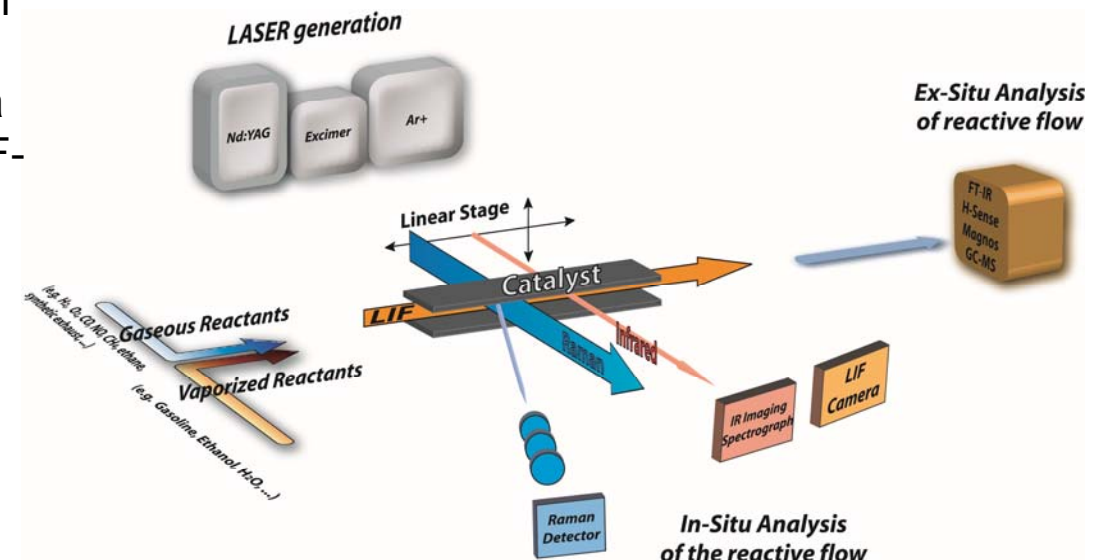
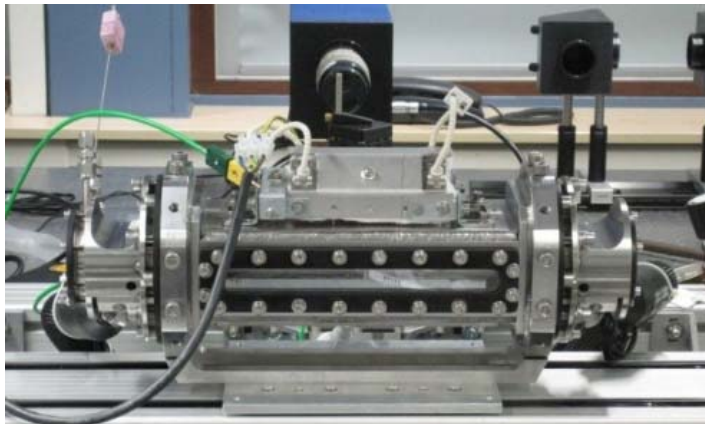
M. Hettel, C. Diehm, O. Deutschmann, 2014

Coupling of external diffusion and reaction



Labor CATHLEN: Optical diagnostics of catalytic reactors

In-situ analysis of spatial and temporal profiles of species concentration and temperature in the gas phase above a catalytic surface using Raman and LIF-spectroscopy

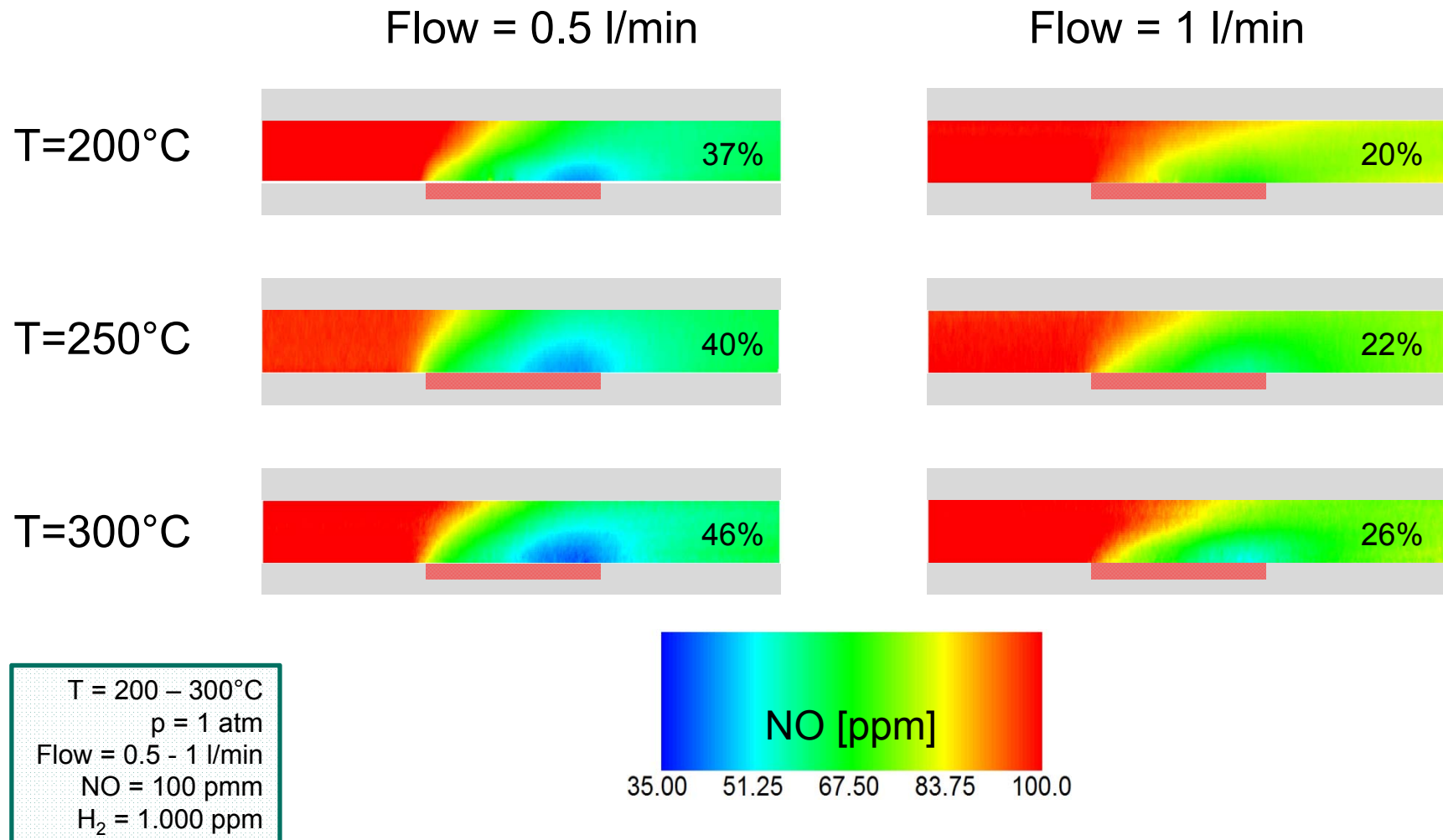


NO LIF profile during reduction by H₂ to NH₃ in Pt/Al₂O₃ one-side-coated single channel of a DOC



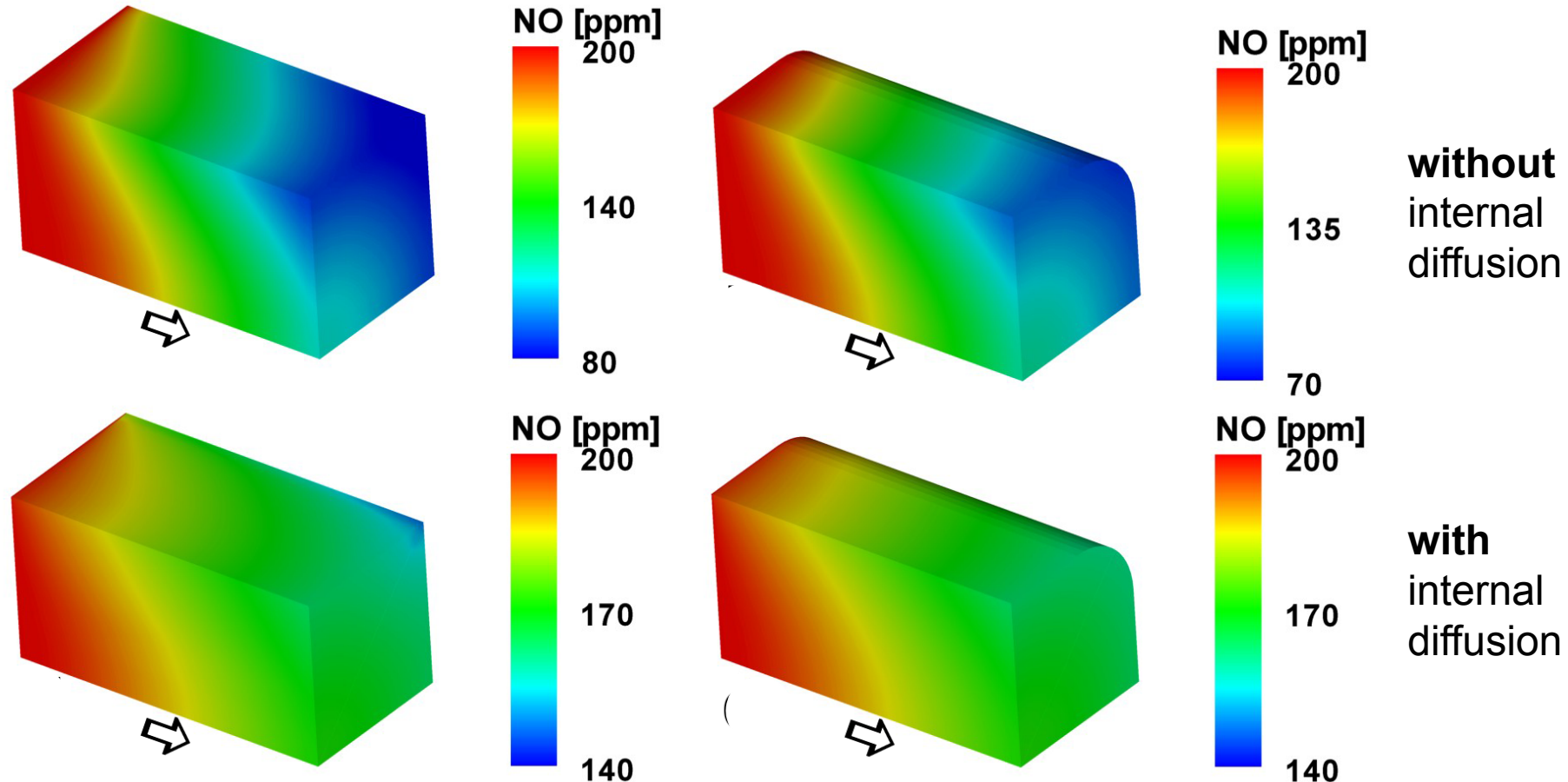
A. Zellner, R. Suntz, O. Deutschmann, Chemie Ingenieur Technik 86 (2014) 538.

NO reduction by H₂ to NH₃ over Pt - DOC catalyst: LIF monitored NO conversion



A. Zellner, R. Suntz, O. Deutschmann, *Angew. Chem., subm.*

Impact of models for channel shape and washcoat diffusion on NO profiles in a DOC

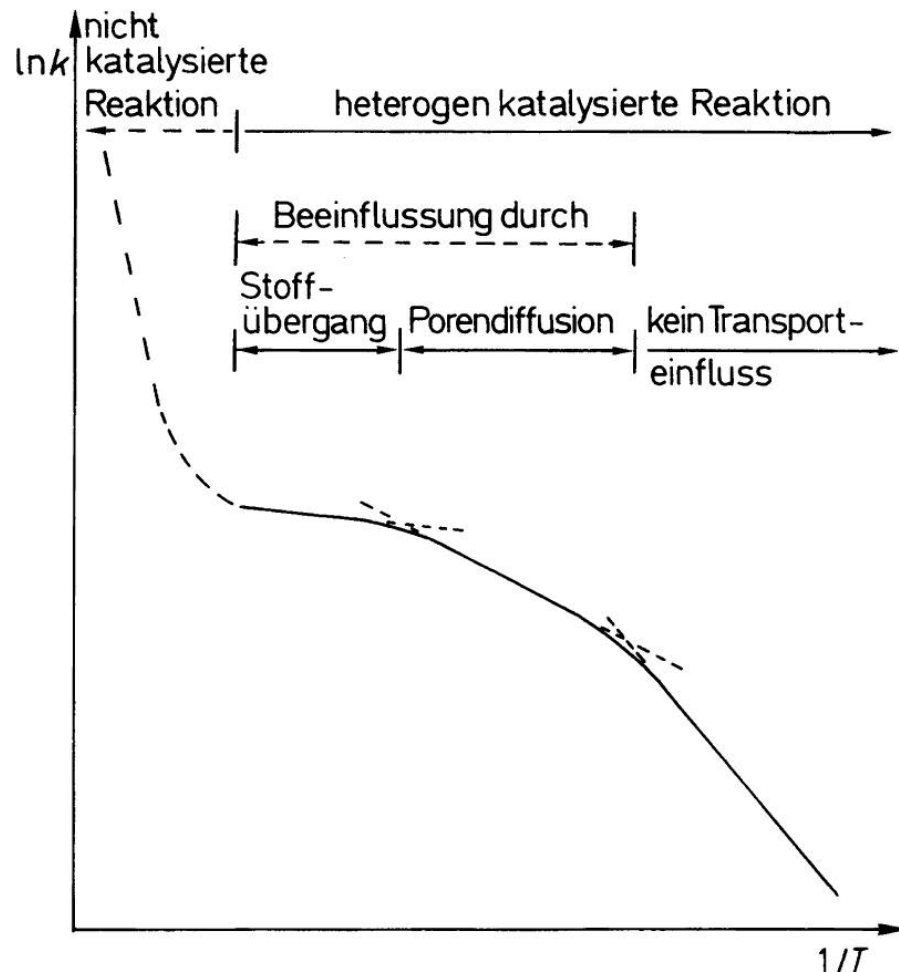


NO profiles at lean conditions at 250°C (steady-state operation)

CFD code: Fluent + DETCHEM

N. Mladenov, J. Koop, S. Tischer, O. Deutschmann. Chem. Eng. Sci. 65 (2010) 812

Zusammenspiel von äußerem und innerem Stofftransport: Temperaturabhängigkeit der effektiven Reaktionsgeschwindigkeit



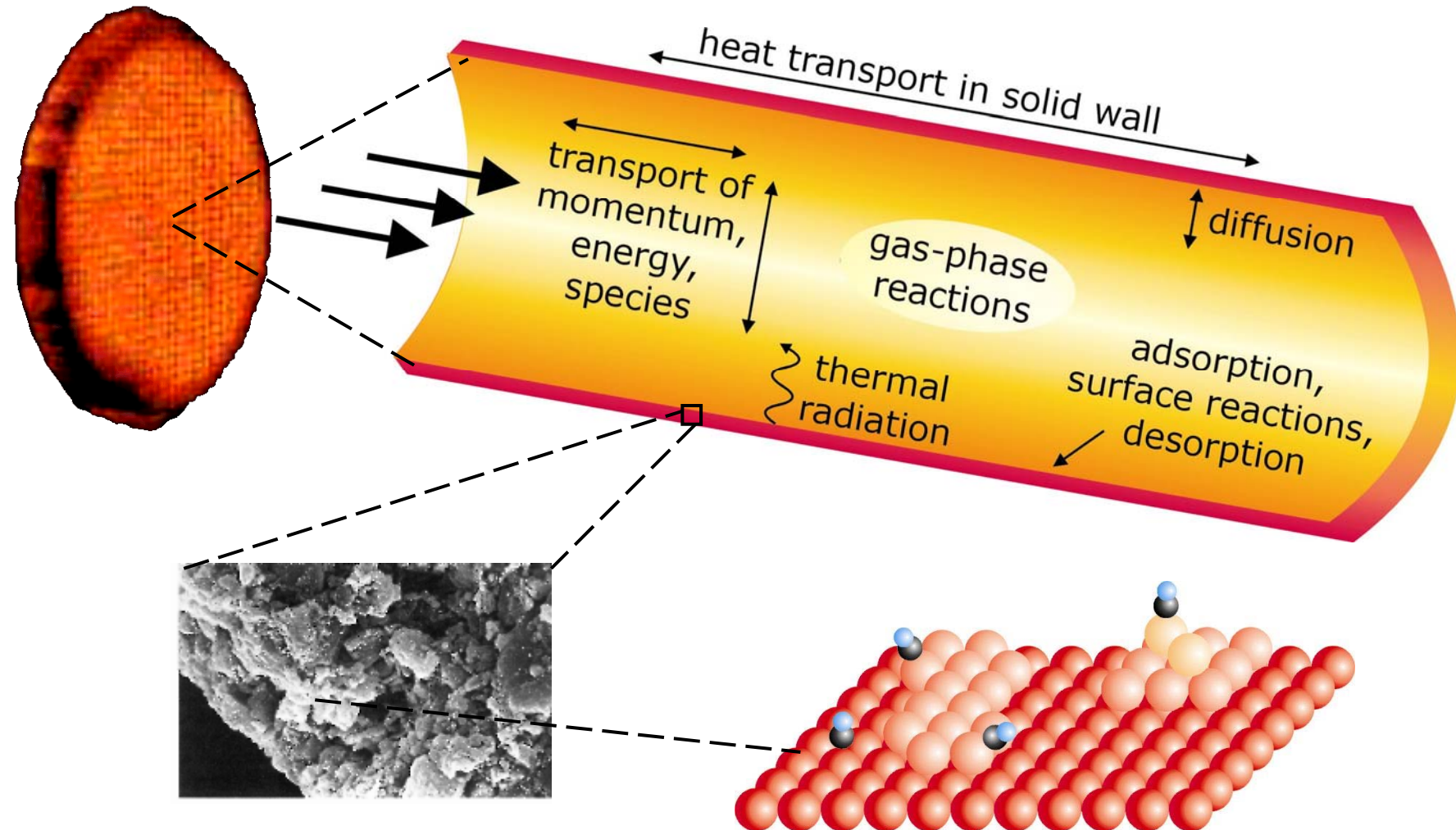
© 2006 Wiley-VCH, Weinheim
Baerns / Technische Chemie
ISBN: 3-527-31000-2 Abb-04-03-09

Kinetics – Interaction between Reaction, Mass and Heat Transfer: Outline



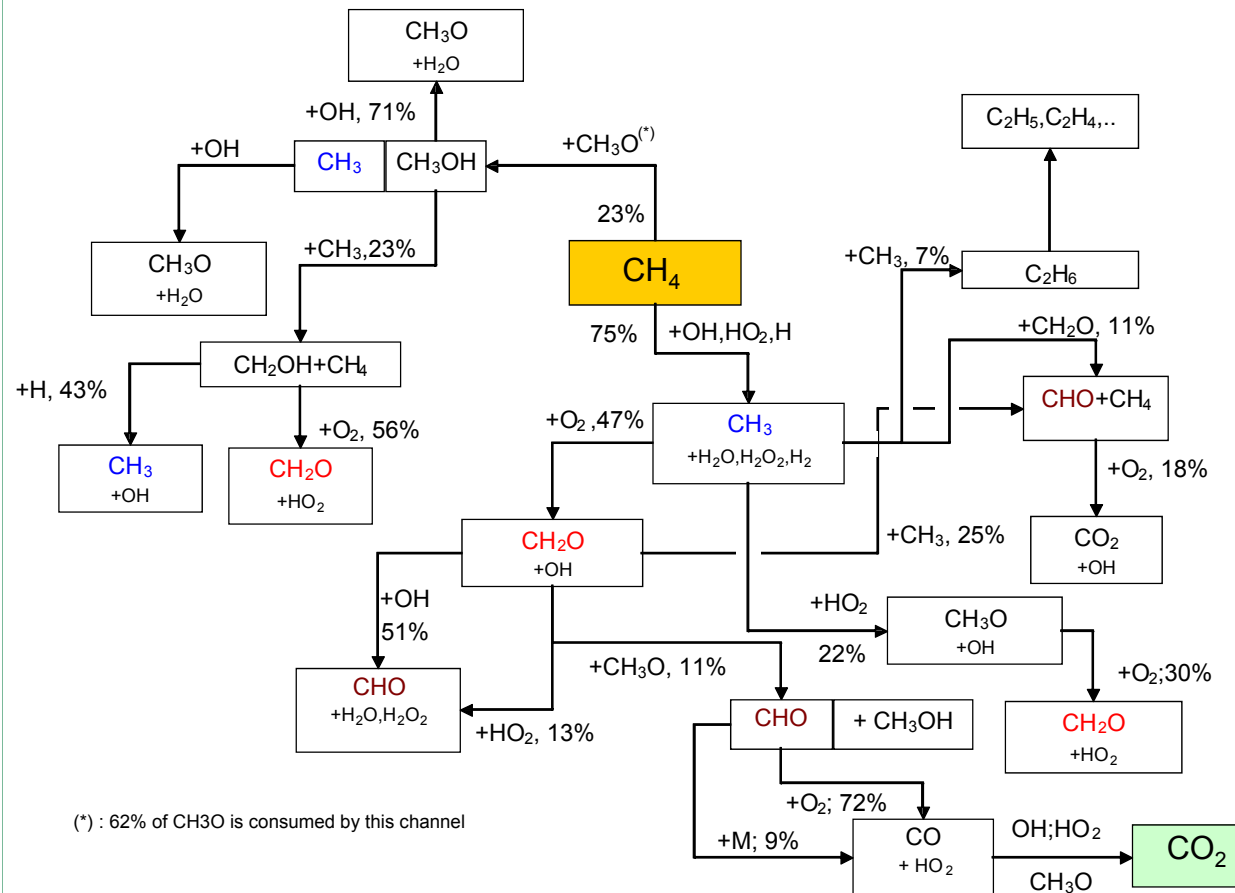
1. Microkinetics of reactions on the catalytic surface
2. Transport and reactions in porous media (internal diffusion)
3. Reactive flow and external diffusion
4. **Gas-phase chemistry**
5. Transient processes and heat transport

Impact of gas-phase reactions



Gas-phase reactions: Complex schemes even for simple fuels - CH₄ partial oxidation

Reaction flow analysis

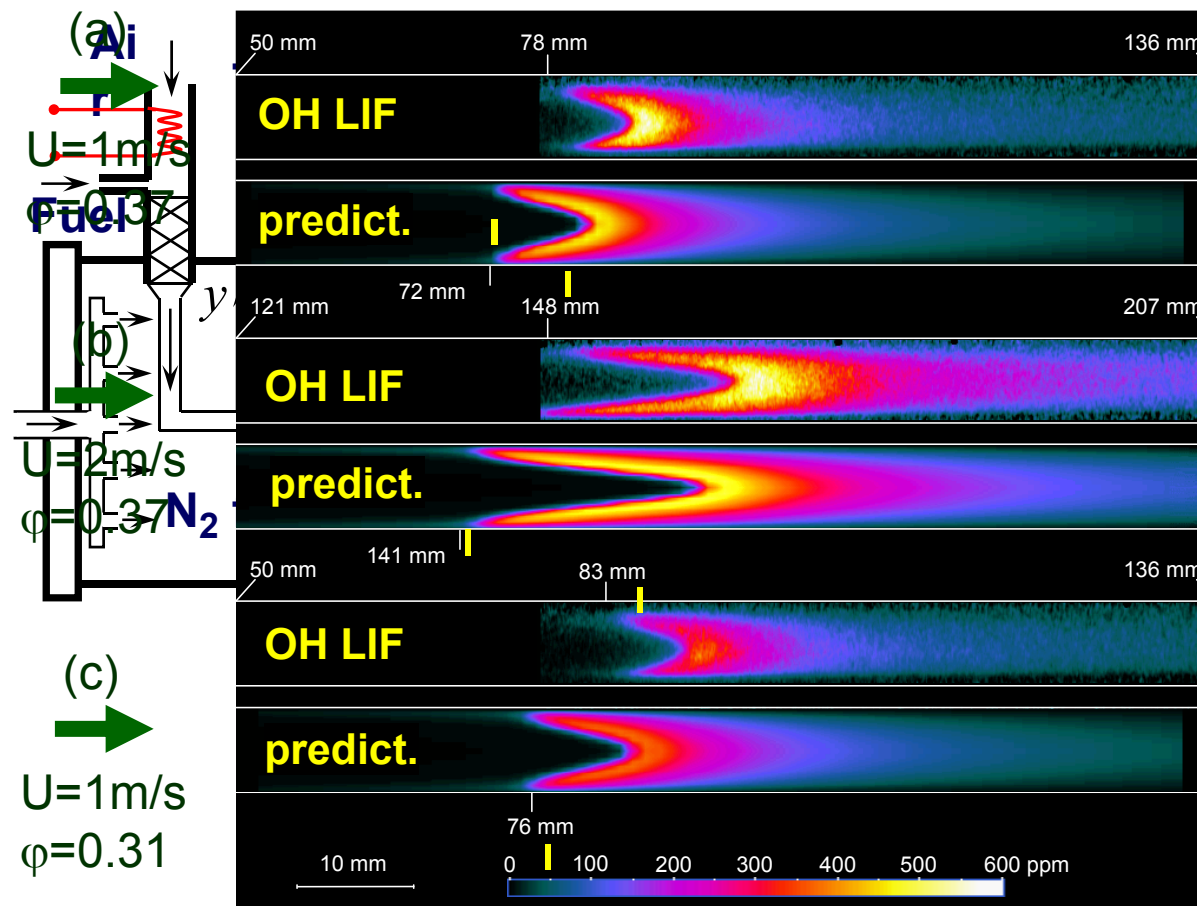


765 reactions among
63 gas phase species

R. Quiceno, J. Perez-Ramirez, J. Warnatz, O. Deutschmann. Appl. Catal. A: General 303 (2006) 166–176

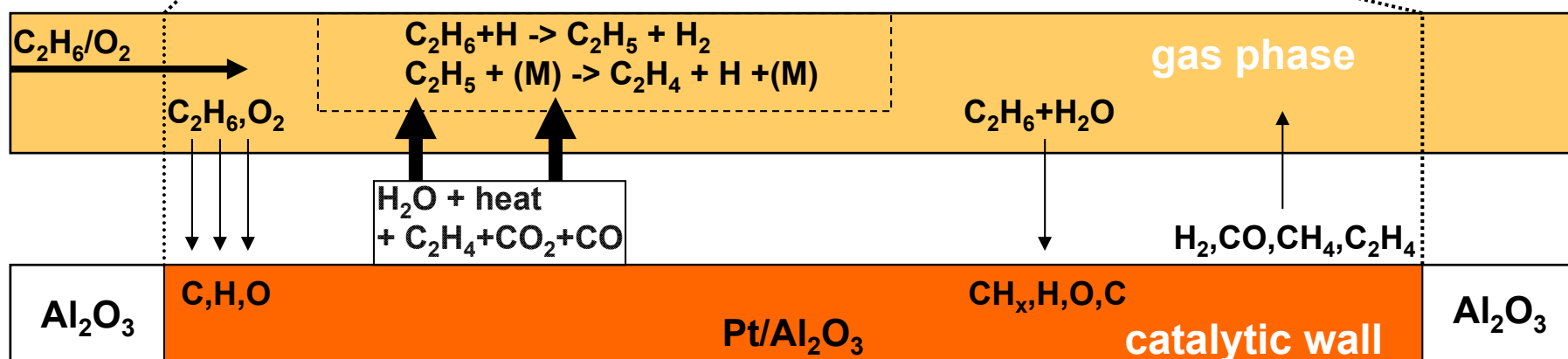
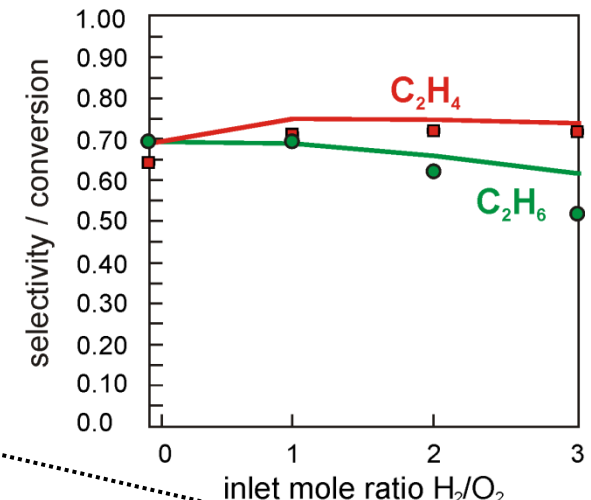
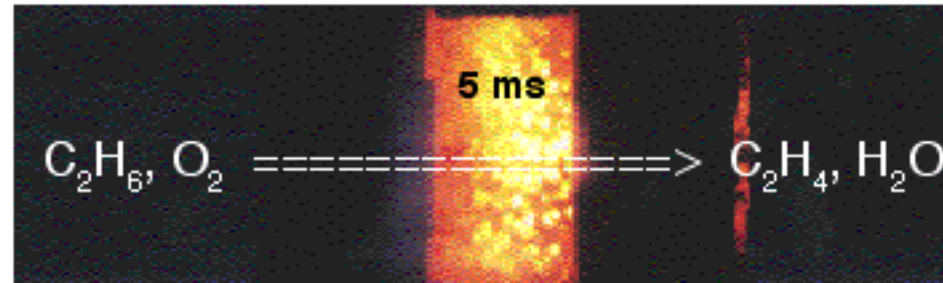
Homogeneous ignition in catalytic combustion of methane/air mixtures over platinum

Comparison of experimentally observed (PLIF) and numerically predicted (2D NS model with detailed gas phase and surface kinetics) OH profiles in a laminar plane channel flow



U. Dogwiler, J. Mantzaras, C. Appel, P. Benz, B. Kaeppli, R. Bombach, A. Arnold. Proc. Combust. Inst. 27 (1998) 2275

Oxidative dehydrogenation of ethane to ethylene on platinum at short contact times

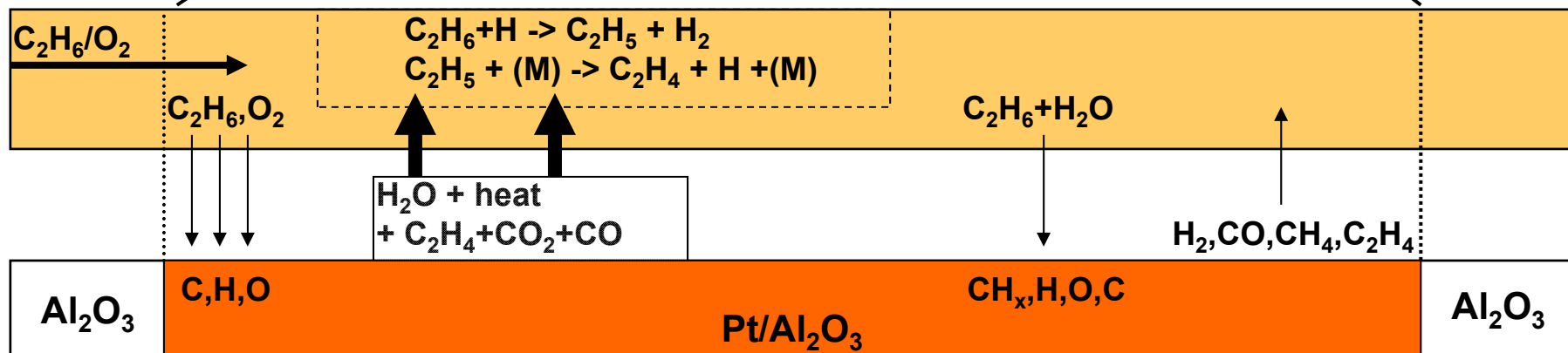
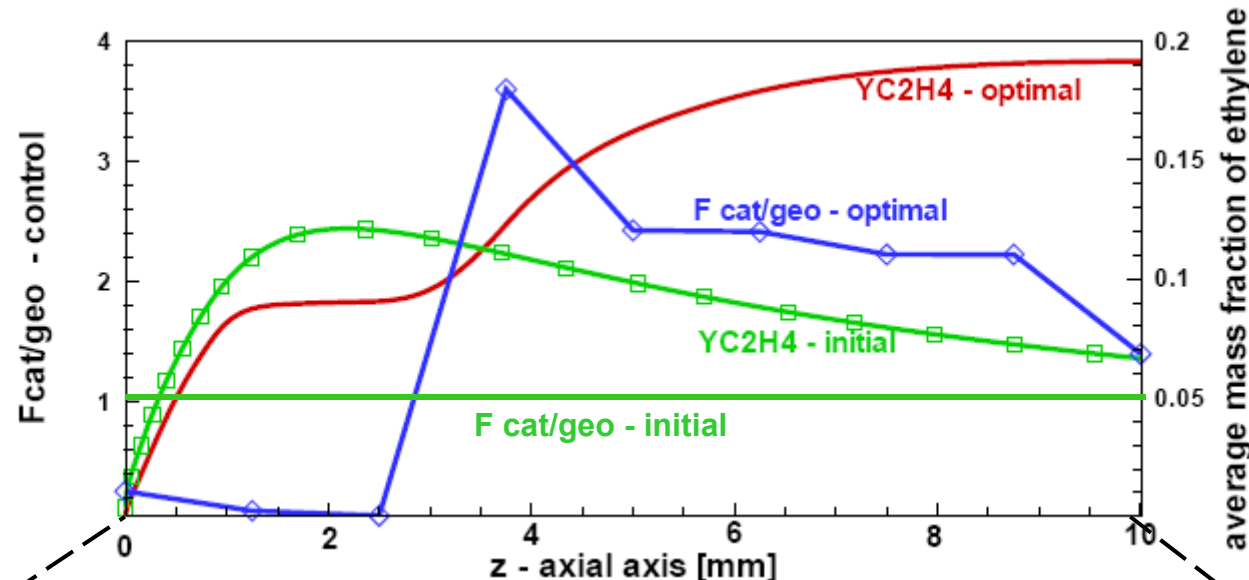


A. Bodke, L.D. Schmidt, J. Catal. 191 (2000) 62

D. K. Zerkle, M. D. Allendorf, M. Wolf, O. Deutschmann. J. Catal. 196 (2000) 18

A. Beretta, E. Ranzi, P. Forzatti, Chem. Eng. Sci. 56 (2001) 779

Mathematical optimization of catalyst loading: Oxy-dehydrogenation of ethane to ethylene over Pt



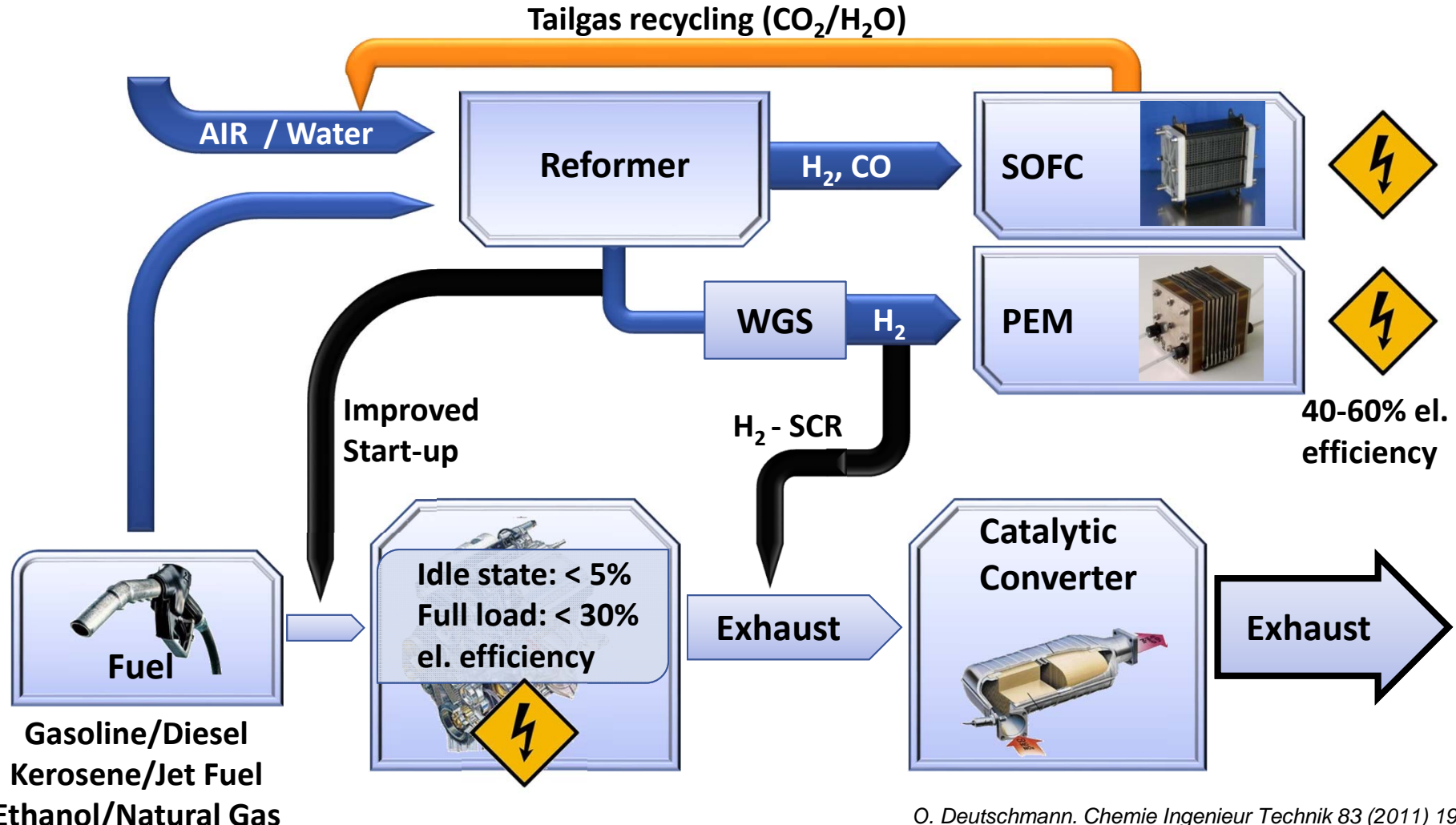
H.D. Minh, S. Tischer, H.G. Bock, O. Deutschmann, AIChE J. 54 (2008) 2432.

More efficient technology for auxiliary power supply in automobile vehicles needed



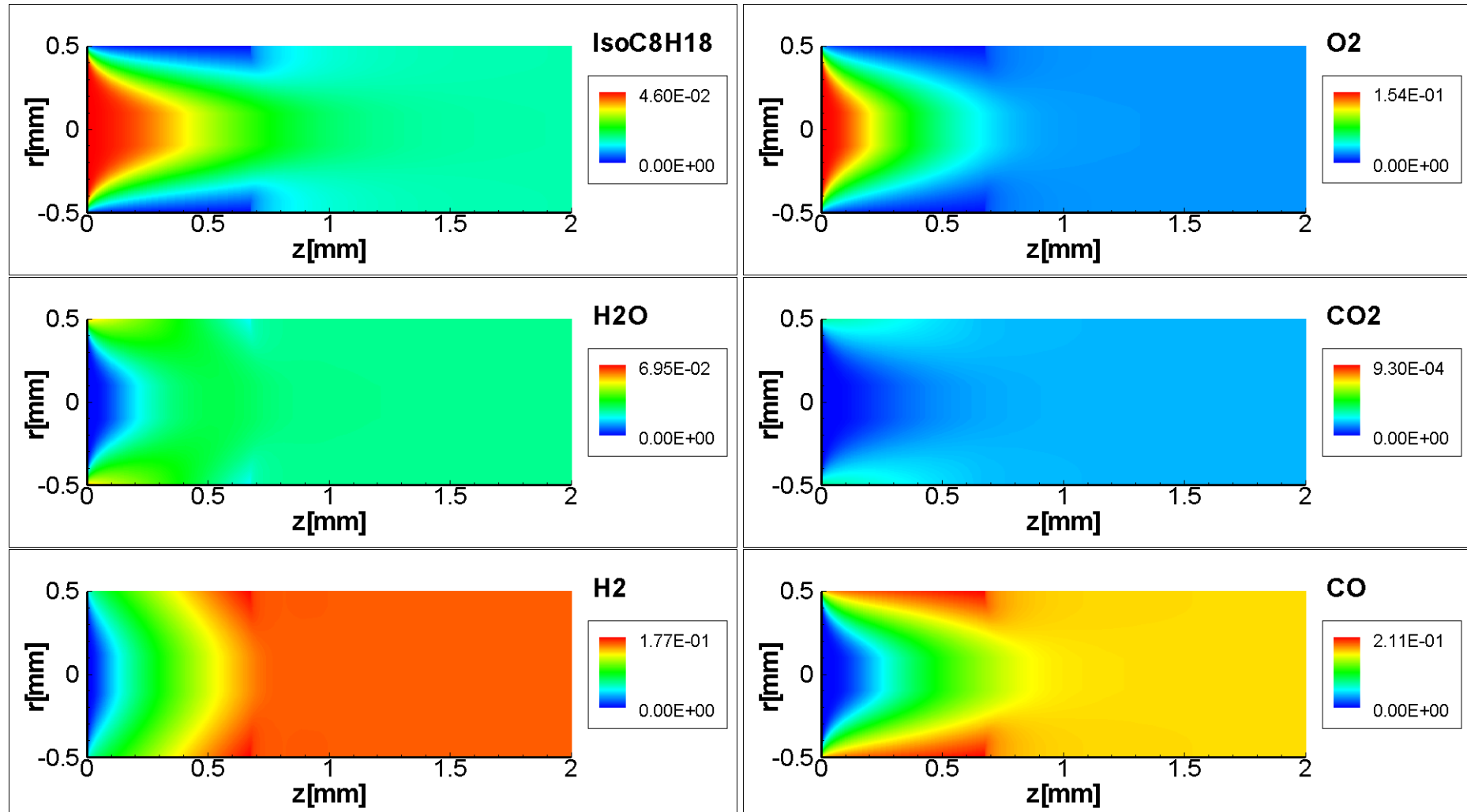
Idling long-haul trucks consumes 1 billion gallons of diesel fuel annually in the USA
→ 11 million tons CO₂, 180,000 tons NO_x, 5000 tons particulates!

Conversion of logistic fuels provides electricity and reduces fuel consumption, pollutant emissions, and noise



O. Deutschmann. Chemie Ingenieur Technik 83 (2011) 1954
T. Kaltschmitt, C. Diehm, O. Deutschmann. Ind.& Eng. Chemi. Res. 51 (2012) 7536

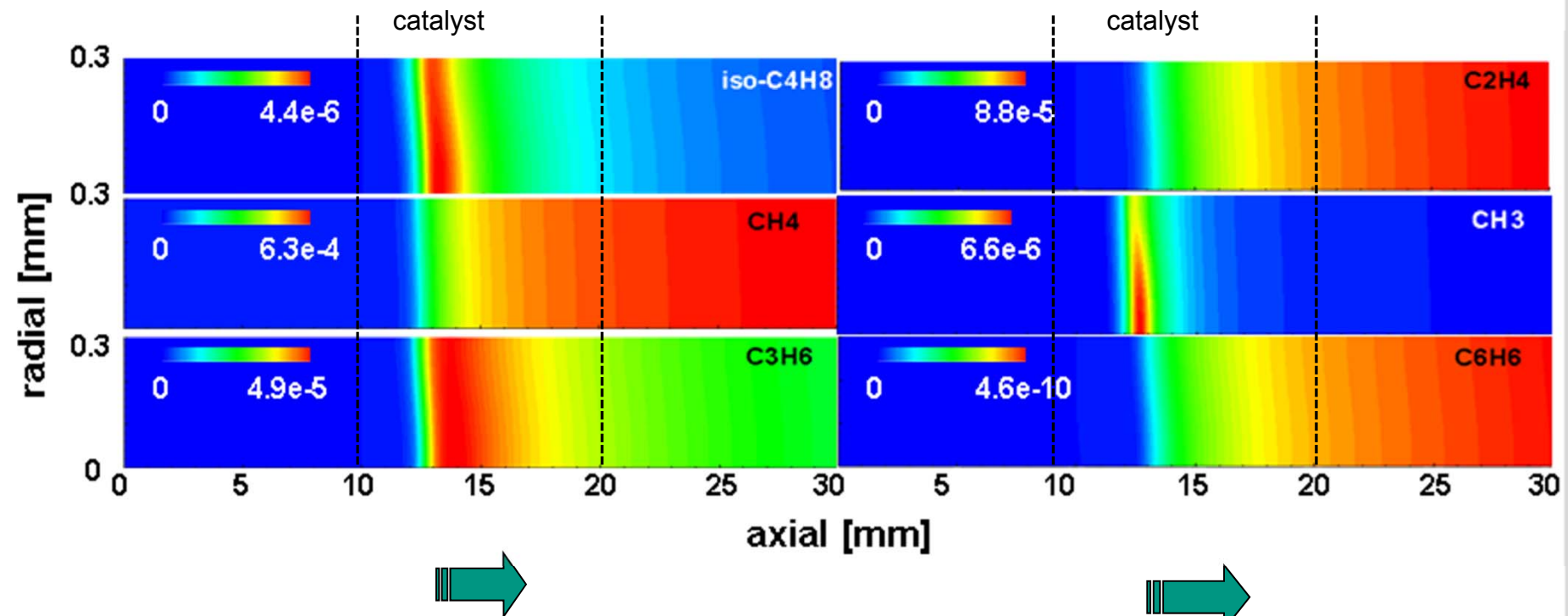
CPOX of iso-octane in catalytic channel: Numerically predicted 2D species profiles in gas-phase



$\text{C}/\text{O} = 1.2, 800^\circ\text{C}$

M. Hartmann, L. Maier, O. Deutschmann, Combust. Flame 157 (2010) 1771

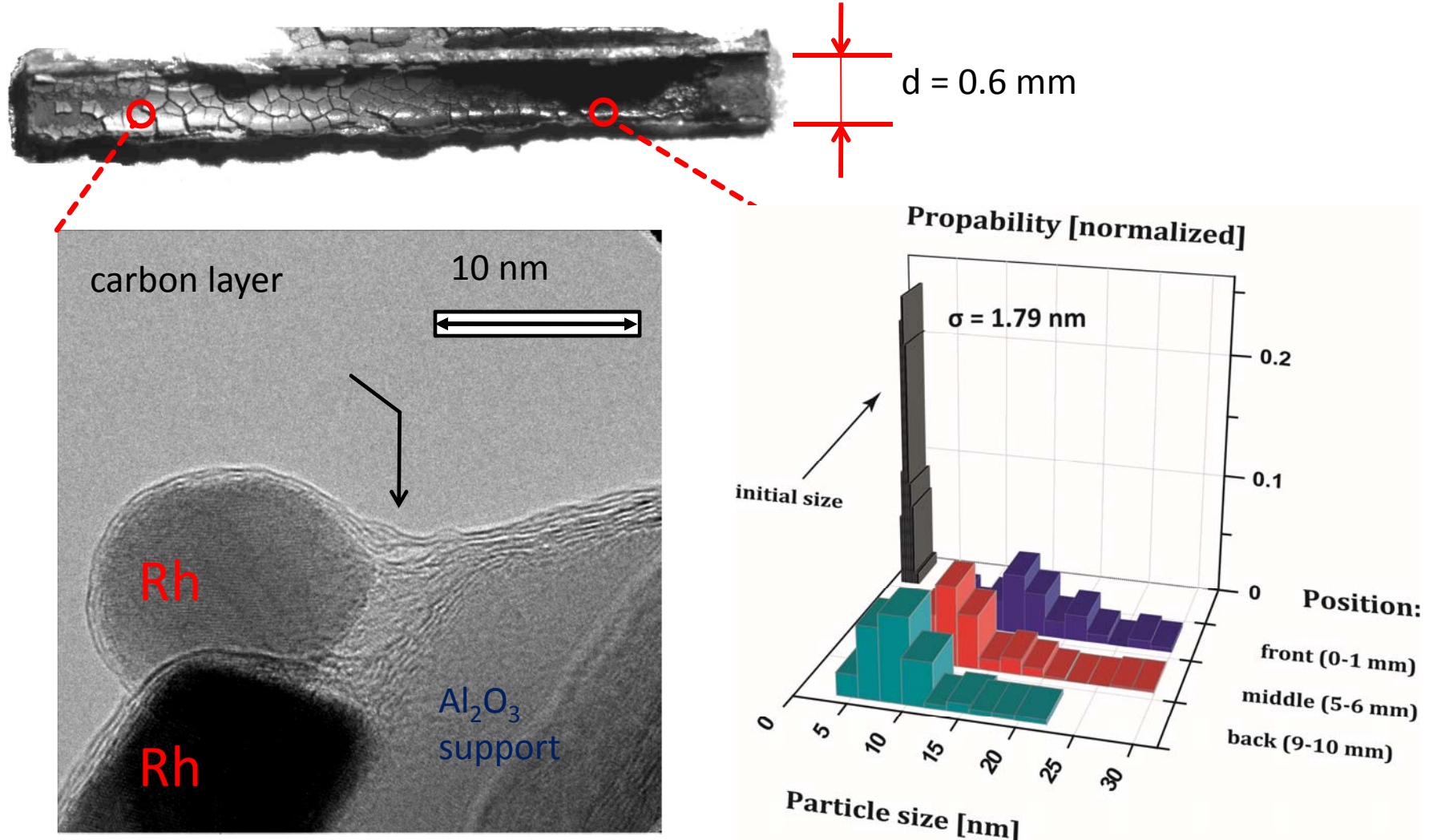
CPOX of i-octane: Coke precursors are formed in the gas phase in the catalytic zone and downstream



C/O = 1.0 5 slpm

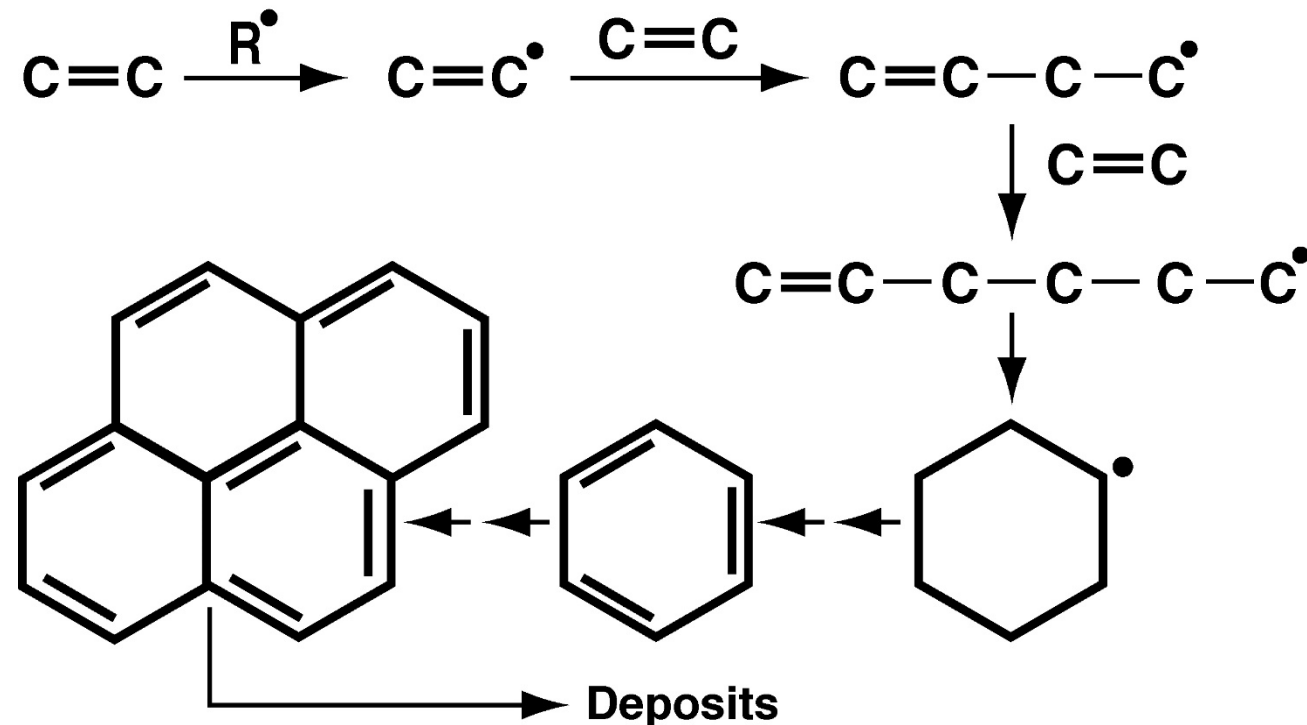
L. Maier, M. Hartmann, O. Deutschmann, Combust. Flame 158 (2011) 796–808.

Catalyst deactivation by coking: TEM-Images of the Rh particles



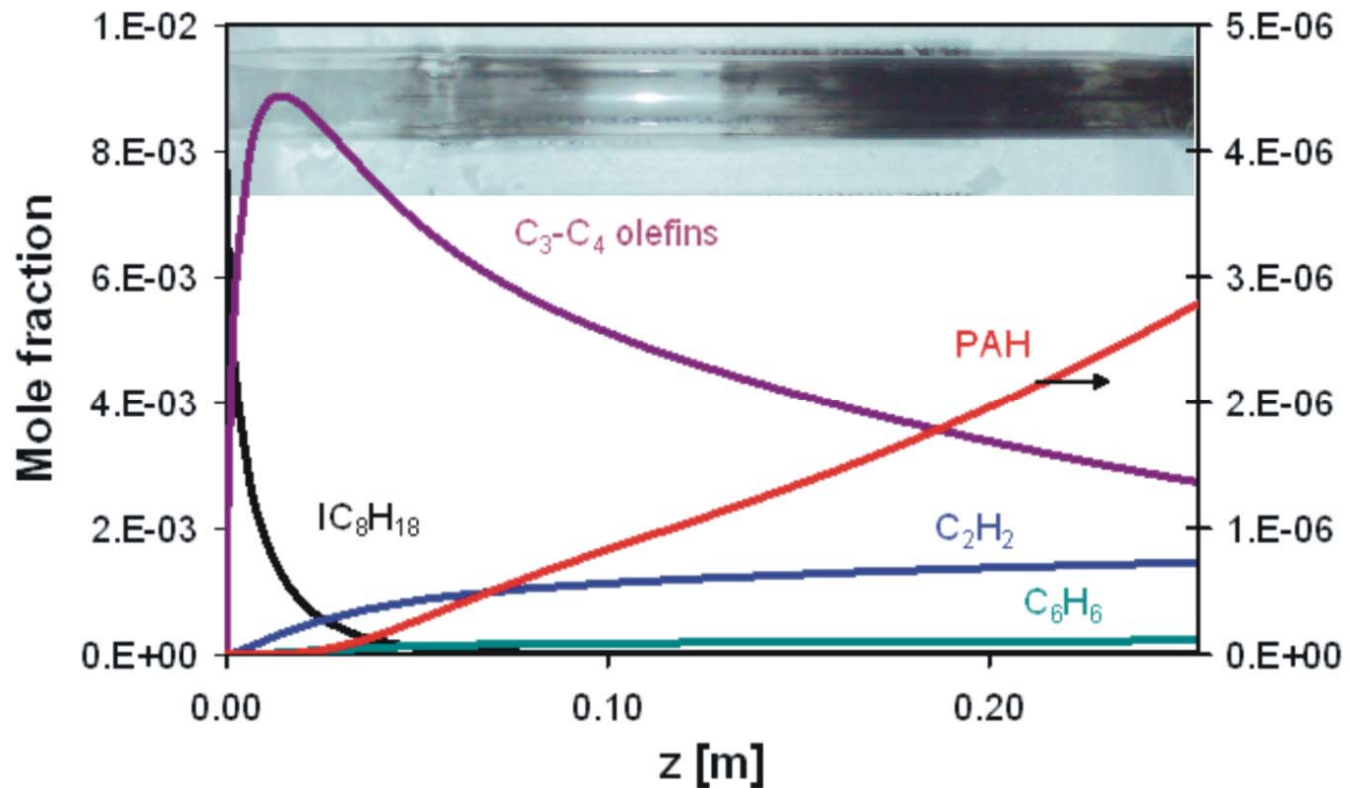
M. Hartmann, B. Reznik, O. Deutschmann, 2010, to be published

Small olefins in reformate gas can lead to gas-phase molecular-weight growth and carbon deposits



A. Dean, Colorado School of Mines

Coke formation in partial oxidation of iso-octane: Carbon distribution along the reactor (w/o catalyst)



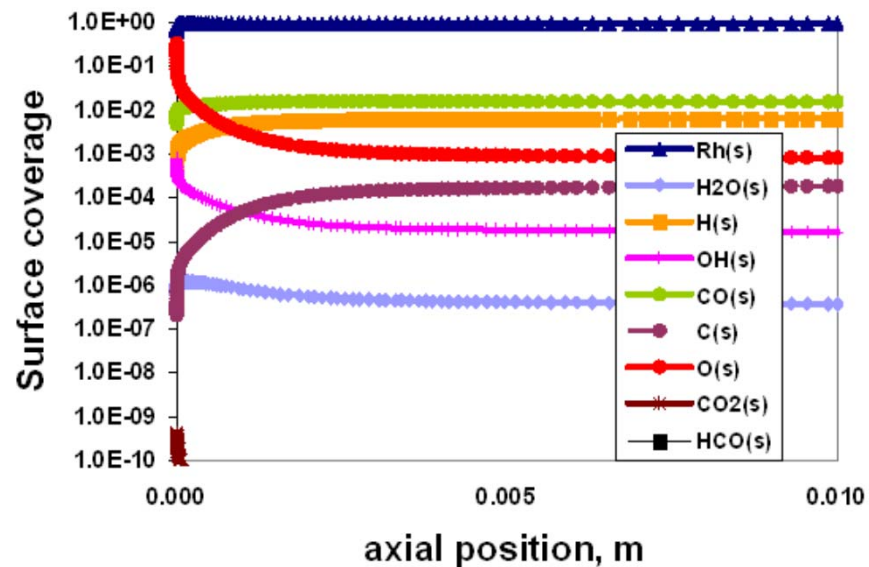
$\text{C}/\text{O} = 1.6$, 1108 K, 6 SLPM. $\text{C}_3\text{-C}_4$ olefins contain 1,2-propadiene, propene, propyne, n-butene (1-butene, 2-butene), iso-butene, 1,3-butadiene; PAH contains naphthalene, anthracene, pyrene.
Embedded photo shows the tubular quartz reactor after operation.

T. Kaltschmitt, L. Maier, O. Deutschmann. Proceedings of the Combustion Institute 33 (2011) 3177

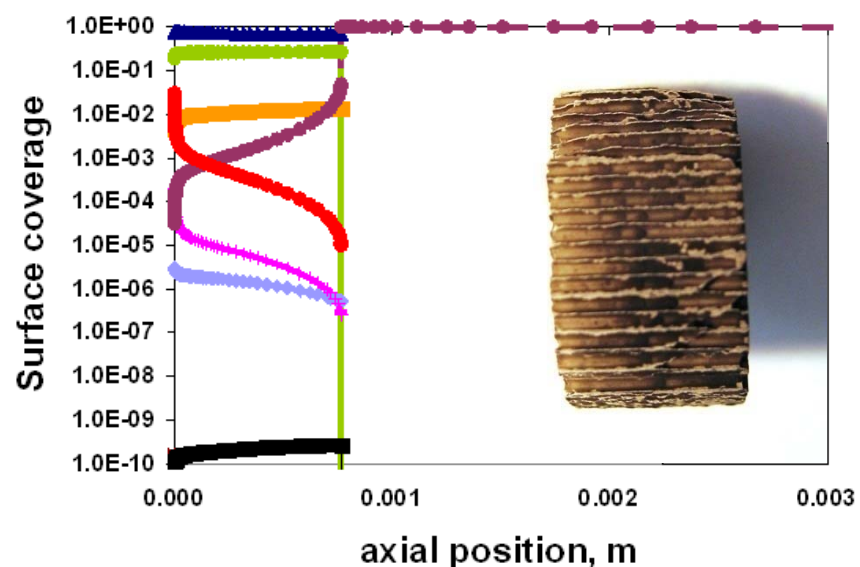
CPOX of i-octane: Coke formation on the downstream section of the catalyst at rich conditions

Numerically predicted surface coverage along the monolithic catalyst

C/O = 0.8



C/O = 1.2



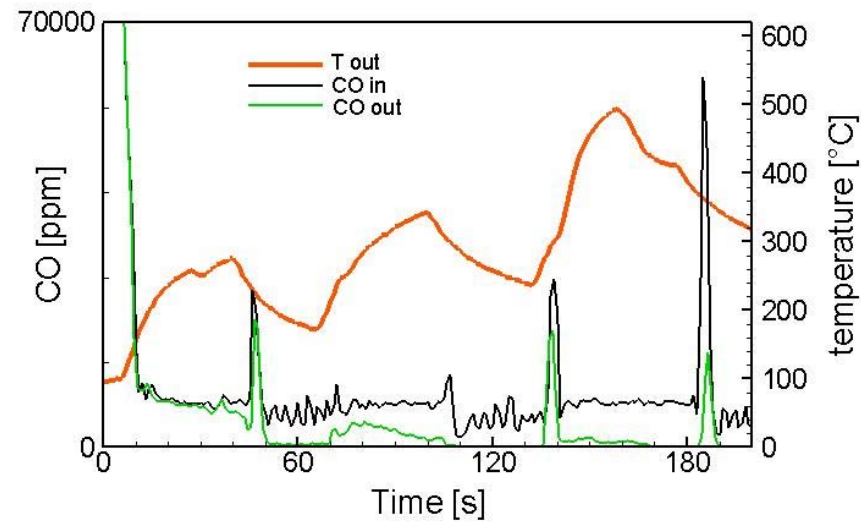
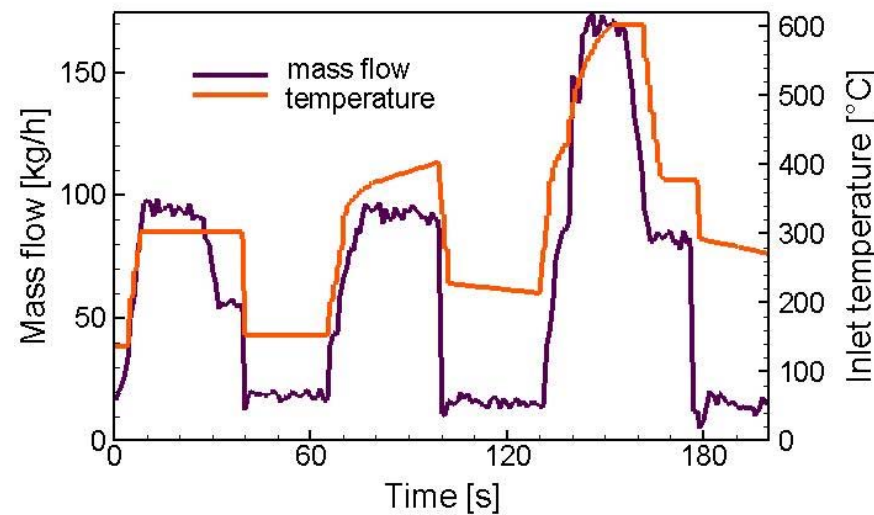
M. Hartmann, L. Maier, O. Deutschmann, Combust. Flame 157 (2010) 1771

Kinetics – Interaction between Reaction, Mass and Heat Transfer: Outline



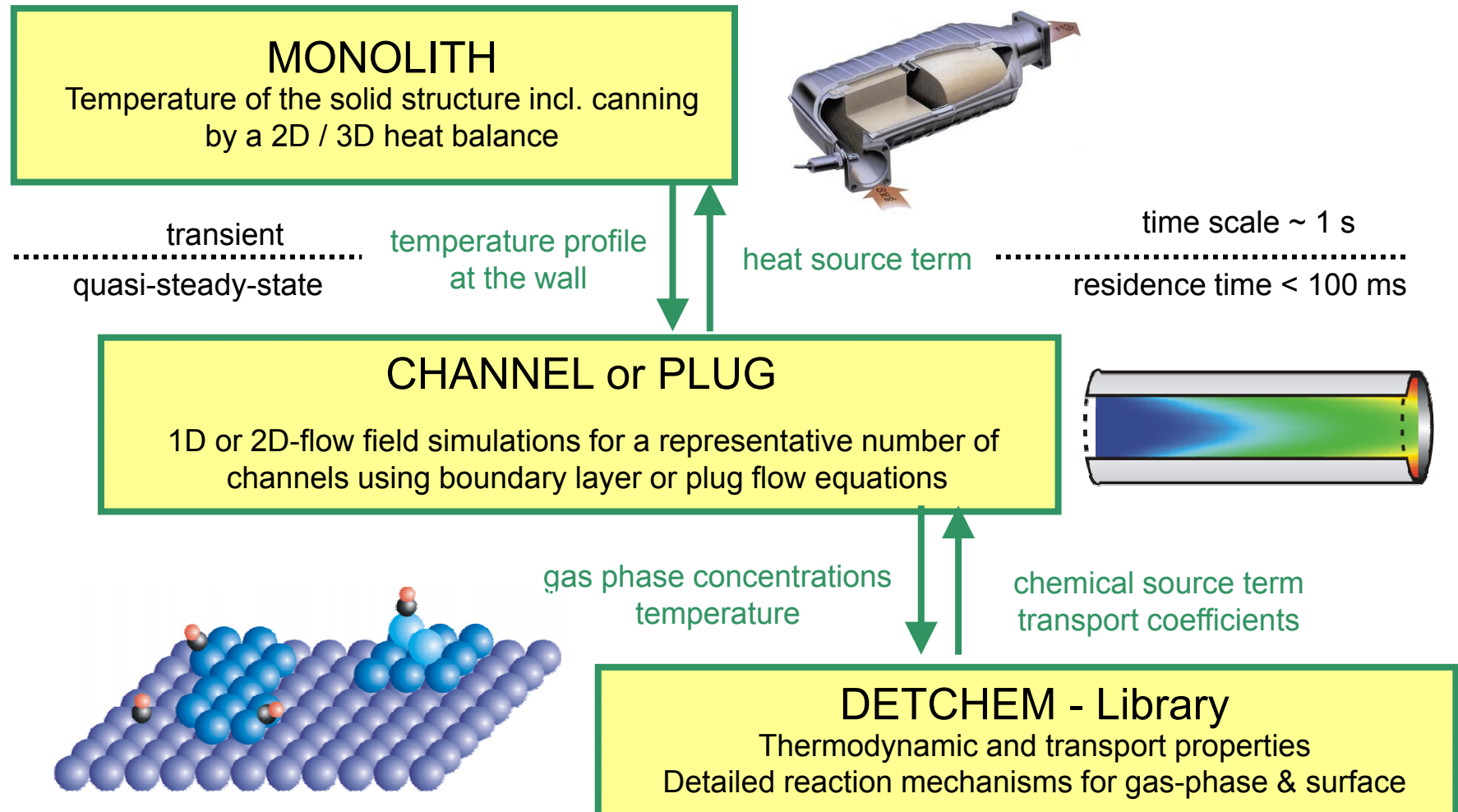
1. Microkinetics of reactions on the catalytic surface
2. Transport and reactions in porous media (internal diffusion)
3. Reactive flow and external diffusion
4. Gas-phase chemistry
5. **Transient processes and heat transport**

Simulation at real driving conditions is very challenging: Continuous variation of all inlet variables



J. Braun, T. Hauber, H. Többen, J. Windmann, P. Zacke, D. Chatterjee, C. Correa, O. Deutschmann, L. Maier, S. Tischer, J. Warnatz, SAE paper 2002-01-0065

DETACHEM^{MONOLITH}: Computer program for the numerical simulation of transients in catalytic monoliths



S. Tischer, O. Deutschmann, Catal. Today 105 (2005) 407, www.detchem.de

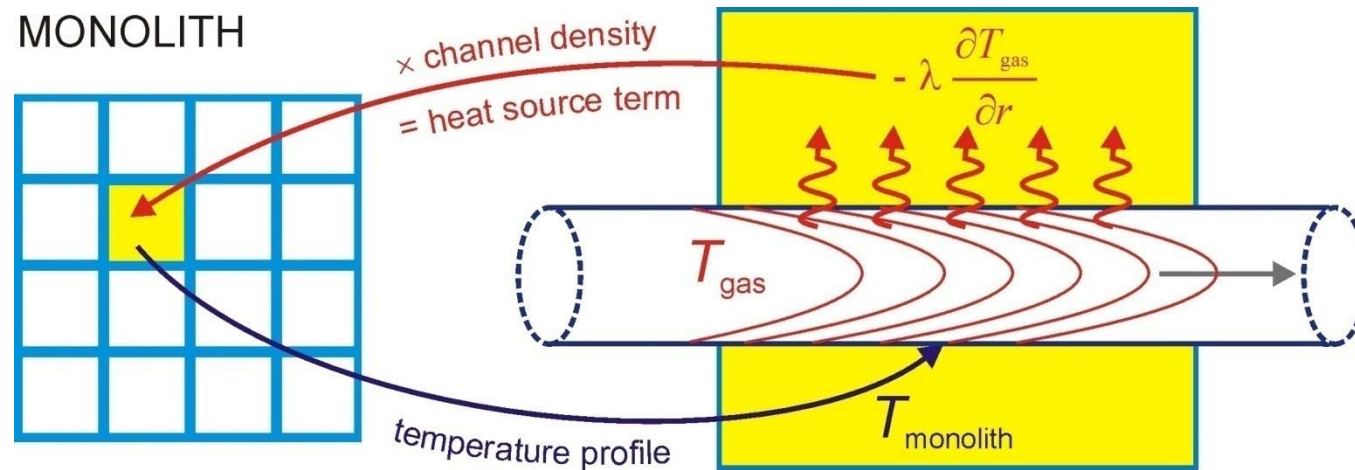
Modeling the temperature of the solid phase of the monolith: Transient three-dimensional heat balance

Temperature

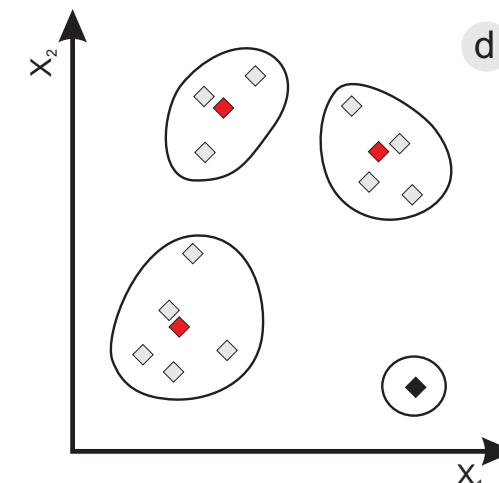
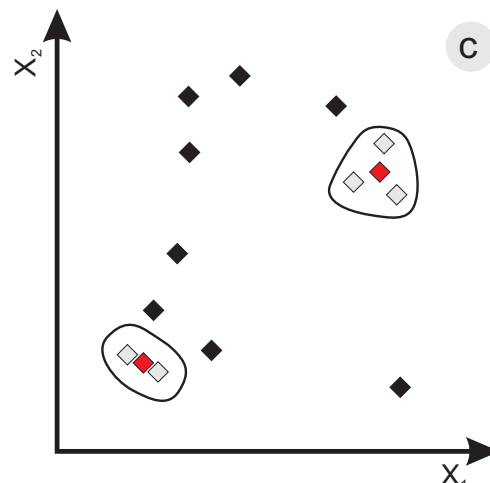
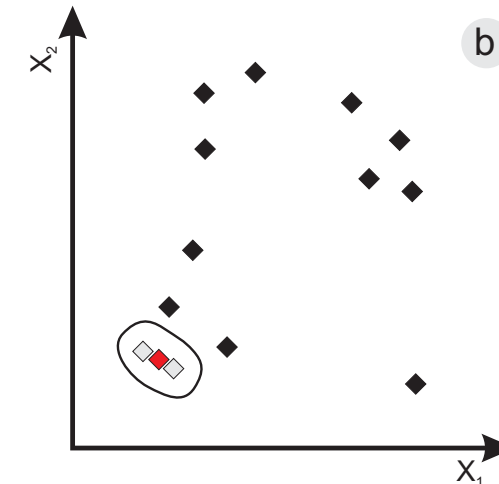
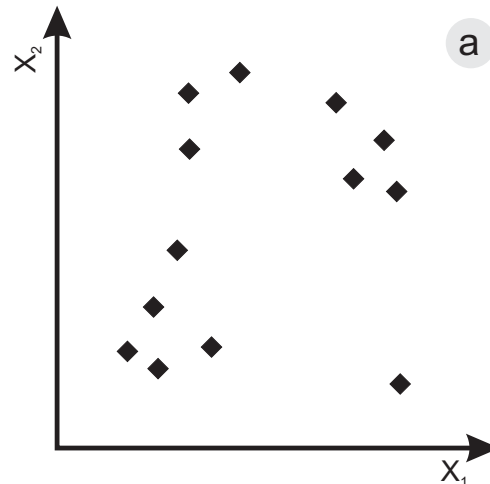
$$\frac{\partial T_{\text{monolith}}}{\partial t} = \nabla^2 \left(\frac{\lambda T_{\text{monolith}}}{\rho c_p} \right) + \frac{q}{\rho c_p}$$

Heat source term

$$q = -\sigma \cdot 2\pi r \lambda \frac{\partial T_{\text{gas}}}{\partial r} \Big|_{\text{surface}}$$



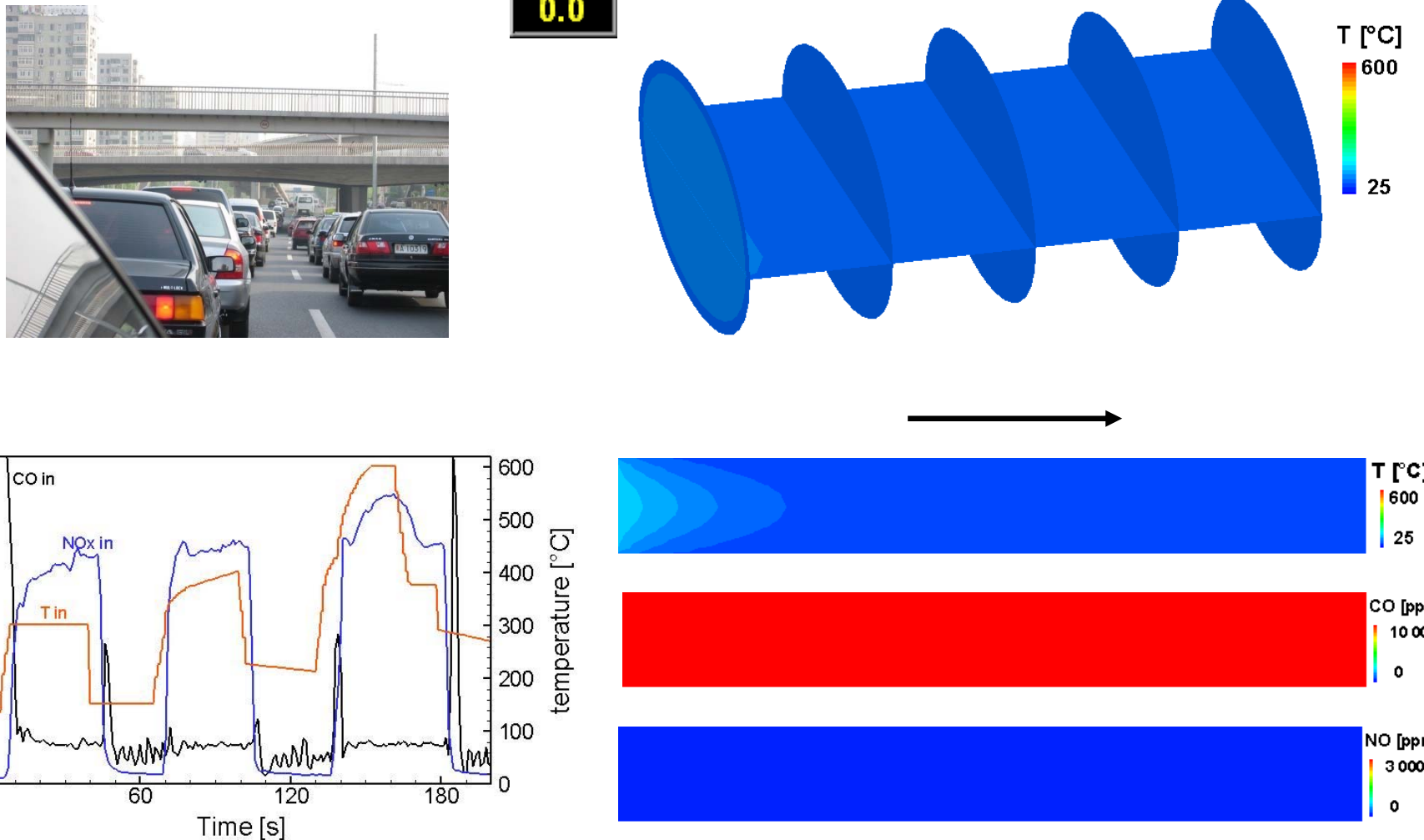
- Cluster-Agglomeration:
- channels may differ in:
wall temperature profile
inlet conditions
- → discrete vectors
- $x=(x_1, x_2, \dots)$



Clustering of „similar“ vectors

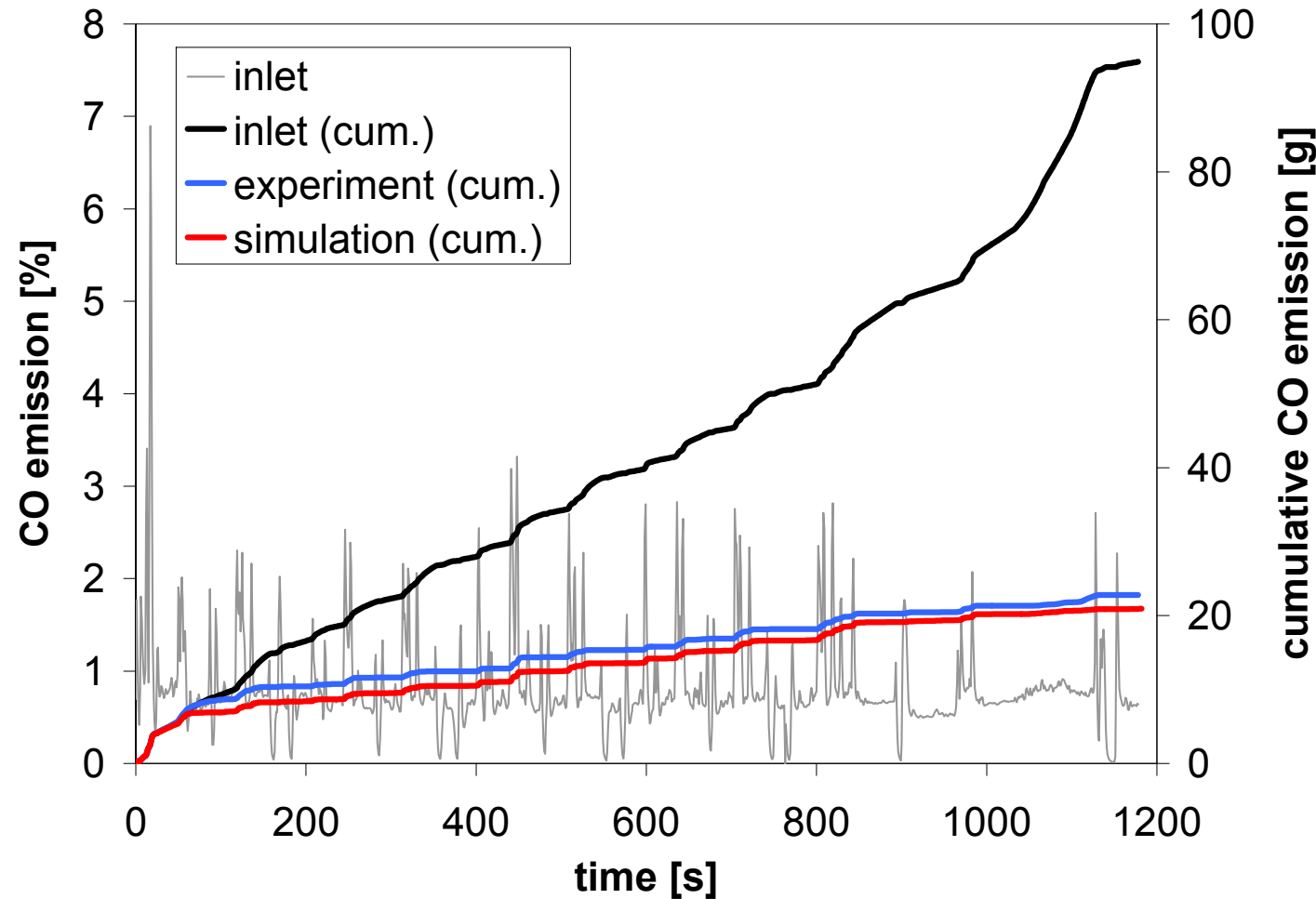
Vectors in one cluster are represented by an averaged vector

Pollutant reduction in a three-way catalyst during cold start-up: Simulation of a driving cycle



J. Braun, T. Hauber, H. Többen, J. Windmann, P. Zacke, D. Chatterjee, C. Correa, O. Deutschmann, L. Maier, S. Tischer, J. Warnatz, SAE paper 2002-01-0065

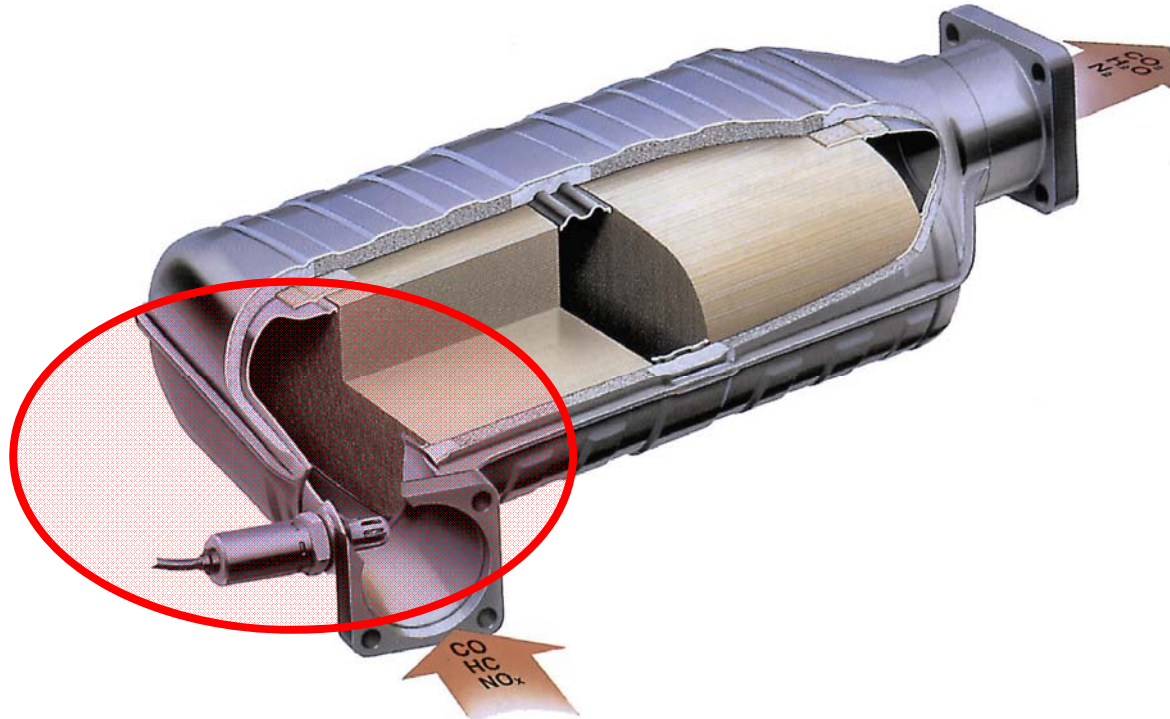
Cumulative CO emission in MEVG cycle: Experiment vs. simulation



Funded by Corning, 2006-2009

Tischer et al. SAE Technical paper 2007-01-1072 2007

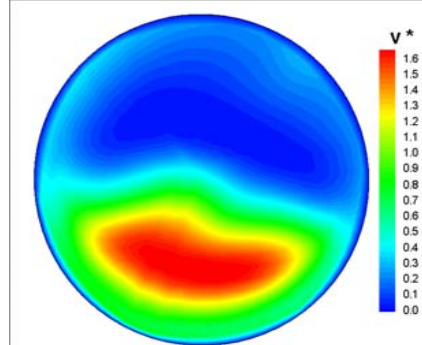
Spatially non-uniform inlet conditions: Non-efficient use of catalyst materials



Courtesy of J. Eberspächer GmbH& Co

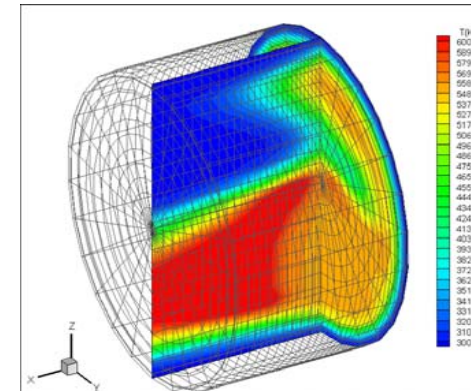
Simulation reveals consequences of design restrictions: Spatial non-uniformity increases pollution emissions

Non-uniform flow distribution
at converter front face

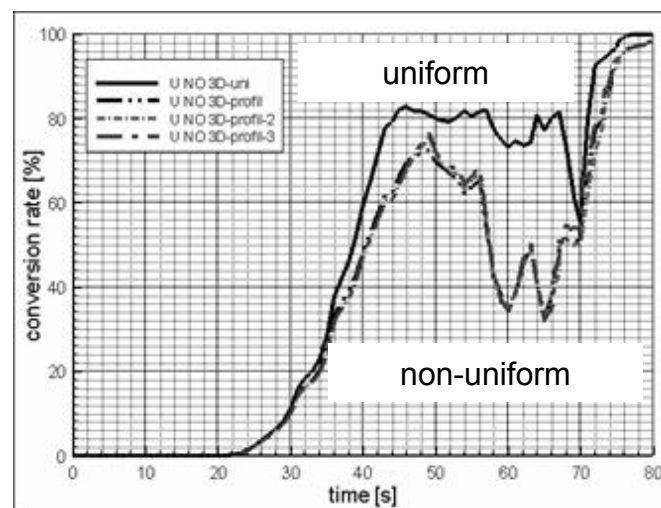
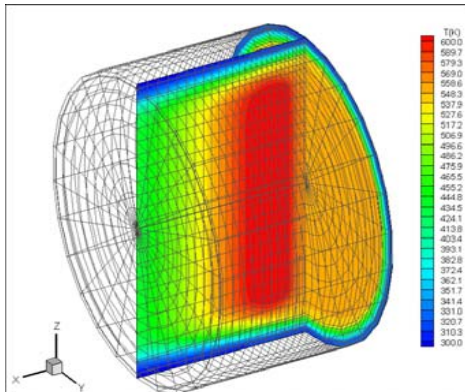


Temperature after 40 s
Non-uniform flow distribution

Temperature after 40 s
Non-uniform flow distribution



Temperature after 40 s
Uniform flow distribution



J. Windmann, P. Zacke, S. Tischer, O. Deutschmann, J. Warnatz, SAE paper 2003-01-0937 (2003)

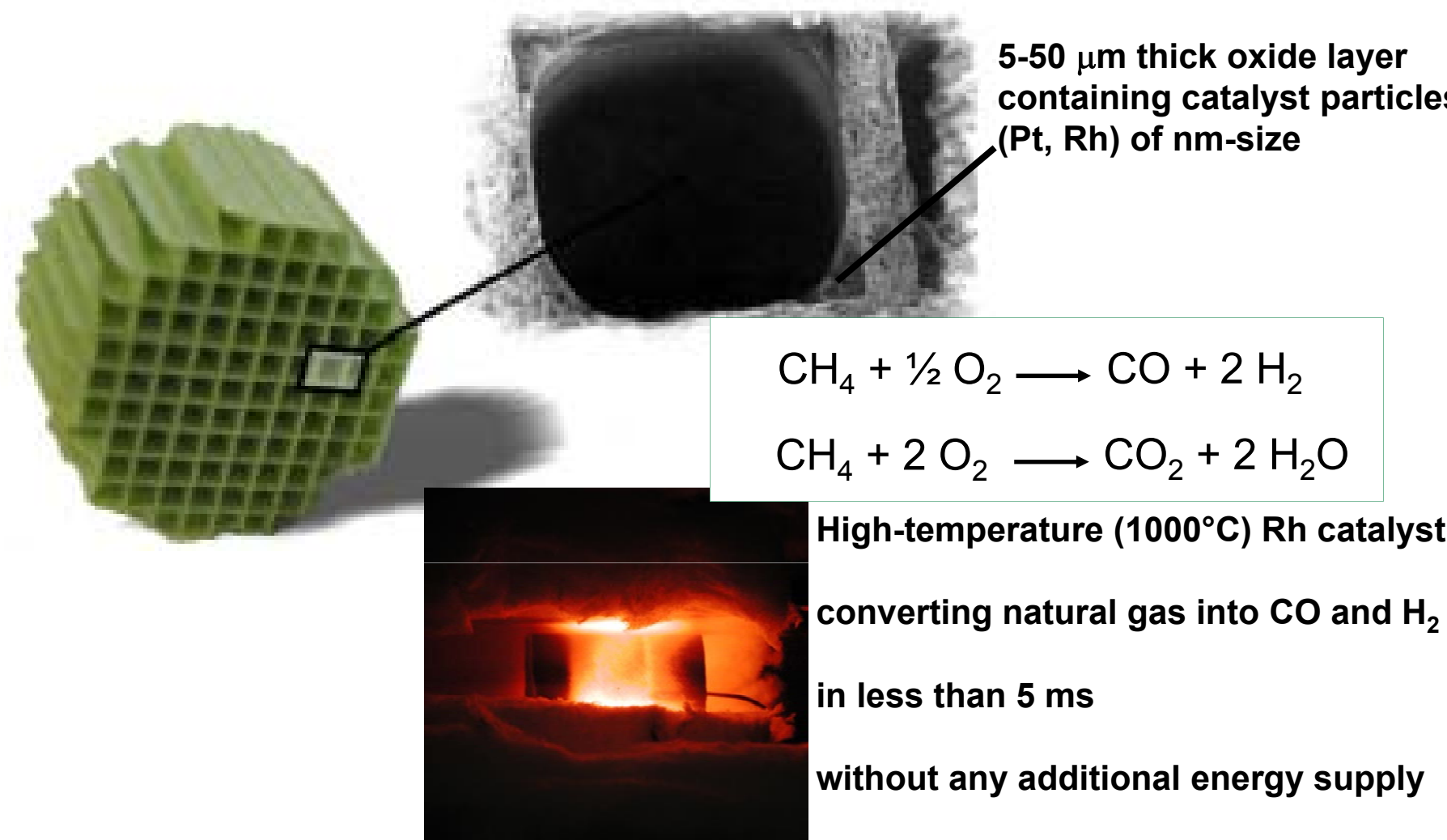
Natural gas → Liquid fuels

Syngas production by partial oxidation over Rh



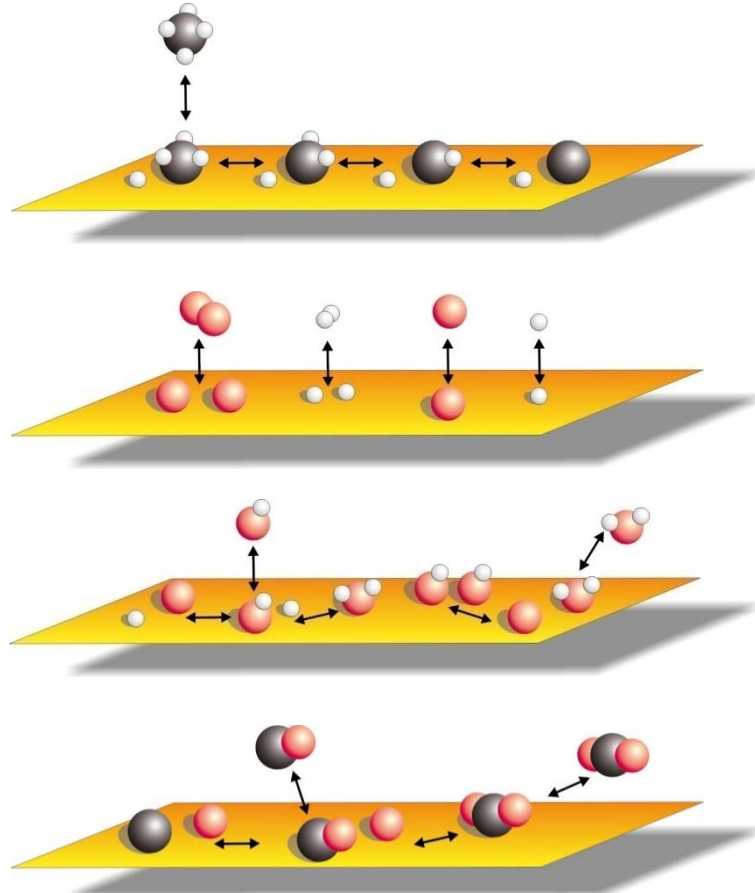
Collaboration with Conoco Inc., 2002

High-temperature catalysis: Compact and autothermal production of hydrogen in few milliseconds



D.A. Hickman, L.D. Schmidt, Science 259 (1993) 343

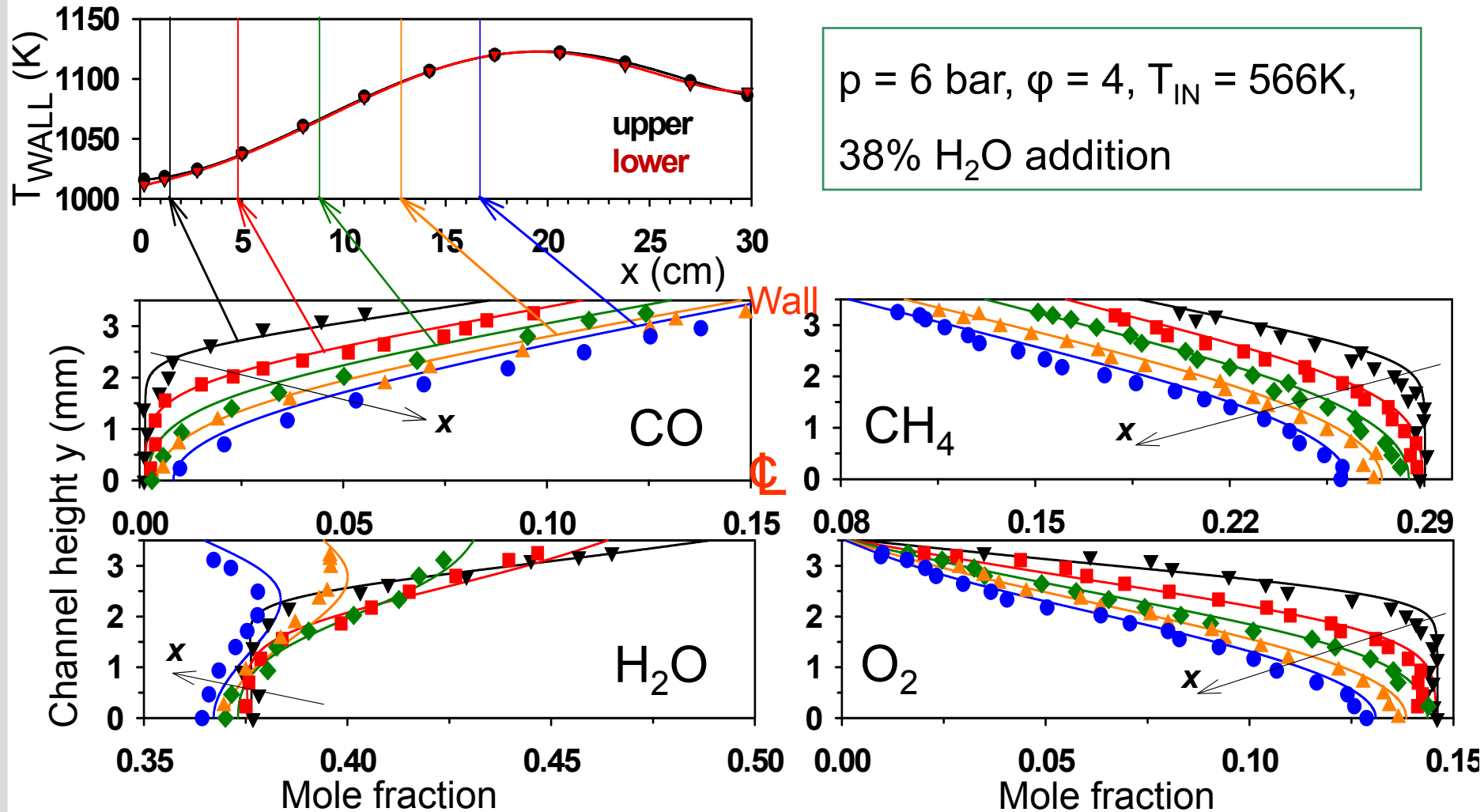
Surface reaction mechanisms: Scheme of partial oxidation of CH₄ over Rh



R. Schwiedernoch, S. Tischer, C. Correa, O. Deutschmann,
Chem. Eng. Sci. 58 (2003) 633

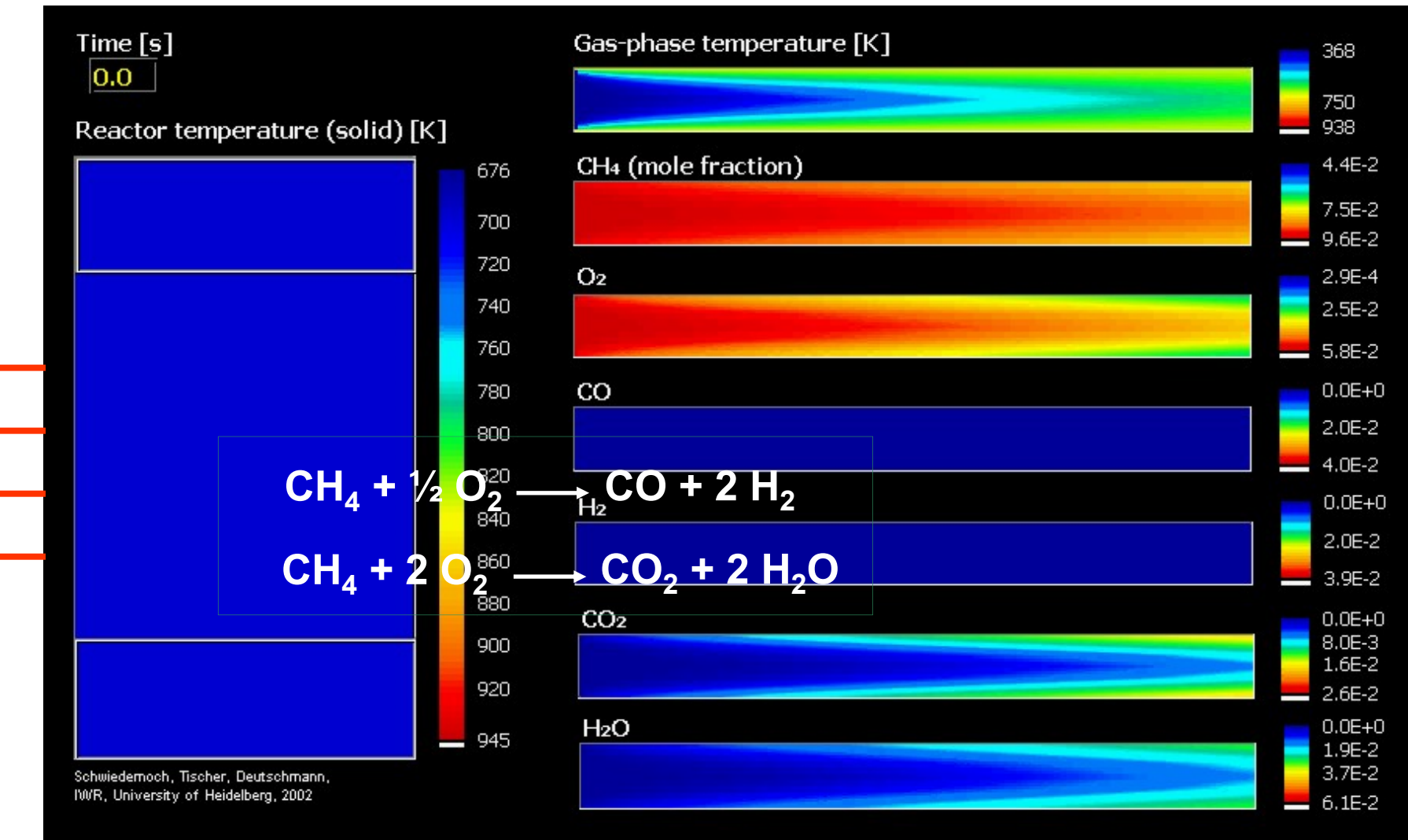
Reaction		A/[cm, mol, s]	E _a /[kJ/mol]		
H ₂	+ Rh(s) + Rh(s)	→ H(s)	+ H(s)	1.000·10 ⁻⁰²	S.C.
O ₂	+ Rh(s) + Rh(s)	→ O(s)	+ O(s)	1.000·10 ⁻⁰²	S.C.
CH ₄	+ Rh(s)	→ CH ₄ (s)		8.000·10 ⁻⁰³	S.C.
H ₂ O	+ Rh(s)	→ H ₂ O(s)		1.000·10 ⁻⁰¹	S.C.
CO ₂	+ Rh(s)	→ CO ₂ (s)		1.000·10 ⁻⁰⁵	S.C.
CO	+ Rh(s)	→ CO(s)		5.000·10 ⁻⁰¹	S.C.
H(s)	+ H(s)	→ Rh(s)	+ Rh(s) + H ₂	3.000·10 ⁺²¹	77.8
O(s)	+ O(s)	→ Rh(s)	+ Rh(s) + O ₂	1.300·10 ⁺²²	355.2-280θ _O
H ₂ O(s)		→ H ₂ O	+ Rh(s)	3.000·10 ⁺¹³	45.0
CO(s)		→ CO	+ Rh(s)	1.330·10 ⁺¹⁴	135.2-150θ _{CO}
CO ₂ (s)		→ CO ₂	+ Rh(s)	1.000·10 ⁺¹³	21.7
CH ₄ (s)		→ CH ₄	+ Rh(s)	1.000·10 ⁺¹³	25.1
H(s)	+ O(s)	→ OH(s)	+ Rh(s)	5.000·10 ⁺²²	83.7
OH(s)	+ Rh(s)	→ H(s)	+ O(s)	3.000·10 ⁺²⁰	37.7
H(s)	+ OH(s)	→ H ₂ O(s)	+ Rh(s)	3.000·10 ⁺²⁰	33.5
H ₂ O(s) + Rh(s)		→ H(s)	+ OH(s)	5.000·10 ⁺²²	104.7
OH(s) + OH(s)		→ H ₂ O(s)	+ O(s)	3.000·10 ⁺²¹	100.8
H ₂ O(s) + O(s)		→ OH(s)	+ OH(s)	3.000·10 ⁺²¹	171.8
C(s)	+ O(s)	→ CO(s)	+ Rh(s)	3.000·10 ⁺²²	97.9
CO(s) + Rh(s)		→ C(s)	+ O(s)	2.500·10 ⁺²¹	169.0
CO(s) + O(s)		→ CO ₂ (s)	+ Rh(s)	1.400·10 ⁺²⁰	121.6
CO ₂ (s) + Rh(s)		→ CO(s)	+ O(s)	3.000·10 ⁺²¹	115.3
CH ₄ (s) + Rh(s)		→ CH ₃ (s)	+ H(s)	3.700·10 ⁺²¹	61.0
CH ₃ (s) + H(s)		→ CH ₄ (s)	+ Rh(s)	3.700·10 ⁺²¹	51.0
CH ₃ (s) + Rh(s)		→ CH ₂ (s)	+ H(s)	3.700·10 ⁺²⁴	103.0
CH ₂ (s) + H(s)	+ 1/2CH ₃ (s)	→ CH ₂ (s) + H(s)	+ Rh(s)	3.700·10 ⁺²¹	44.0
CH ₂ (s) + Rh(s)	+ 2H(s)	→ CH ₂ (s) + H(s)		3.700·10 ⁺²⁴	00.0
CH ₂ (s) + H(s)		→ CH ₂ (s)	+ Rh(s)	3.700·10 ⁺²¹	68.0
CH ₂ (s) + Rh(s)		→ C(s)	+ H(s)	3.700·10 ⁺²¹	21.0
C(s) + H(s)	+ CH ₃ (s)	→ CH ₂ (s)	+ Rh(s)	3.700·10 ⁺²¹	172.0
CH ₄ (s) + O(s)	+ CH ₃ (s)	→ CH ₂ (s) + OH(s)	+ Rh(s)	3.700·10 ⁺²¹	00.0
CH ₃ (s) + OH(s)		→ CH ₄ (s)	+ O(s)	3.700·10 ⁺²¹	24.3
CH ₃ (s) + O(s)		→ CH ₂ (s)	+ OH(s)	3.700·10 ⁺²⁴	120.3
CH ₂ (s) + OH(s)		→ CH ₃ (s)	+ O(s)	3.700·10 ⁺²¹	15.1
CH ₂ (s) + O(s)		→ CH ₂ (s)	+ OH(s)	3.700·10 ⁺²⁴	158.4
CH(s) + OH(s)		→ CH ₂ (s)	+ O(s)	3.700·10 ⁺²¹	36.8
CH(s) + O(s)		→ C(s)	+ OH(s)	3.700·10 ⁺²¹	30.1
C(s) + OH(s)		→ CH(s)	+ O(s)	3.700·10 ⁺²¹	145.5

CPOX of CH_4 on Rh in single channel at steady state: 2d Raman profiles vs. computation (Mantzaras et al.)



A. Schneider, J. Mantzaras, P. Jansohn et al. Proc. Comb. Inst. 31 (2007)

Partial oxidation of CH₄ on Rh at 1 bar: Computed temperature and concentration profiles during light-off



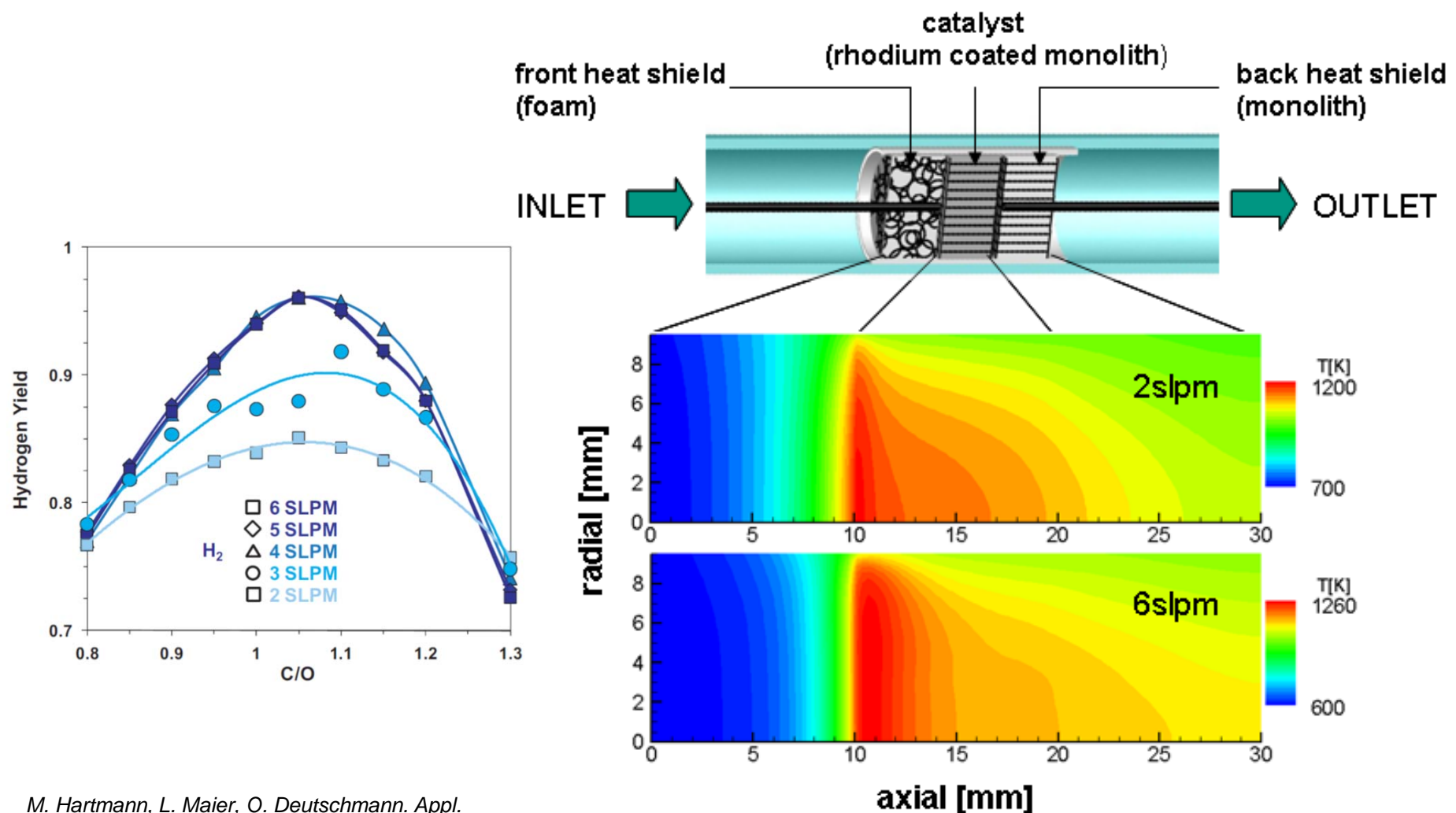
R. Schwiedernoch, S. Tischer, C. Correa, O. Deutschmann, Chem. Eng. Sci., 58 (2003) 633-642

More efficient technology for auxiliary power supply in automobile vehicles needed



Idling long-haul trucks consumes 1 billion gallons of diesel fuel annually in the USA
→ 11 million tons CO₂, 180,000 tons NO_x, 5000 tons particulates!

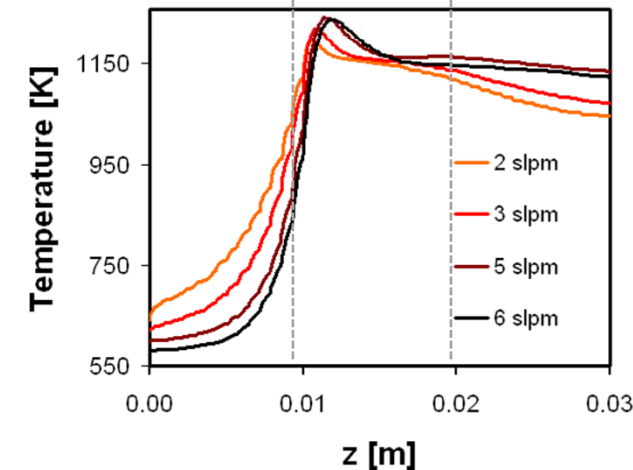
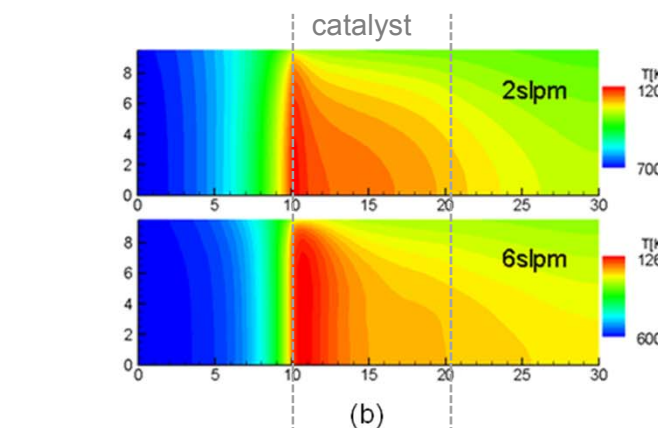
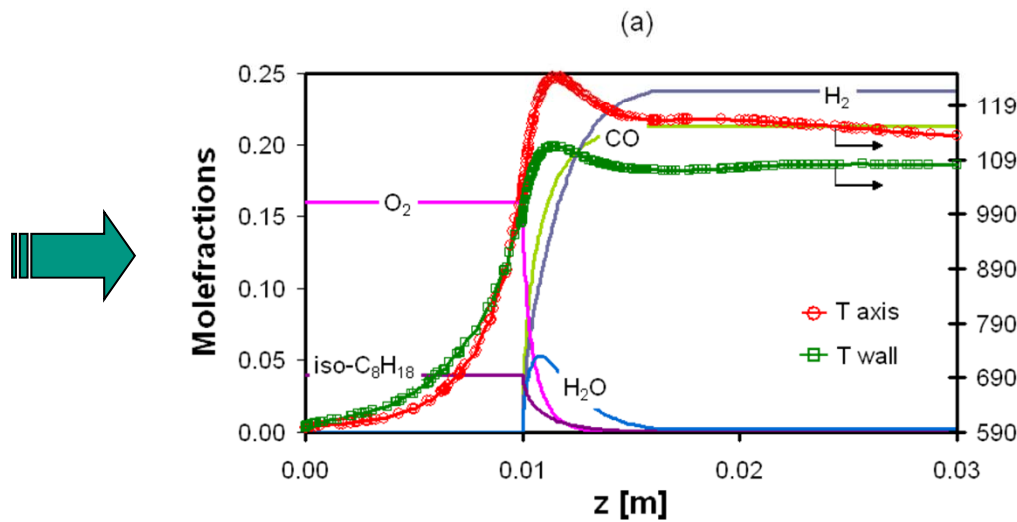
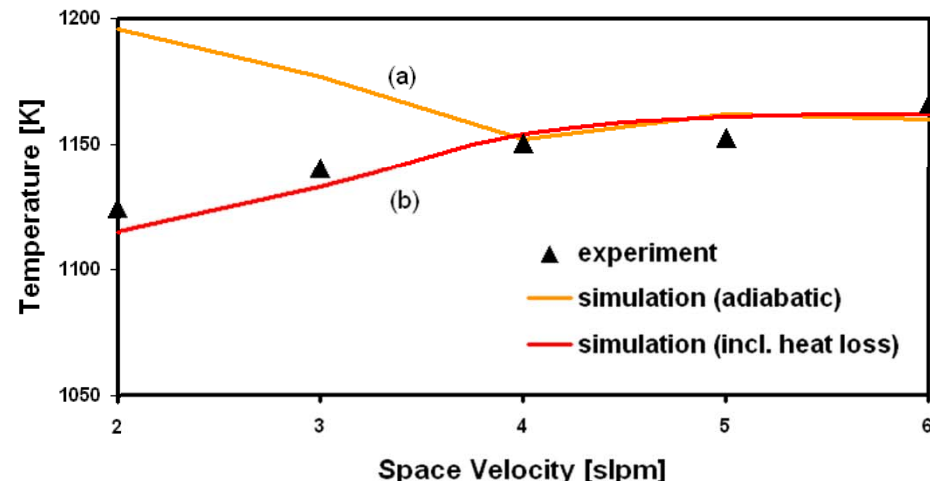
CPOX of i-octane: Impact of flow rate on hydrogen yield Computed temperature distribution in the reactor



M. Hartmann, L. Maier, O. Deutschmann. *Appl. Catalysis A: General* 391 (2011) 144.

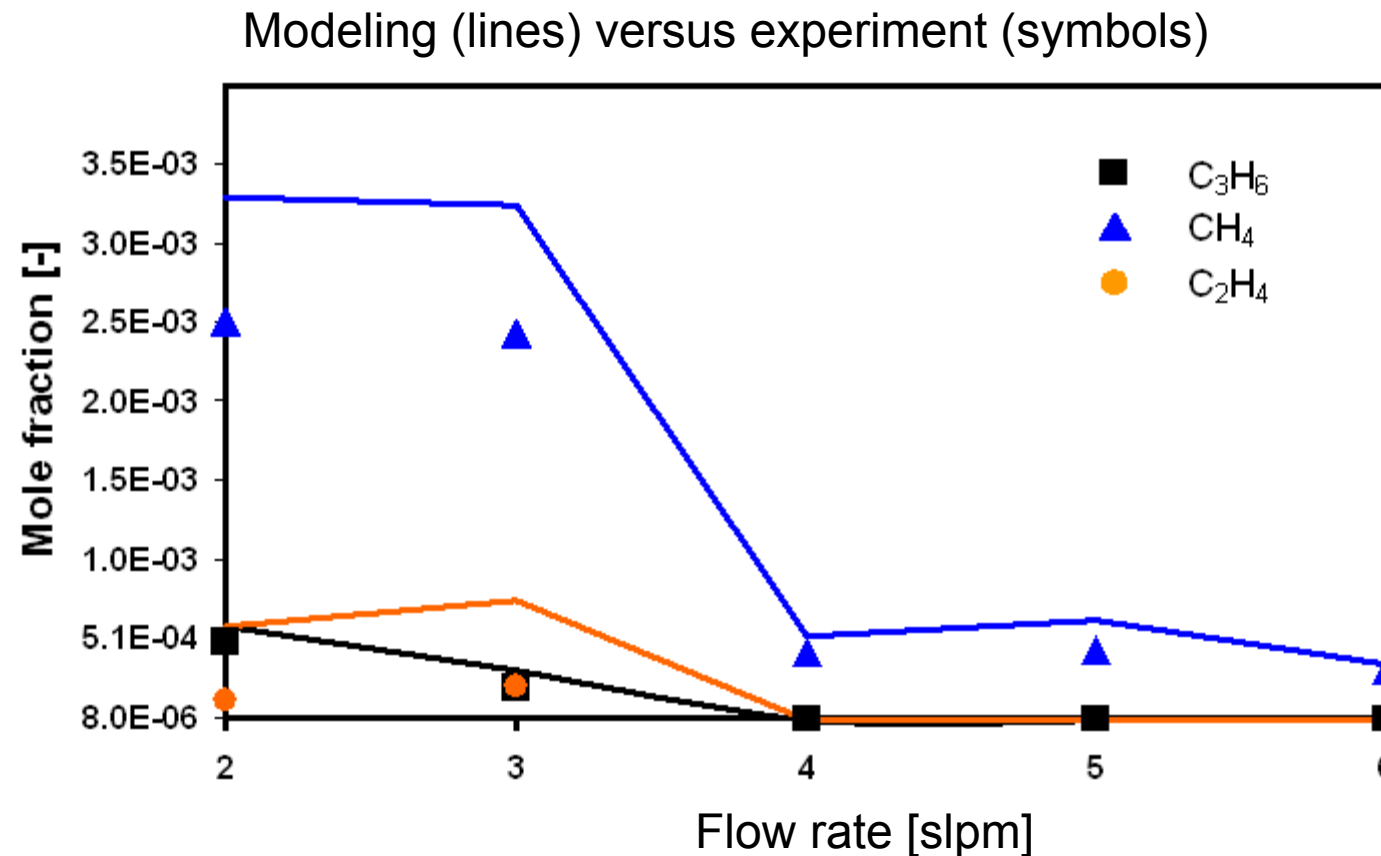
L. Maier, M. Hartmann, O. Deutschmann, *Combust. Flame* 158 (2011) 796–808.

CPOX of HC: Counter-intuitive increase of yields with decreasing residence time understood



L. Maier, M. Hartmann, O. Deutschmann, Combust. Flame 158 (2011) 796–808.

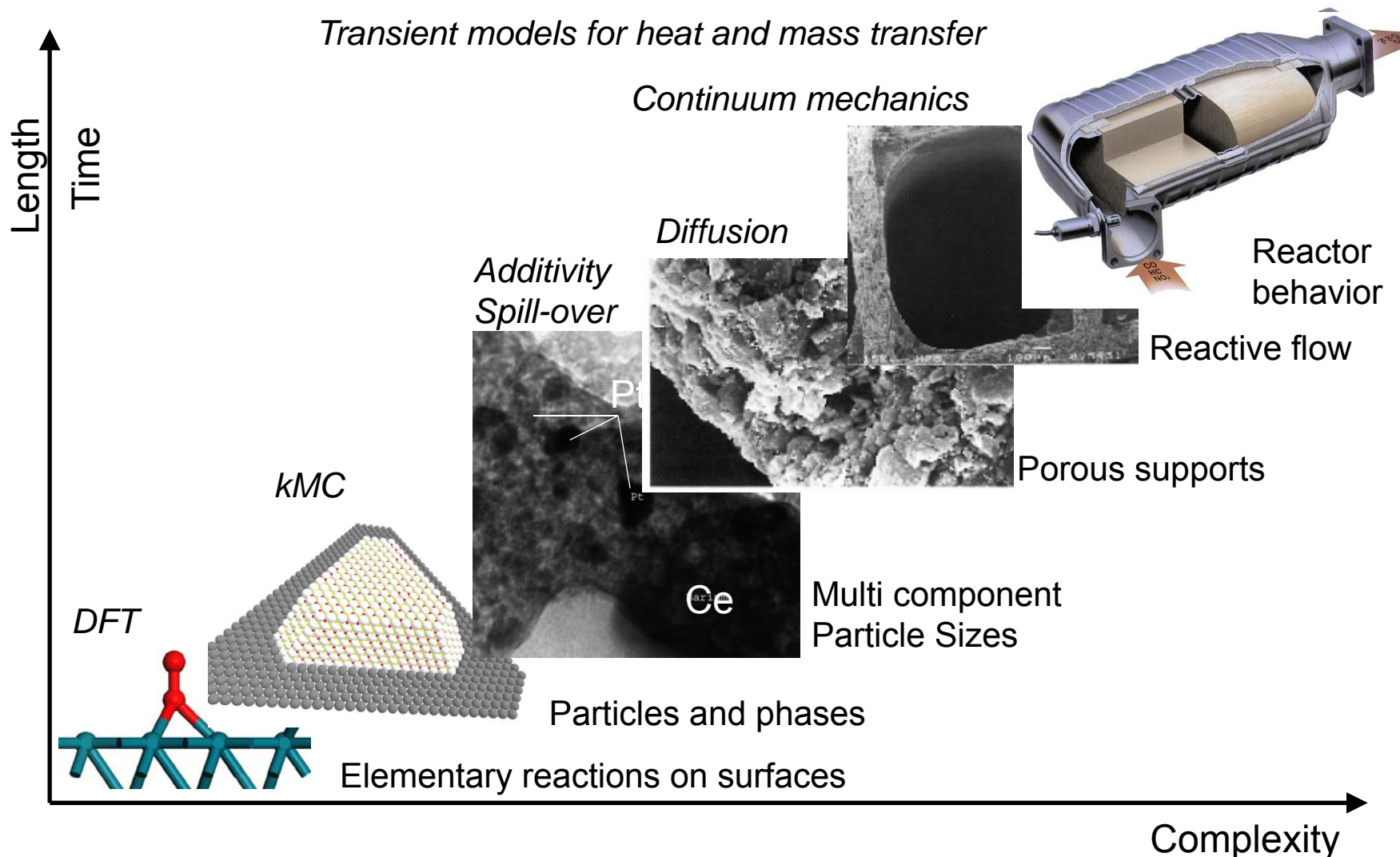
CPOX of iso-octane: Coke precursor formation also depends on flow rate



$\text{C}/\text{O} = 1.0$

L. Maier, M. Hartmann, O. Deutschmann, Combust. Flame 158 (2011) 796–808.

Simulation of catalytic reactors by multi-scale modeling: Information flux over the time and length scales



Literature

M. Baerns, A. Behr, A. Brehm, J. Gmehling, H. Hofmann, U. Onken, A. Renken. **Technische Chemie**. Wiley-VCH, 2006 (1 Band), ISBN 3527310002

M. Baerns, H. Hofmann, A. Renken, **Chemische Reaktionstechnik**, Wiley-VCH, 2006

G. Emig, E. Klemm, **Technische Chemie – Einführung in die chemische Reaktionstechnik**, Springer-Lehrbuch (ursprüngl. erschienen unter E. Fitzer, W. Fritz), 2005

A. Behr, D.W. Agar, J. Jörissen, **Einführung in die Technische Chemie**, Spektrum-Verlag, 2008

Dittmeyer, R. / Keim, W. / Kreysa, G. / Oberholz, A. (Hrsg.) **Winnacker-Küchler: Chemische Technik**, 5., erweiterte und aktualisierte Auflage, 2003-2005. 9677 Seiten, 4661 Abbildungen. Gebunden. ISBN: 978-3-527-30430-1

ENGLISH:

A. Jess, Wasserscheid, **Chemical Technology**, Wiley-VCH, 2014

O. Levenspiel, **Chemical Reaction Engineering**. J. Wiley, New York

H. Scott Fogler, **Elements of Chemical Reaction Engineering**, Prentice-Hall International Series in the Physical and Chemical Engineering Sciences, 2004.

Lanny D. Schmidt. **The Engineering of Chemical Reactions**, Oxford Univ Pr; Auflage: 2nd revised international ed , 2009.

Modeling Heterogeneous Catalytic Reactions. O. Deutschmann (Ed.), Wiley-VCH, 2011

